A MECHANISTIC INVESTIGATION OF *AGROBACTERIUM* β-GLUCOSIDASE

By

JULIE B. KEMPTON

B. Sc., The College of William and Mary, 1984

A THESIS SUBMITTED IN PARTIAL FULFILLMENT OF

THE REQUIREMENTS FOR THE DEGREE OF

MASTER OF SCIENCE

in

THE FACULTY OF GRADUATE STUDIES

(Department of Chemistry)

We accept this thesis as conforming

to the required standard

THE UNIVERSITY OF BRITISH COLUMBIA

July 1990

In presenting this thesis in partial fulfilment of the requirements for an advanced degree at the University of British Columbia, I agree that the Library shall make it freely available for reference and study. I further agree that permission for extensive copying of this thesis for scholarly purposes may be granted by the head of my department or by his or her representatives. It is understood that copying or publication of this thesis for financial gain shall not be allowed without my written permission.

Department of Chemistry

The University of British Columbia
Vancouver, Canada

Date August 4, 1990

DE-6 (2/88)

ABSTRACT

The mechanism of glucoside hydrolysis by *Agrobacterium* β-glucosidase has been investigated through the study of linear free energy relationships and α-secondary deuterium kinetic isotope effects. A two-step mechanism has previously been proposed for this process, consisting of;

(1) cleavage of the glucosidic bond and formation of a covalent glucosyl-enzyme intermediate ("glucosylation"), and

(2) hydrolysis of the intermediate to yield free enzyme and glucose ("deglucosylation").

Values of k_{cat} and K_m were determined for enzymic hydrolysis of fifteen substituted phenyl β-D-glucopyranosides with leaving group pK_a's ranging from 3.96 to 10.34. A linear free energy correlation of $\log(k_{cat})$ *vs.* leaving group pK_a resulted in a concave-downward plot with a break near pK_a 8, indicating a change in rate-determining step of a multistep reaction. The rates of hydrolysis of substrates with leaving group pK_a's < 8 are independent of phenol structure, indicating that deglucosylation is rate-limiting. Glucosides with leaving group pK_a's > 8 exhibit a linear dependence of hydrolysis rate upon pK_a, and thus it is proposed that glucosylation is the rate-determining step for these substrates. The value of the Hammett reaction constant, ρ, is 1.6, indicating that cleavage of the glucosidic bond is significantly advanced at the transition state.

The α-secondary deuterium kinetic isotope effects on hydrolysis of five substituted phenyl β-D-glucopyranosides were determined (deuterium substitution at the anomeric center), and the values were found to be segregated into two groups. The faster substrates (leaving group $pK_a < 8$) exhibited k_H/k_D values of approximately 1.11, while values for the slower substrates averaged 1.06. These results support the hypothesis of a change in rate-determining step as leaving group pK_a decreases. The magnitude of the isotope effect on glucosylation indicates a small amount of sp^3 to sp^2 rehybridization at the transition

state, which combined with the ρ value for this process suggests a substantial degree of nucleophilic participation of the enzymic carboxylate.

2-Deoxy-2-fluoro-D-glucosides with highly activated leaving groups are potent covalent inactivators of *Agrobacterium* β-glucosidase which operate by trapping the enzyme as its glucosyl-enzyme intermediate. Values of k_i and K_i were determined for six substituted phenyl 2-deoxy-2-fluoro-β-D-glucopyranosides whose leaving group pK_a's ranged from 3.96 to 7.18. A linear correlation was observed for both $\log(k_i)$ and $\log(k_i/K_i)$ *vs.* leaving group pK_a, with ρ values of 2.0 and 2.7, respectively, which indicates that cleavage of the glycosidic bond is virtually complete at the transition state. Such an observation of a linear free energy relationship between the rate of enzyme inactivation and the electronic structure of the inactivator is rarely accomplished in enzymology. Preliminary investigation of the α-secondary deuterium kinetic isotope effect on enzyme inactivation by 2',4'-dinitrophenyl 2-deoxy-2-fluoro-β-D-glucopyranoside indicates that the effect is quite small, probably 0-5%. These results suggest that the inactivation proceeds *via* an essentially concerted mechanism and that the transition state has little oxocarbonium ion character.

TABLE OF CONTENTS

CHAPTER II
RESULTS AND DISCUSSION

CHAPTER III
MATERIALS AND METHODS

LIST OF FIGURES

LIST OF TABLES

LIST OF SCHEMES

LIST OF ABBREVIATIONS AND DEFINITIONS

Abbreviations

BSA	bovine serum albumin
GalOH	galactopyranose
GalOMe	methyl galactoside
PNPG	4'-nitrophenyl-β-D-glucopyranoside
2d-PNPG	4'-nitrophenyl-2-deoxy-β-D-glucopyranoside
2F-PNPG	4'-nitrophenyl-2-deoxy-2-fluoro-β-D-glucopyranoside
G1P	α-D-glucopyranosyl phosphate
Asp	Aspartic acid
Glu	Glutamic acid
TMS	tetramethylsilane
nmr	nuclear magnetic resonance
m.p.	melting point
pABG-5 β-glucosidase	cloned *Agrobacterium* β-glucosidase isolated from *E. coli*

Kinetic and Physical Constants

T	Temperature (K)
k	Boltzmann constant
h	Planck's constant
K_m	Michaelis-Menten constant (the apparent dissociation constant for all bound enzyme-substrate species)
K_s	dissociation constant of the enzyme-substrate complex
V_{max}	Maximal rate of an enzyme-catalyzed reaction

k_{cat}	First-order rate constant for catalysis (turnover number)
K_i	Inhibitor constant (the apparent dissociation constant for all bound enzyme-inhibitor species)
k_i	First-order rate constant of inactivation

ACKNOWLEDGEMENT

I would like to express my gratitude to my supervisor, Dr. Stephen Withers, for his advice and encouragement during the course of my research. Thanks also to my coworkers for useful suggestions and especially for their friendship. Assistance from Karen Rupitz and Mark Namchuk has been particularly appreciated. I also thank the University of British Columbia for financial support, and the technical support staff of the Department of Chemistry for their assistance.

Special thanks go to my good friends Bev McLagan and Michael Nel for all their help and support.

And finally, my deepest thanks to my husband, Jim, for his belief in me and for his love, support, and friendship.

CHAPTER I

INTRODUCTION

1. Glycosidases and Glycoside Hydrolysis

Glycosidases are a broad class of enzymes which catalyze the hydrolysis of the C-O bond of glycosidic linkages, according to the reaction shown below (Scheme 1). Their function in nature is generally to cleave disaccharides into two sugar molecules. Thus, in natural substrates, the aglycone portion, R, is another sugar residue, but it may also be an alkyl or aryl group.

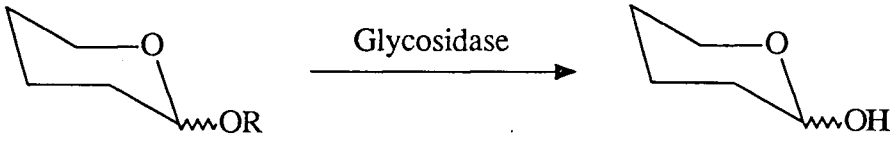

Scheme 1. Reaction catalyzed by a glycosidase.

The large family of glycosidases is divided into subgroups based on several characteristics. First, they are classified according to the sugar, or glycone, moiety toward which they are most reactive (e.g., a galactosidase is most reactive toward galactosides). Sugar specificity is often further characterized with regard to ring size, i.e. pyranose, furanose, etc. Next, these enzymes are classed as "α" or "β" depending on the stereochemistry of the glycosidic bond which they cleave. It should be noted that many glycosidases show a relatively relaxed specificity for the glycone portion of their substrate. For example, β-glucosidases have been shown to have some mannosidase and galactosidase activity. Conversely, they are nearly totally specific in regards to the configuration (α or β) of the bond which they hydrolyze.

One further classification of glycosidases is as "retaining" or "inverting" enzymes, indicating the relative anomeric configurations of the substrate cleaved and the product released (Scheme 2). This work will focus on "retaining" glycosidases.

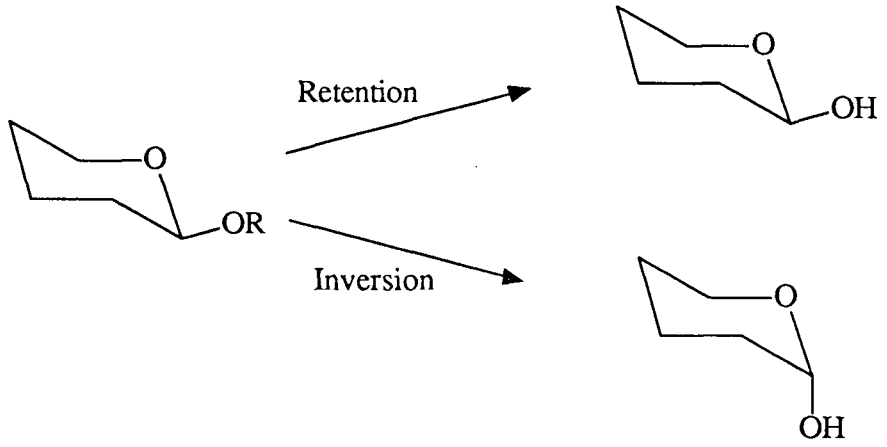

Scheme 2. Stereochemical outcomes of glycosidase-catalyzed hydrolysis.

2. The Catalytic Mechanism of Glycosidases

The mechanism for "retaining" glycosidases was first suggested by Koshland in 1953[1] (Scheme 3), and this earliest proposal can accommodate all subsequent mechanistic data for these enzymes. The mechanism has the following features:

1). An enzymic carboxylate group is located adjacent to the anomeric center, on the opposite side of the sugar ring to the aglycone.

2). A covalent glycosyl-enzyme intermediate forms between the carboxylate and C(1) of the sugar.

3). This covalent intermediate is reached, in both directions, *via* an oxocarbonium-ion-like transition state.

4). General acid catalysis may assist aglycone departure, but is not essential for all substrates. General base catalysis may assist attack of the acceptor (e.g. water) in the deglycosylation step.

5). Non-covalent interactions provide most of the rate acceleration.

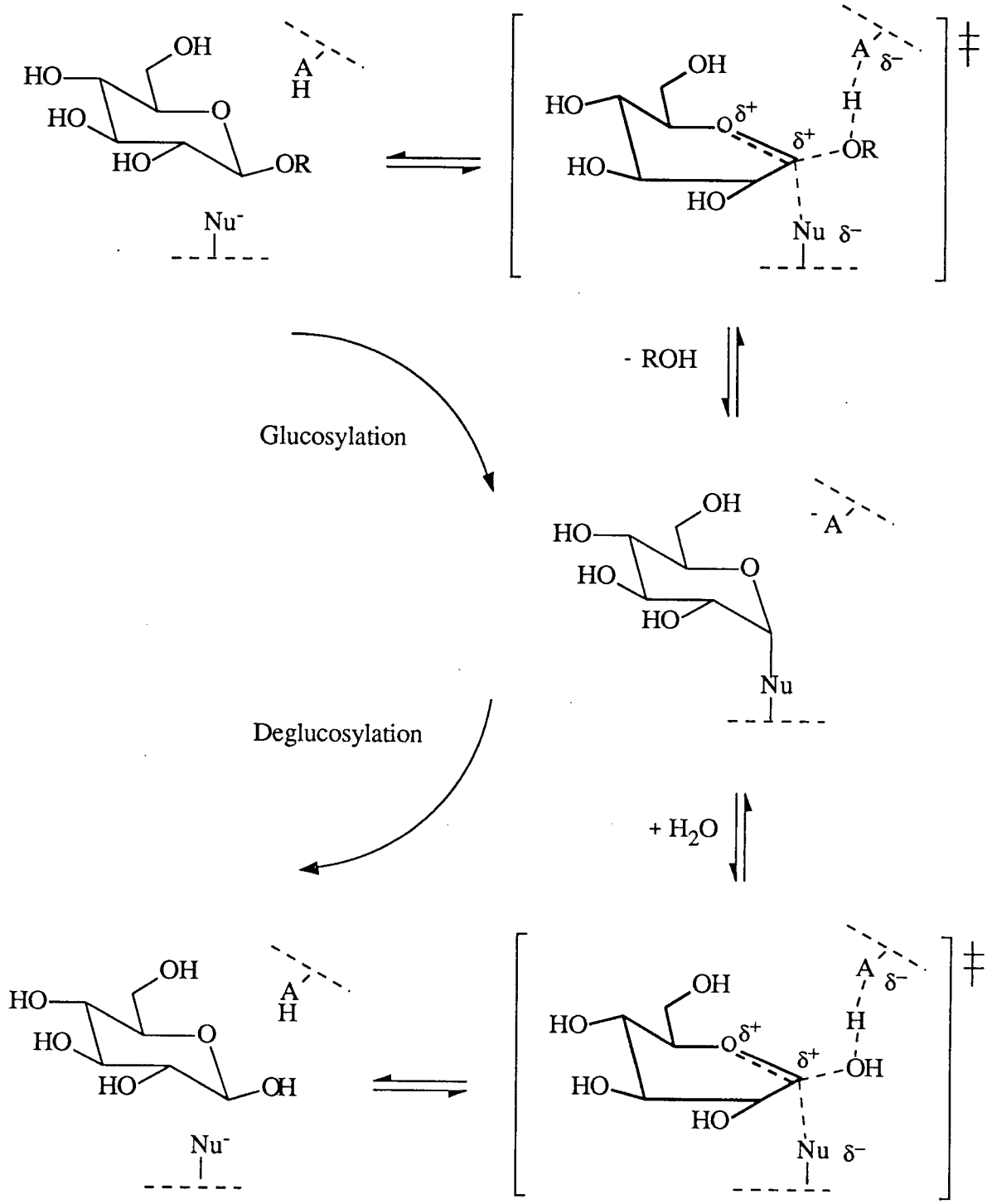

Scheme 3. Mechanism for hydrolysis of β-glucosides by a β-glucosidase.

These features will be discussed in some detail below. Points 2, 3, and 4 will be of particular importance to the scope of this work.

2.1. Enzymic Carboxylate Group

The strongest evidence for a strategically-placed enzyme carboxylate comes from X-ray structural data on the enzyme lysozyme, a glycosidase responsible for the degradation of the polysaccharide component of bacterial cell wall peptidoglycans (Scheme 4).

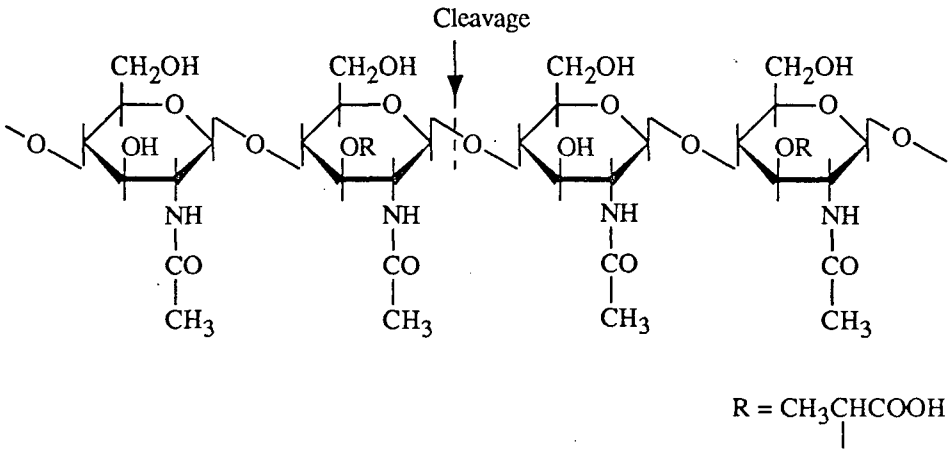

Scheme 4. Lysozyme-catalyzed cleavage of bacterial-cell-wall polysaccharide.

The three-dimensional structures of two lysozymes have been determined, and both have an aspartate residue correctly positioned in the active site. This residue is Asp20 in the lysozyme from bacteriophage T4[2], and Asp52 in that of hen's egg white[3]. Additional information has been gained using mechanism-based inactivators. One such class of inactivators, cyclohexane polyol epoxides, appropriately substituted to mimic gluco- or galacto-derivatives, have been used to identify carboxylates in affinity-labelling studies of two β-glucosidases (from *A. wentii*[4] and from sweet almond[5]), and the *lac-Z* β-

galactosidase of *E. coli*[6]. These compounds inactivate the enzymes according to Scheme 5. An aspartate residue was labelled in both of the β-glucosidases, while Glu461 was identified in the β-galactosidase.

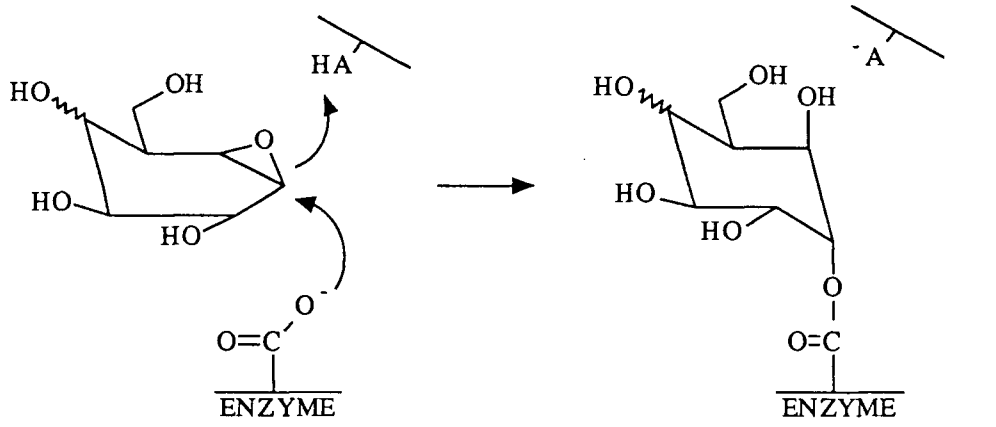

Scheme 5. Affinity labelling of β-glycosidases by cyclohexane polyol epoxides.

A second class of mechanism-based inhibitor has also been used to tag an active-site carboxylate. The β-glucosidase from *Agrobacterium* was inactivated using 2',4'-dinitrophenyl 2-deoxy-2-fluoro-β-D-glucopyranoside, and the labelled amino acid proved to be Glu358 (Scheme 6)[7].

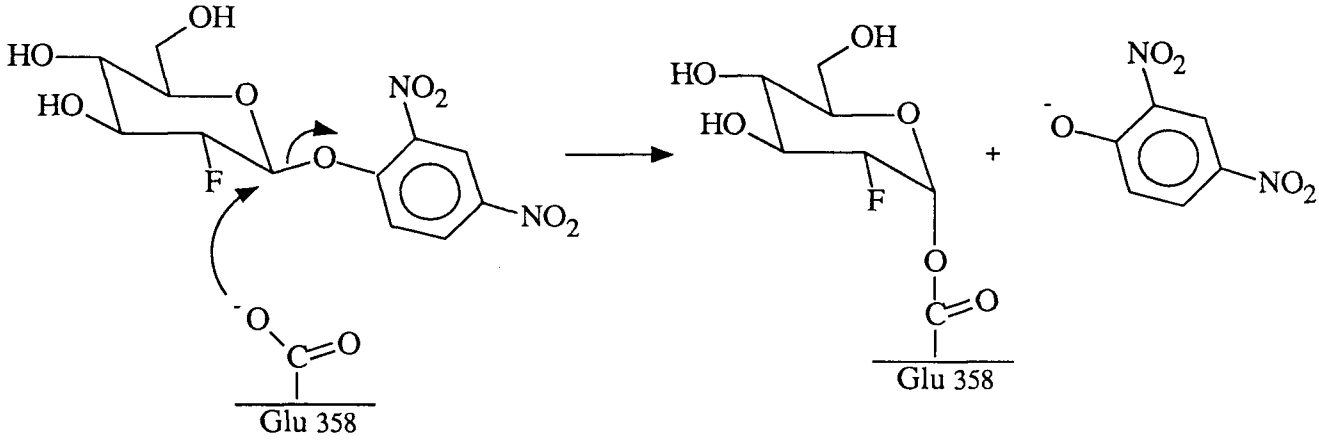

Scheme 6. Identification of nucleophilic carboxylate in Agrobacterium β-glucosidase.

2.2. Covalent Glycosyl-Enzyme Intermediate

Some excellent evidence for the existence of a glycosyl-enzyme intermediate was obtained by Stokes and Wilson in 1972[8]. They observed the partitioning ratios between hydrolysis and methanolysis products formed by β-galactosidase-catalyzed solvolysis of a series of aryl β-galactosides in a mixture of buffer and methanol.

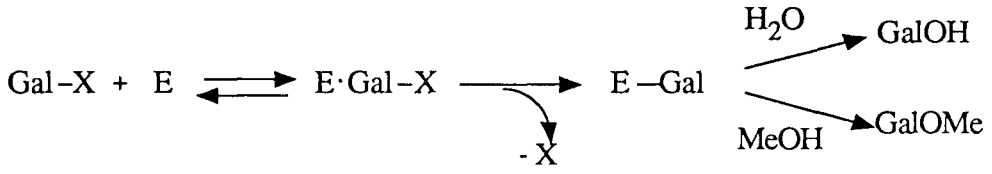

Scheme 7. Hydrolysis vs. methanolysis of aryl β-galactosides.

The data showed a constant ratio of methanolysis product to hydrolysis product, although the reactivity of the enzyme toward the substrates varied greatly, as reflected by the V_{max} values. These results suggest that the nucleophiles attack an enzymatic intermediate common to all substrates, but say little about the nature of that intermediate.

Table 1. Partitioning of Galactosyl β-Galactosidase between Water and Methanol[8].

Aglycone	Methanolysis/Hydrolysis	V_{max} (relative)
2'-nitrophenyl	1.97	1.0
3'-nitrophenyl	1.96	0.9
3'-chlorophenyl	2.08	0.5
4'-nitrophenyl	1.99	0.2
phenyl	1.94	0.1
4'-methoxyphenyl	2.14	0.1
4'-chlorophenyl	2.13	0.02
4'-bromophenyl	2.02	0.02
methyl	2.02	0.06

Koshland's original mechanism for "retaining" glycosidases suggested a covalent glycosyl-enzyme intermediate, but there is not complete agreement on this point. Based on X-ray crystal structure data of hen's egg white lysozyme, Phillips[9] has proposed that an intimate ion pair between an oxocarbonium ion and Asp52 could be sufficiently long-lived to allow the leaving group to diffuse away and the acceptor (e.g. water) to diffuse in and react before the ion pair collapses to a covalent species. However, glycosyl cations are of comparable stability to tertiary alkyl cations, the latter having an estimated lifetime in water on the order of 10^{-10} seconds[10]. It is possible (but as yet unproven) that an intimate ion pair is indeed the intermediate species in lysozyme, but for other glycosidases, such an intermediate seems quite unlikely. Some glycosyl-enzymes formed at ambient temperature have lifetimes in the 1 to 100 ms range; low temperature can increase lifetimes to minutes[11]. It is difficult to accept that even an extremely favorable environment could increase the duration of a glycosyl cation by factors of 10^9 to 10^{12}.

An extraordinarily long-lived covalent glucosyl-enzyme intermediate is formed in the reaction of β-glucosidase with 2',4'-dinitrophenyl 2-deoxy-2-fluoro-β-D-glucopyranoside[12]. The substitution of fluorine for hydroxyl at the C(2) position of the glycone causes both the glycosylation and deglycosylation steps to be extremely slow; however, incorporation of the highly-activated leaving group, 2,4-dinitrophenol, accelerates glucosylation significantly and allows the covalent 2-deoxy-2-fluoro-glucosyl enzyme intermediate to be trapped (Scheme 6, above), thus temporarily inactivating the enzyme. ^{19}F Nmr studies have confirmed the covalent nature of this intermediate[13]. This species is remarkably stable, with a half-life of over 500 hours at 30°C in buffer. Yet, when the inactivated enzyme is incubated with a glucoside which can act as an acceptor [for example, 4'-nitrophenyl β-D-glucopyranoside (PNPG) or glucosyl benzene], first-order reactivation kinetics are observed ($t_{1/2}$ = 85 min in 10 mM PNPG), and full activity can be

restored (Scheme 8). Thus a covalent glucosyl-enzyme intermediate has been confirmed as a catalytically competent intermediate in glucoside hydrolysis.

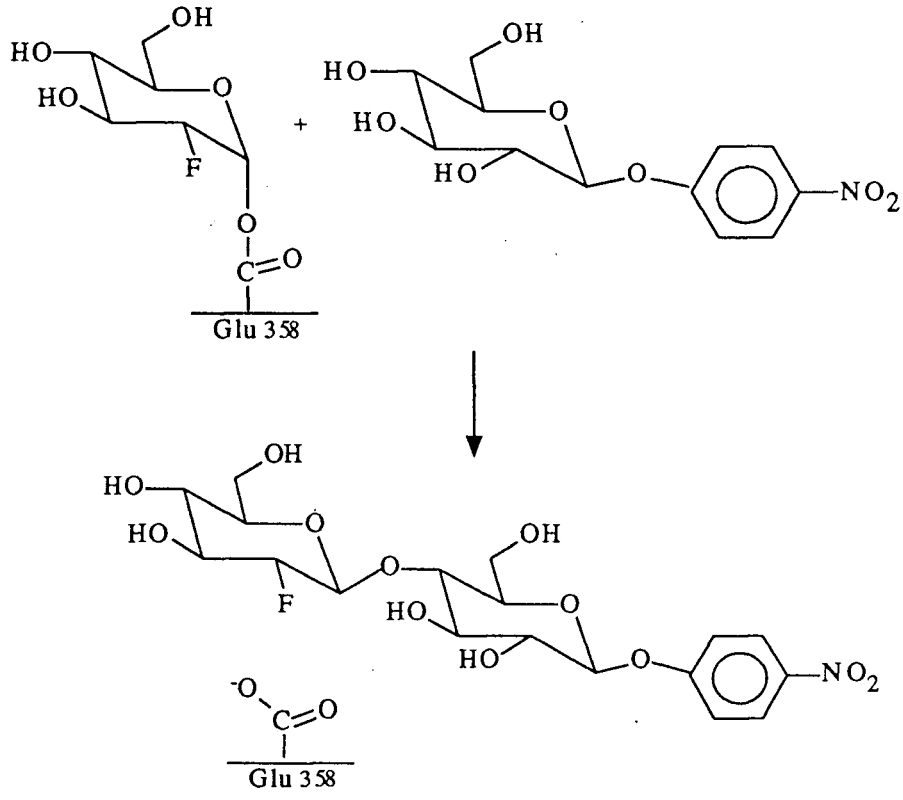

Scheme 8. Reactivation of β-glucosidase via transglycosylation.

2.3. Oxocarbonium-Ion-Like Transition State

While the existence of a covalent glycosyl-enzyme intermediate seems likely for most glycosidase enzymes, there is also a great deal of evidence suggesting that the transition states for formation and hydrolysis of the covalent intermediate have substantial oxocarbonium ion character. Much of the kinetic evidence comes from studies of kinetic isotope effects. (See Section 5 for a discussion of kinetic isotope effects as transition state probes). By careful choice of substrate, one can obtain conditions in which the glycosylation or deglycosylation steps are rate-limiting, and it is then possible to measure the kinetic isotope effect of each individual step.

Several studies have shown large kinetic isotope effects for substrates for which glycosylation is known to be rate-limiting. One such reaction, the β-galactosidase-catalyzed hydrolysis of C(1)-deuterated β-galactosyl pyridinium salts (Figure 1) exhibited α-secondary deuterium isotope effects of 1.15 to 1.20[14]. This indicates a large degree of sp^2 character at the transition state for formation of the galactosyl-enzyme intermediate. Similar conclusions have been drawn for this step with the β-glucosidase A3 from *A. wentii*[15].

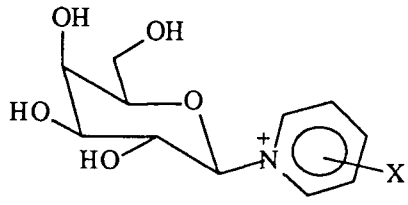

Figure 1. β-Galactosyl pyridinium salt.

Large α-deuterium kinetic isotope effects have also been observed in cases where deglycosylation is known to be rate-limiting. Such isotope effects indicate an increase in sp^2 character on going from glycosyl-enzyme to the transition state, and thus constitute evidence for the covalent (sp^3) character of the intermediate. For example, the *E. coli* β-galactosidase-catalyzed hydrolysis of 2',4'-dinitrophenyl β-D-galactopyranoside showed a kinetic isotope effect[14] of 1.21. Van Doorslaer et al.[16] also observed a large isotope effect on deglycosylation of β-glucosidase. If the intermediate were a stable ion pair, an inverse isotope effect would be observed.

Transition state analogues offer additional evidence for the oxocarbonium ion nature of the transition state. There are two main features of a glycosyl cation which distinguish it from its parent glycoside. First, O(5) and C(1) carry a full positive charge between them. Also, the four atoms C(5), O(5), C(1), and C(2) are coplanar[17]. There exist stable monosaccharide derivatives which have one or both of these features, and many of them

have exhibited enhanced binding relative to normal glycosides, as would be expected for a molecule which mimics the transition state. These molecules, termed "transition state analogues", provide supportive evidence for the oxocarbonium-ion-like nature of the transition state.

Table 2 presents a sampling of the binding constants exhibited by such transition state analogues. (A decreased K_i indicates tighter binding).

Table 2. Inhibition of Glycosidases by Transition State Analogues.

Enzyme	Inhibitor	K_i (mM)
β-glucosidase		
--*A. wentii*	glucose[15]	2.8
	β-glucosylamine[15]	0.0016
	glucono-(1,5)-lactone[15]	0.0096
	glucono-(1,5)-lactam[15]	0.036
	nojirimycin[18]	0.00036
--sweet almond	glucose[19]	189
	glucono-(1,5)-lactone[19]	0.2
	glucono-(1,5)-lactam[19]	0.037
	nojirimycin[18]	0.0009
--*Helix pomata*	glucose[18]	46
	nojirimycin[18]	0.0011
--sheep liver	glucose[20]	> 50
	glucono-(1,5)-lactone[20]	0.010
β-N-acetylglucosaminidase		
--rat kidney	N-acetylglucosamine[21]	4.4
--rat epididymis	N-acetyl-glucosaminolactone[22]	0.00072

Glucono-(1,5)-lactone binds 2 to 3 orders of magnitude better than normal substrates. The lactone has the same coplanarity between C(5) and C(2) as does a glucosyl cation, and also by resonance has some positive charge on O(5) (Figure 2).

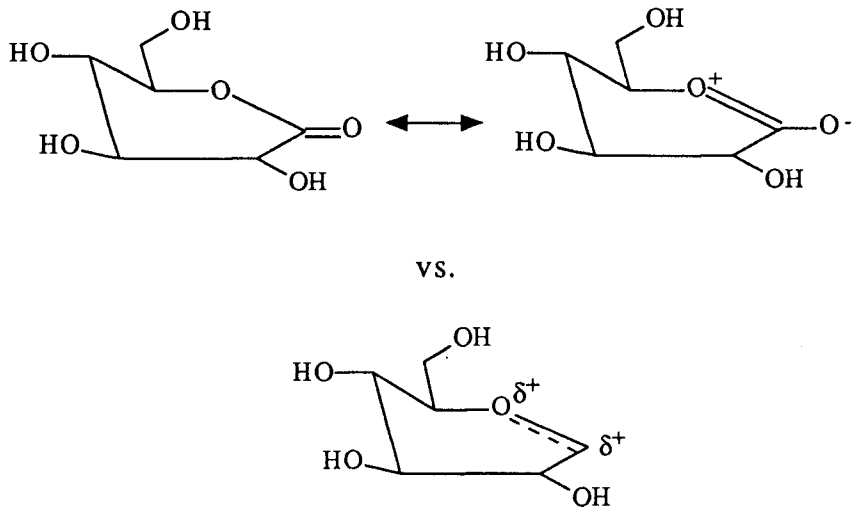

Figure 2. Structural and electronic similarity of glucono-(1,5)-lactone and glucosyl cation.

Inhibitors like nojirimycin exist in several forms, and when protonated can be both isosteric and isoelectronic with a glucosyl cation (Scheme 9). Such compounds containing positively-charged groups are among the tightest binding glycosidase inhibitors[23].

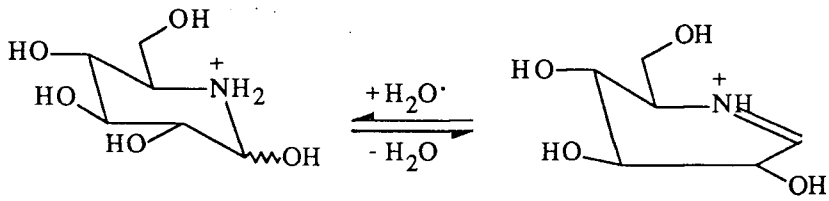

A B

Scheme 9. Different structures of nojirimycin. (A) is isoelectronic with a glucosyl cation; (B) is isosteric as well.

2.4. Acid Catalysis

As mentioned previously, acid catalysis is of variable importance to aglycone departure, and in some cases does not occur at all. The primary evidence for this is provided by the study of glycosidase-catalyzed hydrolysis of glycosyl pyridinium salts. For such compounds, protonation of the leaving group is structurally impossible. Yet Sinnott et al. observed[24] that β-galactosidase caused rate accelerations of 10^8-10^{13}-fold relative to spontaneous hydrolysis of a series of substituted β-galactosyl pyridinium salts. These are enormous rate enhancements even though acid catalysis is not involved, thus it may not be a significant factor in the hydrolysis of normal substrates.

Other evidence for a strategically-placed acid group is found in the glycosidase-catalyzed hydration of C(1)-unsaturated heptopyranosyl derivatives. For example, the stereochemistry of the product of the reaction in Scheme 10 indicates that the substrate was protonated from the β-face[25].

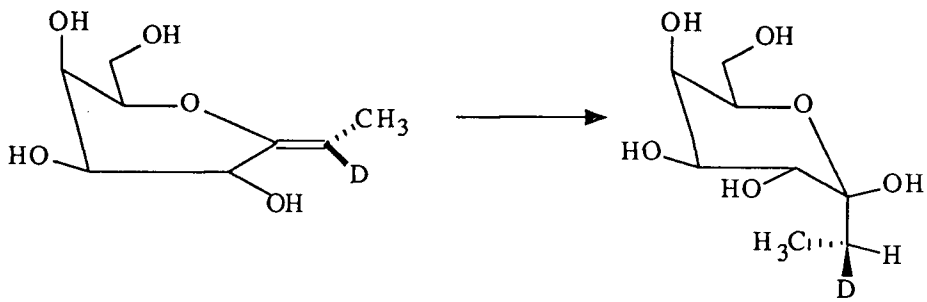

Scheme 10. E. coli β-galactosidase-catalyzed hydration of a heptenitol derivative.

Several glycosidase residues have been identified that could act as general acid catalysts. From X-ray structural data of hen's egg white lysozyme, Glu35 seems the likely proton donor group. Other residues, suggested on the basis of affinity-labelling and mutagenesis studies include tyrosine (β-galactosidase from *E. coli*[26]) and histidine (yeast α-glucosidase[27]).

2.5. Non-covalent Interactions

The enormous rate enhancements of glycoside hydrolysis achieved by glycosidases cannot be accounted for solely by attack of a nucleophilic carboxylate and acid-catalyzed assistance of aglycone departure. Clearly, the majority of the acceleration arises from a different source. It is now generally accepted that all enzymes derive their tremendous catalytic power from their ability to stabilize the transition state, a theory first put forth in 1946 by Pauling[28]. (A theoretical treatment of transition state stabilization and enzyme catalysis is presented in Appendix I). In glycosidases this would mean that the active site is more complementary in structure to the oxocarbonium ion transition state than the ground state, as evidenced by the tight binding of glucono-(1,5)-lactone.

The importance of individual non-covalent interactions in stabilization of such a transition state has been explored by modification of these interactions through modification of the substrates. In *A. wentii* β-glucosidase, two important non-covalent interactions were identified by use of modified substrates. Roeser and Legler[29] determined that when the C(2) hydroxyl group of glucose is removed and replaced by H, the enzymatic rate of hydrolysis drops by at least a factor of 10^6. Clearly, the interaction of this hydroxyl with a moiety in the enzyme is crucial to transition state stabilization. The C(4) hydroxyl group is also important, with the 4-deoxy substrates being hydrolyzed 10^4 to 10^5 times slower. Similar rate reductions have been observed in *E. coli* β-galactosidase; the hydrolysis of 2-deoxygalactosides is 10^4 times slower than the normal substrates[30]. In lysozyme, Ballardie et al. have studied substrate analogues to determine the importance of the C(6) hydroxyl to catalysis using the substrate analogues shown in Figure 3. Compound 3-b was hydrolyzed by lysozyme at least 1300 times slower than 3-a[31]. This reduction in rate when the CH_2OH group is replaced by H indicates that there must be an energetically favorable interaction between this group and the enzyme in the transition state, most likely a hydrogen-bond.

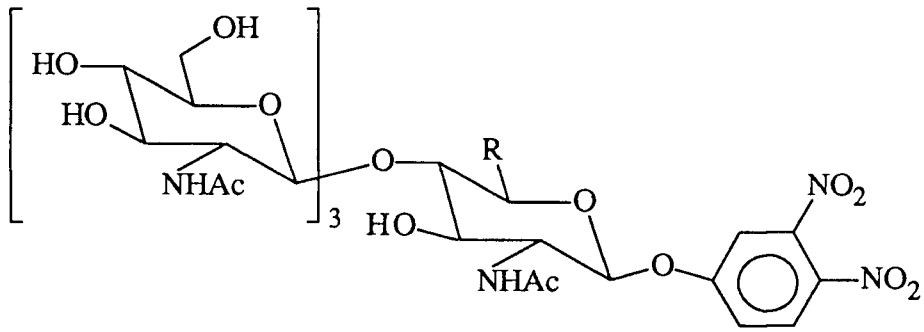

Figure 3. Substrate analogues for lysozyme.

3. *Agrobacterium* β-Glucosidase (ATCC 21400)

The wild-type β-glucosidase from *Agrobacterium** was originally isolated and characterized by Han and Srinivasan[32], and was later reinvestigated by Day and Withers[33]. It was found to have a monomeric molecular weight of 50,000 Daltons, and in its active form exists as a dimer. This enzyme shows a relatively relaxed specificity for glycone and aglycone portions of its substrate. In addition to cellobiose, its natural substrate, it hydrolyzes a variety of β-glucosides, β-galactosides, and β-mannosides with varying efficiencies, as well as glycosyl derivatives with C-F, C-N, and C-S bonds.

The enzyme has been cloned and expressed in high yield in *E. coli*[34]. The clone (pABG-5 β-glucosidase) has been fully characterized and determined to be essentially identical to the wild type in amino acid content and kinetic behavior. The kinetic experimentation described in this thesis was performed with the cloned β-glucosidase.

The amino acid content determined for this enzyme from the DNA sequence has been found to be homologous to only one other β-glucosidase, that from the thermophilic bacterium *Caldocellum saccharolyticum*[35]. The two proteins have greater than 50% identity in their primary sequences.

The catalytic carboxylate residue in pABG-5 β-glucosidase has been identified through affinity labelling as Glu358[7] (Scheme 6, above).

*This bacterium was previously identified as *Alcaligenes Faecalis*.

4. Linear Free Energy Relationships as Mechanistic Probes

4.1. Concepts of Linear Free Energy Relationships

Structure-reactivity relationships are an important tool for elucidating reaction mechanisms. Systematic perturbations in the structure of reactants may affect a reaction process in such a manner as to provide evidence concerning rate-determining-step(s), existence of intermediates, unusual reaction pathways, and other mechanistic features.

A series of changes in reaction conditions (for instance, changing the electronegativity of substituents on a reagent) will nearly always cause a series of changes in the rate or equilibrium position of a reaction. If the same series of changes affects the rate (k) or equilibrium (K) of a second reaction in exactly the same way as it affects the first (except for some constant amount dependent on the second substrate), it is said that a linear free energy relationship exists between the two sets of effects. That is,

$$\log (k_{X,2}/k_{O,2}) = \log (k_{X,1}/k_{O,1}) \times \text{constant} \qquad (1)$$

where k_X refers to the rate for the substituted compound, and k_O to the rate for the unsubstituted compound. (Equilibrium constants, K, can be likewise correlated.) The term "linear free energy relationship" is appropriate because log(k) is related to the free energy of activation and log(K) is related to the standard free energy change of the reaction.

Hammett was the first to attempt to quantify the electronic effects of a given substituent on reaction rates or equilibrium constants. He observed a relationship between the acid strengths of substituted benzoic acids and a number of chemical reactions involving compounds of the type shown in Figure 4, where X is a *meta-* or *para-* substituent, Z is the reacting center, and Y is a side chain of varying length. For instance, he noted a

correlation between the pK_a's of substituted benzoic acids and the rates of alkaline hydrolysis of identically-substituted ethyl benzoates[36]. (Figure 5).

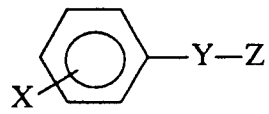

Figure 4. General substrate structure for linear free energy relationship analysis.

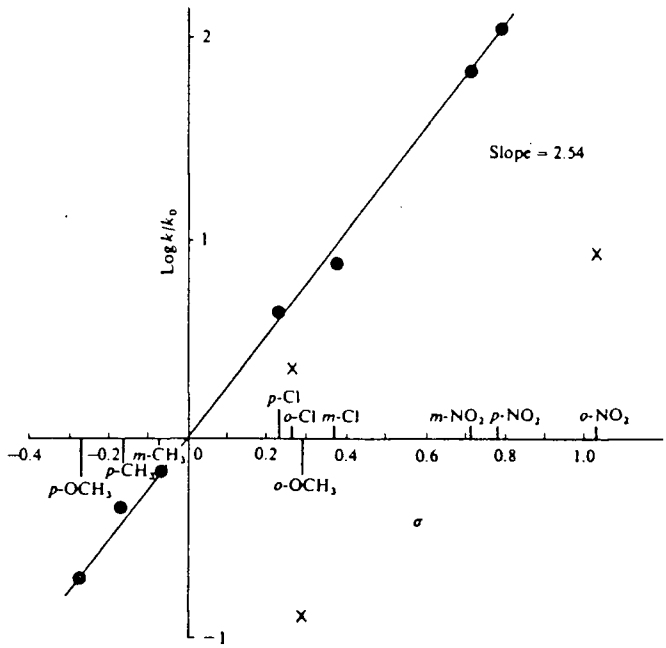

Figure 5. Hammett plot of alkaline hydrolysis of substituted ethyl benzoates[36].

Hammett postulated that, in the absence of steric and proximity considerations, the effects of resonance and induction of a particular group should be essentially constant over a wide spectrum of reaction types. This observation led to the postulation of the Hammett equation:

$$\log \left(\frac{k_x}{k_o}\right) = \rho\sigma \qquad (2)$$

where k_x is the rate constant of the substituted compound and k_o that for the unsubstituted compound. The parameter ρ is the "reaction constant", and is determined by the nature of the reaction and its conditions (solvent, catalyst, temperature). It is independent of substituent. The parameter σ is the substituent constant, and does not vary with reaction type. (Specific exceptions will be discussed below.) The numerical values of ρ and σ are defined by selection of a reference reaction, chosen by Hammett to be the ionization of unsubstituted benzoic acid. This reaction is arbitrarily assigned a reaction constant $\rho = 1$, and $\sigma = 0$. σ values can then be determined for a series of substituent groups by measuring the acid dissociation constant of the appropriately-substituted benzoic acid. Table 3 gives a sampling of σ values for common substituent groups. By convention a positive σ value indicates an electron-withdrawing group and a negative σ value indicates an electron-donating group.

Table 3. Substituent Constants for the Hammett Equation[37].

	σ			σ	
Substiutent	*meta*	*para*	Substituent	*meta*	*para*
$N(CH_3)_2$	-0.05	-0.83	SH	+0.25	+0.15
NH_2	-0.04	-0.66	Cl	+0.37	+0.23
OH	+0.12	-0.37	CO_2H	+0.37	+0.41
OCH_3	+0.11	-0.27	$COCH_3$	+0.38	+0.50
CH_3	-0.07	-0.17	CF_3	+0.47	+0.54
$(CH_3)_3Si$	-0.12	-0.07	CN	+0.61	+0.66
C_6H_5	+0.06	-0.01	NO_2	+0.71	+0.78
H	0.00	0.00	$(CH_3)_3N^+$	+0.86	+0.82
SCH_3	+0.15	0.00	$(CH_3)_2S^+$	+1.00	+0.90
F	+0.34	+0.06	N_2^+	+1.76	+1.91

These σ values can be used to determine ρ values for many other reactions. For example, a plot of pK_a of substituted phenols *vs.* σ gives an excellent correlation with a

slope $\rho = 2.21$ (Figure 6). Values of ρ for several common reactions are given in Table 4. The absolute magnitude of ρ can be interpreted as a measure of the susceptibility of the reaction or equilibrium to substituent effects; a large ρ value thus implies a large charge change on going from the ground state to the transition state. The value of ρ is positive for those reactions which are favored by electron-withdrawing groups (e.g. nucleophilic substitution) and negative for reactions enhanced by electron-donating groups (e.g. electrophilic reactions).*

---

*As an explicit demonstration of the free energy relationship between a given reaction and benzoic acid ionization, consider the following:

$$\log (K_X/K_O) = \sigma$$

(K_O and K_X are the equilibrium constants for ionization of benzoic acid and a substituted benzoic acid, respectively), and

$$\log (k_X/k_O) = \rho\sigma$$

(k_O and k_X are rate constants for a related reaction, for example the hydrolysis of benzoate esters.)

Since $$2.303\ RT \log (K) = -\Delta G^o,$$

the difference in free energy of ionization between substituted and unsubstituted benzoic acids (B) is;

$$\Delta G_{X(B)} - \Delta G_{O(B)} = -2.303\ RT\sigma$$

Also, $$2.303\ RT \log (k) = -\Delta G^{\ddagger}$$

so the difference in activation energies between the substituted and unsubstituted species in the related reaction (A) is;

$$\Delta G^{\ddagger}_{X(A)} - \Delta G^{\ddagger}_{O(A)} = -2.303\ RT\sigma\rho$$

Thus,

$$\Delta G^{\ddagger}_{X(A)} - \Delta G^{\ddagger}_{O(A)} = \rho\ (\Delta G_{X(B)} - \Delta G_{O(B)})$$

So, the extent to which the free energy of activation of a particular reaction is altered by adding a substituent X is linearly related to the extent to which the free energy of ionization of benzoic acid is altered by placing that same substituent on the benzene ring.

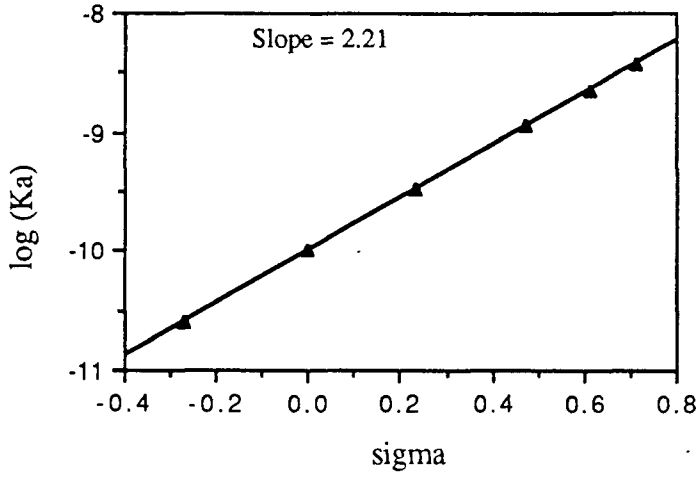

Figure 6. Correlation of phenol dissociation constants with substituent constant[37].

Table 4. Some Typical Reaction Constants[36].

Equilibria		ρ
$XC_6H_4COOH \rightleftharpoons XC_6H_4COO^- + H^+$	(H_2O, 25 °C)	1.00
	(50% aq. C_2H_5OH, 25 °C)	1.60
	(C_2H_5OH, 25 °C)	1.96
$XC_6H_4CH_2COOH \rightleftharpoons XC_6H_4CH_2COO^- + H^+$	(H_2O, 25 °C)	0.49
$XC_6H_4CH_2CH_2COOH \rightleftharpoons XC_6H_4CH_2CH_2COO^- + H^+$	(H_2O, 25 °C)	0.21
$XC_6H_4CH{=}CHCOOH \rightleftharpoons XC_6H_4CH{=}CHOO^- + H^+$	(H_2O, 25 °C)	0.47
$XC_6H_4\overset{+}{N}H_3 \rightleftharpoons XC_6H_4NH_2 + H^+$	(H_2O, 25 °C)	2.77
	(30% aq. C_2H_5OH, 25 °C)	3.44
$XC_6H_4OH \rightleftharpoons XC_6H_4O^- + H^+$	(H_2O, 25 °C)	2.11
$XC_6H_4PO(OH)_2 \rightleftharpoons XC_6H_4PO.OH.O^-$	(H_2O, 25 °C)	0.76
Reactions		
$XC_6H_4COOC_2H_5 + OH^- \rightleftharpoons XC_6H_4COO^- + C_2H_5OH$	(85% aq. C_2H_5OH, 25 °C)	2.54
$XC_6H_4CH_2OCOCH_3 + OH^- \rightleftharpoons XC_6H_4CH_2OH + CH_3COOH$	(60% aq. $(CH_3)_2CO$, 25 °C)	0.47
$XC_6H_4N(CH_3)_2 + CH_3I \rightleftharpoons XC_6H_4N^+(CH_3)_3I^-$	(90% aq. $(CH_3)_2CO$, 35 °C)	−3.30
$XC_6H_4NH_2 + C_6H_5COCl \rightleftharpoons XC_6H_4NHCOC_6H_5 + HCl$	(C_6H_6, 26 °C)	−2.78

In some reactions, certain *para*-substituents deviate from behavior predicted by the Hammett equation. For example, in the ionization of N'-aryl-sulphanilamides (Figure 7),

the *meta*-substituted compounds are well-correlated (open circles), but the *para*-compounds (filled circles) are consistently above the line. Such deviations occur when the substituent is in direct conjugation with a developing charge at the reaction center. This conjugation enhances the electron-donating or -withdrawing effect of the substituent. This has given rise to sets of modified σ constants; σ^+ values apply when a substituent is in conjugation with a positive charge at the reaction center, and σ^- values are used for groups conjugated to a negative charge (also termed σ* by Jaffe[38]) (Table 5). Another proposed σ scale is Taft's σ^o values[39] (or σ^{n}[40] or σ_G[41]), which are valid only when no conjugation is possible.

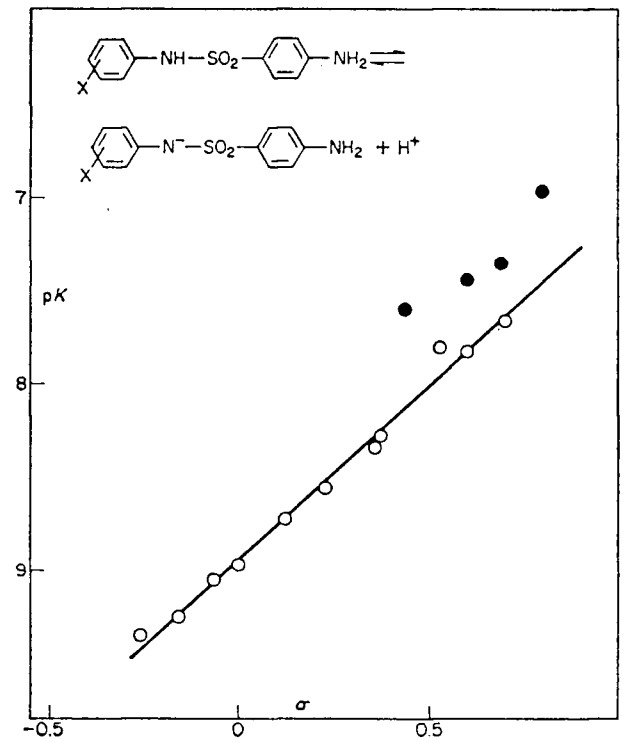

Figure 7. A Hammett plot with deviating para-substiutents due to an electron-rich reaction center; ionization of N-arylsulphanilamides[42].

Table 5. Comparison of σ Scales[43].

Subsituent	σ_{para}	σ^{+}_{para}	σ^{-}_{para}
H	0.00	0.00	0.00
OCH_3	-0.66	-1.30	--
NH_2	-0.27	-0.78	--
CH_3	-0.17	-0.31	--
Cl	+0.23	-0.18	+0.11
$COCH_3$	+0.50	--	+0.84
CN	+0.66	--	+0.88
NO_2	+0.78	--	+1.27
$(CH_3)_3N^+$	+0.82	--	+1.77

Certain substituents may violate the linear relationship no matter which σ constants are used. This is often the result of an interaction with solvent (e.g. ionization, complex formation, chemical reaction), or a change in mechanism with that particular substituent (e.g. intramolecular catalysis). Such deviations must be examined individually.

It has also been noted that substituent effects are additive for polysubstituted compounds[44]. That is,

$$\log(\frac{k}{k_o}) = \rho\Sigma\sigma \qquad (3)$$

Deviations from this ideal behavior are sometimes observed, usually resulting from steric interactions of neighboring substituents[45], or from cross-conjugation[46].

In general, *ortho*-substituted compounds do not correlate well with *meta*- and *para*-substituted reactants. This is usually caused by one or more of the following effects[43]:

1) steric bulk at the reaction center,

2) steric hindrance to coplanarity (i.e. disruption of conjugation),

3) steric inhibition of solvation,

4) hydrogen-bond formation.

Several attempts have been made to devise a general σ_{ortho} scale[37,47] (Table 6). These constants do have some predictive value, but cannot reliably be applied over the same wide range of reactions as σ_{meta} and σ_{para} constants.

Table 6. Apparent σ_{ortho} Constants for Benzoic Acid Ionization[37].

Substituent	σ_o	Substituent	σ_o
CH_3	+0.29	H_3N^+	+2.15
CH_2CH_3	+0.41	OCH_3	+0.12
C_6H_5	+0.74	F	+0.93
CN	+1.06	Cl	+1.28
$CONH_2$	+0.45	Br	+1.35
NO_2	+1.99	I	+1.34

4.2. Use of Linear Free Energy Relationships in Elucidating Reaction Mechanism

In simple reactions and equilibria, for instance hydrolysis of ethyl benzoates, knowledge of reaction mechanisms allows one to make deductions of the sign and size of ρ and σ[36]. This can also be applied in reverse: the ρ value and the type of σ value (i.e. σ, σ^+, or σ^-) necessary for correlation of substituent effects with reaction rates can be used to shed light on the nature of the reaction mechanism. Several characteristics of the data may provide evidence for a mechanism:

1) magnitude and sign of ρ;

2) type of σ values required;

3) concave upward or downward plots;

4) two separate lines for *meta-* and *para-* substituents;

5) no observable correlation.

As stated above, the sign and magnitude of ρ can reveal much about the nature of the transition state. A negative ρ is indicative of an increase in positive charge on attainment of the transition state, while a positive ρ implies increased negative charge. The absolute magnitude of ρ is a measure of sensitivity to electronic substituent effects: a large ρ implies a high sensitivity and therefore a large redistribution of charge on forming the transition state. Also, in general, the closer the reacting center is to the aromatic ring, the larger ρ will be[43].

Hopkinson[48] used ρ values to distinguish between mechanisms for acid-catalyzed hydrolysis of substituted primary and tertiary benzoates. Such hydrolyses were believed to proceed *via* one of two pathways (Scheme 11).

$A_{Ac}1$ $A_{Al}1$

Scheme 11. Two possible mechanisms of acid-catalyzed ester hydrolysis.

The first mechanism should be enhanced by electron-donating groups (ρ negative), while electron-withdrawing groups should facilitate the second mechanism (ρ positive). Indeed, Hopkinson found that the ρ value for the hydrolysis of methyl benzoates is -0.825, and for isopropyl benzoates is +1.991. This is quite reasonable, since the release of an alkyl cation in the $A_{Al}1$ pathway makes it unlikely that the methyl benzoate would hydrolyze *via* that route.

Further conclusions can be drawn about a mechanism based on the kind of σ values required to correlate the rate or equilibrium data. For instance, if a better correlation is seen using σ^+ values than by using σ values, the mechanism likely proceeds *via* an electron-deficient transition state which can be in direct conjugation with *para*-substituents. For example, White and Fife[49] observed a good $\rho\sigma^+$ correlation for the Claisen rearrangement

of substituted cinnamyl-*p*-tolyl ethers, and reasoned that the reaction is probably not concerted, but that there is substantial charge separation at the transition state (Scheme 12).

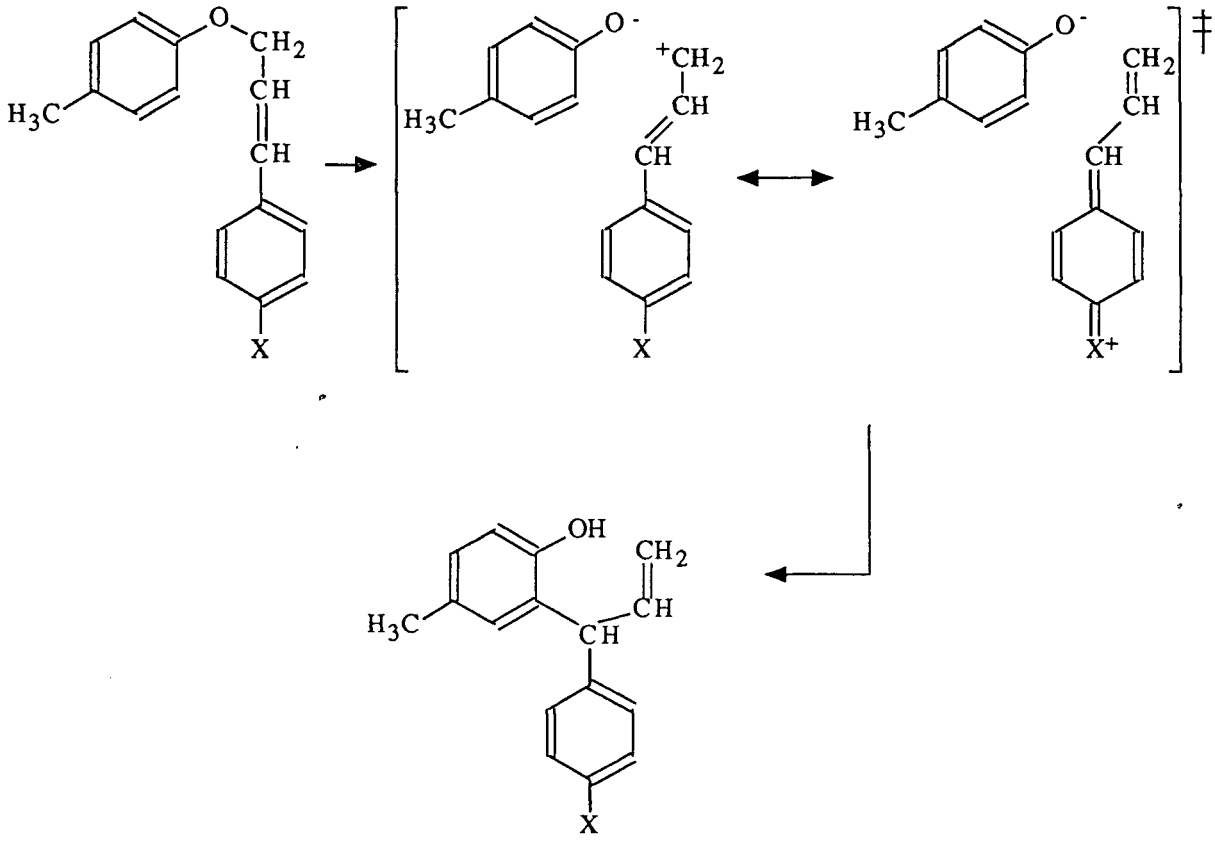

Scheme 12. Claisen rearrangement of X-cinnamyl-p-tolyl ethers[49].

There are several non-linear patterns often observed in Hammett plots which can provide important clues to reaction mechanism. First, a plot of the data may be concave upward (and in the extreme case show a minimum) as demonstrated in Figure 8. This effect arises when a substrate S can yield product P by two different pathways[36]:

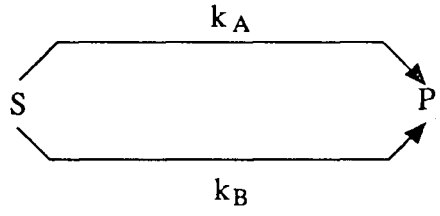

The overall $k_{obs} = k_A + k_B$. If reaction A is favored by electron-donating groups and path B by electron-withdrawing groups, the reaction mechanism will change as σ increases.

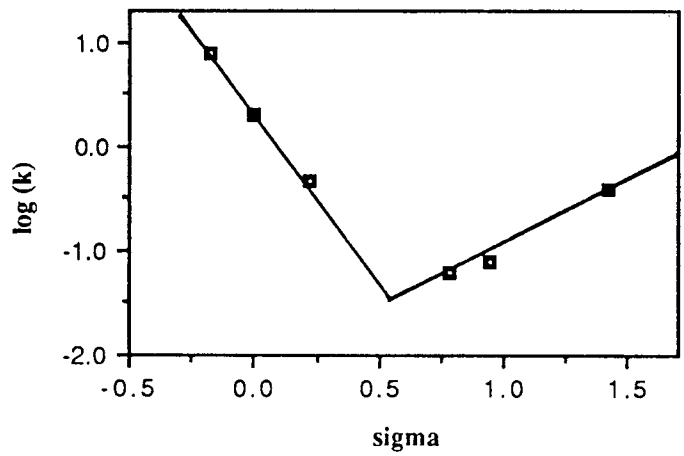

Figure 8. Concave upward Hammett plot due to change in reaction mechanism; hydrolysis of ethyl benzoates in concentrated strong acid[50].

A second case involves a concave downward Hammett plot, which may in the limiting case exhibit a maximum. This type of plot generally arises from a multistep reaction, and indicates a change in rate-determining-step as the electronic nature of the substituent changes. Figure 9 depicts a Hammett plot for the reaction of substituted benzaldehydes and *n*-butylamine (Scheme 13).

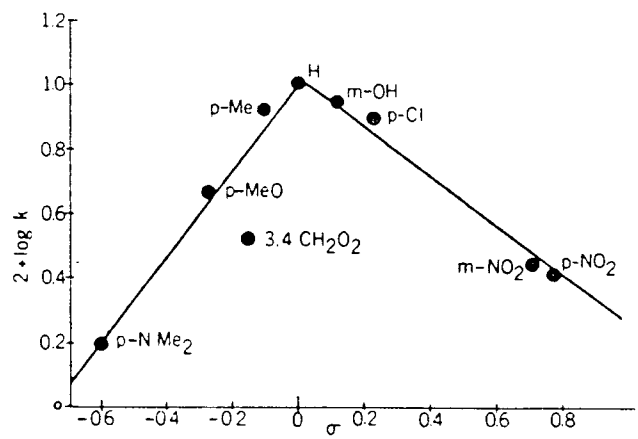

Figure 9. Concave downward Hammett plots due to change in rate-determining-step; reaction of substituted benzaldehydes with n-butylamine[50].

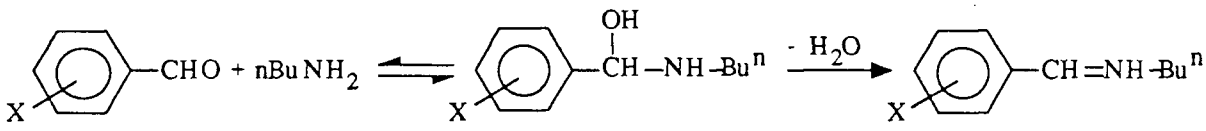

Scheme 13. Reaction of benzaldehyde and n-butylamine.

As the substituent becomes more electronegative, the rate-limiting reversible combination of aldehyde and amine becomes faster, until dehydration becomes the rate-determining-step, around $\sigma = 0$. The dehydration step is facilitated by electron-donating groups, so now as σ continues to rise, the rate decreases.

The two other cases of nonlinearity, segregation of *meta* and *para* substituents (Figure 10A) and random scatter (Figure 10B) cannot be explained as simply as the concave plots[42]. Interpretations of such data are generally unique to the particular experiment.

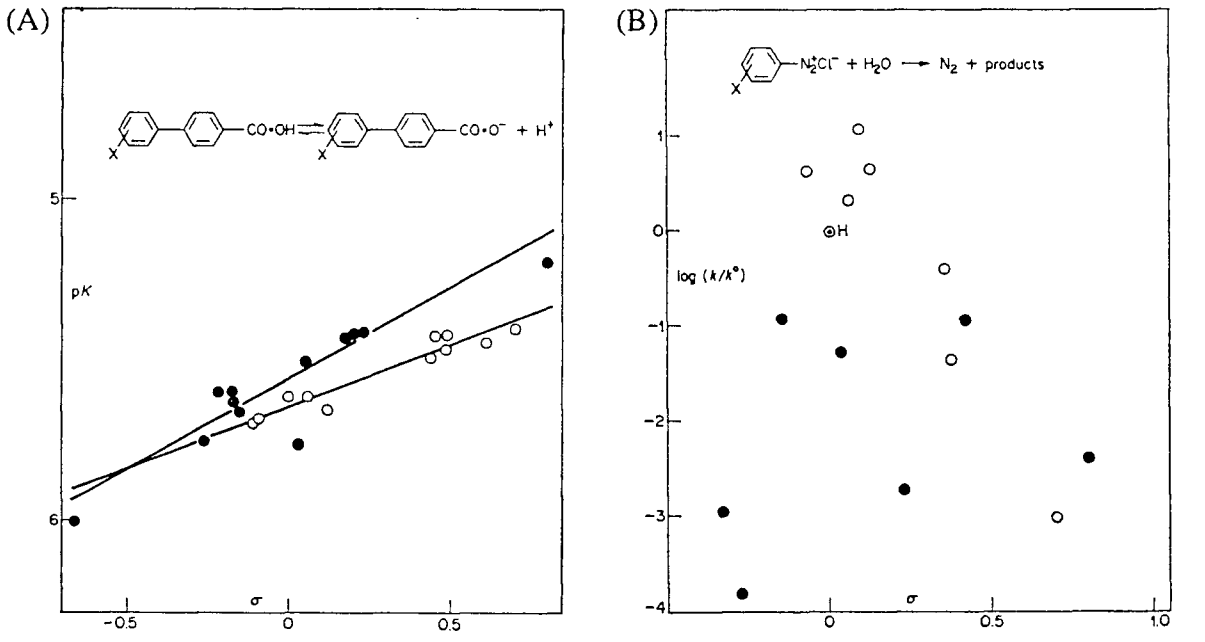

Figure 10. (A). Segregation of meta- and para-substituents in Hammett correlation; ionization of 3'- and 4'-substituted biphenyl-4-carboxylic acids. (B). No observable correlation; decomposition of arenediazonium chlorides in water[42].

4.3. Linear Free Energy Relationships in Enzymology

The primary objective of investigating structure-reactivity relationships in enzymology is the determination of reaction mechanism, and detailed information on the nature of interactions of an enzyme with its substrates may be obtained by correlating structural changes in the substrate with the activity of the enzyme. If the Hammett principles discussed above apply equally well to enzyme substrates with aromatic groups, one should be able to gain insight into the catalytic mechanism by studying the effects of electronic substitution on rates. However, it is usually not this straightforward, since all enzymatic reactions involve at least two steps (i.e. binding and catalysis) which may respond in very different ways to structural alterations in the substrate. Substituent groups interact with the binding site of the enzyme in very specific ways, thus substrate modifications may affect both the enzyme-substrate dissociation constant (K_m) and the precise spatial orientations of the catalytic group(s) and reactive bond(s) of the substrate[51]. The inductive effects of substituents are often obscured by these binding effects. Also, many enzymes are quite specific with regard to substrate, and therefore cannot accommodate the structural changes necessary for linear free energy analysis. Despite these limitations, however, strong mechanistic evidence can often be obtained through structure-reactivity studies with enzymes. These studies have proved most useful when considered in conjunction with additional evidence from other kinds of experiments.

The three enzyme classes most extensively investigated through structure-reactivity studies are glycosyltransferases[52], serine proteases (e.g. chymotrypsin[53]), and acyl transferases (e.g. acetyl-Coenzyme A:arylamine N-acetyltransferase[54]). This work will focus on the first of these, the glycosyltransferases.

Glycosyl transfer enzymes provide an excellent system for structure-reactivity studies since a number of these enzymes are quite reactive toward a large range of aryl α- and β-glycosides. The pioneering investigation of this type was that carried out by Nath and Rydon in an extensive study of the hydrolysis of substituted phenyl β-glucosides

catalyzed by sweet almond β-glucosidase[52]. They measured V_{max} and K_a (= $1/K_m$) for hydrolysis of a series of 21 *ortho*-, *meta*-, and *para*-substituted compounds, and correlated the kinetic parameters against σ values for the phenyl substituents (Figure 11).

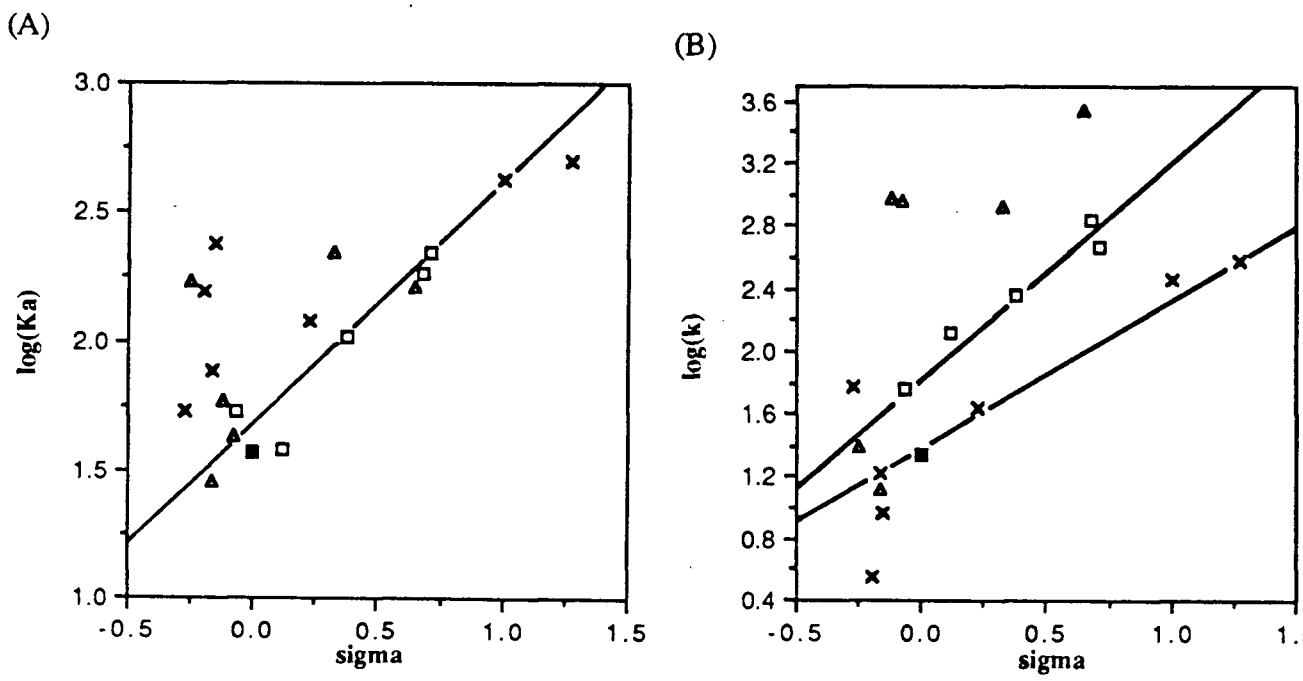

Figure 11. Hammett correlations for almond β-glucosidase-catalyzed hydrolysis of substituted phenyl glucosides. (A). log(Ka) vs. σ. (B). log(rate) vs. σ.
■, phenyl glucoside; Δ, *ortho*-substituted phenyl glucosides; ❑, *meta*-substituted phenyl glucosides; x, *para*-substituted phenyl glucosides. The upper line in (B) represents the best least-squares fit for the *meta*-substituted compounds; the lower line is the best fit for the *para*-substituted compounds[52].

The equilibrium constants, K_a, correlated fairly well with σ (Figure 11A); however, some notable deviations, particularly the greatly enhanced binding of the *p*-Pr^i and *p*-Bu^t derivatives, indicate that steric interactions may be at least as important as electronic effects on the stability of the enzyme-substrate complex.

Several characteristics are apparent in the correlation of reaction rate with σ (Figure 11B). First, the rates of hydrolysis of the *ortho*-substitued compounds showed no clear

trend with regard to σ. However, within the *meta*- and *para*-groupings, rates generally increased with increasing σ, indicating that the reaction is facilitated by electron-withdrawing groups. The *m*- and *p*-substituted compounds are segregated into two separate lines of similar slope, ρ ~ 1.2, suggesting a significant amount of charge buildup at the transition state. The authors propose that the separation of the compounds into two lines results from steric differences between the *m*- and *p*-substituted phenyl glucosides. The *p*-Pr^i and *p*-Bu^t derivatives again deviate substantially, being hydrolyzed quite slowly relative to the other substrates.

This study of almond β-glucosidase was extended by Dale et al. to include phenyl β-glucosides with leaving group pK_a's less than 7[19]. (The most acidic leaving group in Nath and Rydon's study, 4-nitrophenol, has a σ of +1.27, corresponding to a pK_a of 7.18*). Upon plotting their data along with Nath and Rydon's, they observed a break in the curve occurring near pK_a 7 (Figure 12). Below this pK_a, differences in leaving group ionizability have essentially no effect on V/K.

These results strongly suggest the presence of a covalent glucosyl-enzyme intermediate in the β-glucosidase reaction (see Scheme 3, mechanism of a retaining β-glucosidase). For the slower substrates (higher leaving group pK_a's), formation of this covalent intermediate is rate-limiting, and this is reflected in the good correlation between rate and pK_a. As pK_a decreases, however, deglycosylation of the enzyme becomes the rate-determining step, and this is of course independent of aglycone structure. This also points out that linear free energy studies can provide strong evidence for the existence of intermediates in enzyme reactions.

---

*For substituted phenols, $pK_{a,x} = pK_{a,H} - (2.21)\sigma$, and $pK_{a,H} = 9.99$.

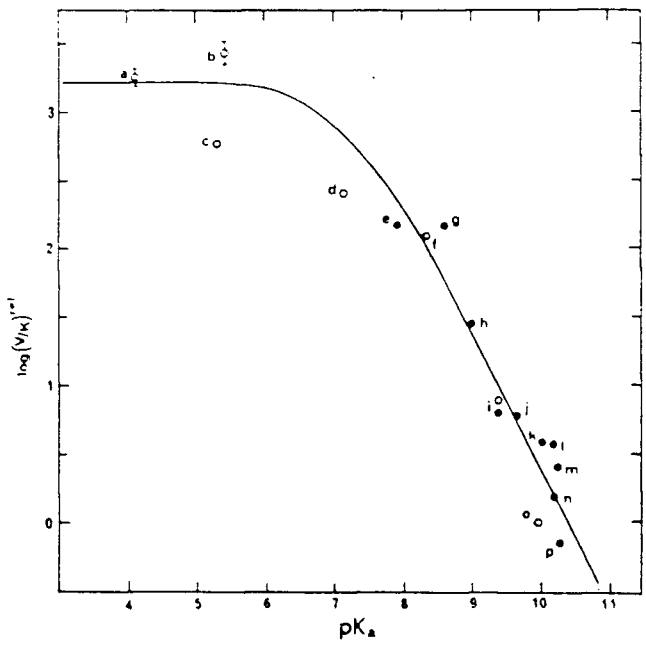

Figure 12. Correlation of log(V/K) with σ for almond β-glucosidase-catalyzed hydrolysis of substituted phenyl glucosides.[19]

The results from linear free energy studies on several glycosidase systems are summarized below (Table 7). A particular point of interest in these data is the difference between hydrolysis of aryl O-glycosides and glycosyl pyridinium salts by *A. wentii* β-glucosidase. The aryl glycosides show little relationship between $\log(k_{cat})$ and leaving-group pK_a, while the pyridinium salts exhibit a strong correlation. Similar results have been noted with *E. coli* β-galactosidase. In the case of β-glucosidase, where cleavage of the C-O or C-N bond is known to be rate-limiting, Legler et al. hypothesized that there is extensive proton donation to the leaving group oxygen of phenyl β-glucosides. This results in minimal buildup of negative charge on the leaving group at the transition state, and thus the electronic nature of substituents on the phenyl ring is of little consequence. Proton donation to the pyridinium leaving group is not structurally possible; hence there is significant charge change on the nitrogen at the transition state, and $\log(k_{cat})$ shows a good correlation with leaving group ability. This study demonstrates another application of enzymatic linear free energy studies, i.e. that they can provide evidence for general acid and general base catalysis.

Table 7. Reaction Constants for Hydrolysis of Substrates by Several Glycosidases.

Enzyme	Substrate series	Parameter correlated	ρ
β-glucosidase (sweet almond)	phenyl β-glucosides	K_m[52]	1.31
		V_m[52]	1.16
		V/K[19]	2.13 ($pK_a > 7$)
			0 ($pK_a < 7$)
(*Asperigillus wentii*)	phenyl β-glucosides	k_{cat}[15]	0.11 (± 0.11)
	β-glucosyl pyridinium salts	k_{cat}[15]	2.11
β-galactosidase (*E. coli*)	phenyl β-galactosides	k_{cat}[55]	*
		k_{cat}/K_m[55]	*
	β-galactosyl pyridinium salts	k_{cat}[14]	2.05
Lysozyme	phenyl β-di-(N-acetylchitobiosides)	k_{cat}[56]	1.20

* No significant correlation; data were greatly scattered, with correlation coefficients of -0.64 (k_{cat}) and -0.61 (k_{cat}/K_m).

In summary, linear free energy analysis of enzymatic reactions can provide evidence regarding:

1) rate-determining-step of the reaction

2) charge distribution at the transition state

3) effects of substrate modification on binding

4) existence of reaction intermediates

5) general acid/general base catalysis.

5. Isotope Effects as Transition State Probes

Isotope effects are very powerful probes of reaction mechanism since they provide insight into the bonding changes which occur during the course of a reaction. A major advantage of studying isotope effects is that the uncharged neutrons of isotopically different compounds do not affect the electronic nature of the transition state. This is particularly important in enzymatic studies, since enzymes are very sensitive to changes in the electronic nature of the substrate. In this regard, isotopic substitution is superior to other substrate modifications which may perturb the true enzymatic mechanism[57]. Isotopic substitutions also do not alter the binding orientation of the substrate in the enzyme active site. While many types of substrate modification can allow one to distinguish between proposed mechanisms through differences in rate, it is very difficult to determine the effect which the modification has on substrate binding. Determining K_m may give an indication of how well or poorly the modified substrate binds, but gives no clue to possible differences in binding orientation between native and modified substrates. This can be significant in enzymes which have one or more nonproductive binding modes in addition to their productive mode (e.g. lysozyme, β-glucosidase)[57].

α-Secondary kinetic isotope effects have been used extensively in studies of reaction mechanism in glycosyl transfer reactions. The magnitude of these effects is usually interpreted as indicating the amount of rehybridization occurring on proceeding from the reactants to the transition state. In general, k_H/k_D values from 1.10 to 1.25 are indicative of a large amount of sp^3 to sp^2 rehybridization in the rate-determining-step, while a mechanism involving little or no change in hybridization would show a k_H/k_D close to unity[16]. However, the validity of extending this to distinguishing S_N1 from S_N2 reactions of acetals (e.g. sugars) has been questioned[58]. Therefore, one must use caution when making mechanistic conclusions based solely upon kinetic isotope effects. (For a general discussion of the origin and interpretation of isotope effects, see Appendix II).

As noted by Dahlquist et al.[57], care must also be taken in interpreting the absence of an isotope effect. While a k_H/k_D value of 1.00 may indicate no hybridization change on approaching the transition state, there are other possible explanations, including a rate-limiting conformational change[55] (see below).

Table 8. α-Secondary Kinetic Isotope Effects of Several Glycosidase-Catalyzed Reactions.

Enzyme	Substrate	Temperature	k_H/k_D
β-glucosidase	4'-nitro-PG*	30°C	1.121
(*S. atra*)[16]	4'-methoxy-PG	"	1.122
	4'-methyl-PG	"	1.114
	4'-nitro-PX*	"	1.154
(almond)[57]	PG	25°C	1.015
(*A. wentii*)[15]	4'-nitro-PG	35°C	1.08
β-galactosidase	2',4'-dinitro-PGal*	30°C	1.25
(*E. coli*)[55]	4'-bromo-PGal	"	1.00
	4'-nitro-PGal	"	1.04
	3'-nitro-PGal	"	1.16
Lysozyme (hen egg white)[57]	NAG-PG*	40°C	1.11

*PG ≡ phenyl glucoside, PX ≡ phenyl xyloside, PGal ≡ phenyl galactoside, NAG ≡ N-acetylglucosamine

A sampling of α-secondary kinetic isotope effects for several glycosidase enzymes is found in Table 8. On inspection, one sees that the isotope effects vary widely, both between and within enzyme systems. For instance, *S. atra* β-glucosidase showed no change in k_H/k_D with substrate variation. Van Doorslaer has suggested that this indicates rate-limiting deglycosylation (hydrolysis of the glycosyl-enzyme intermediate), a step

which would be insensitive to the identity of the aglycone[16]. Sinnott and Souchard have postulated that their very low isotope effects are indicative of a rate-limiting change in conformation of the enzyme-substrate complex[55]. They also offer this as an explanation of the small isotope effect of almond β-glucosidase-catalyzed hydrolysis of phenyl glucoside. Dahlquist, however, attributes this to an associative mechanism with little or no change in hybridization at the transition state[57].

Rosenberg and Kirsch have attempted to circumvent the ambiguity of α-secondary deuterium isotope effects by measuring the primary ^{18}O leaving group isotope effect for reactions catalyzed by almond β-glucosidase[59]. They found an $^{16}O/^{18}O$ isotope effect value for hydrolysis of 4'-nitrophenyl β-D-glucopyranoside equal to 1.038 ± 0.006, corresponding to 89±14% C-O bond cleavage at the transition state. This evidence argues against a rate-limiting conformational change, since such a change would not be sensitive to isotopic substitution. Based on the α-secondary deuterium kinetic isotope effect, and other evidence supporting nucleophilic involvement at the transition state (e.g. observation of a burst of 4-nitrophenolate ion released at low temperature), Rosenberg has suggested an "exploded" transition state structure with minimal rehybridization at C(1) (Scheme 14).

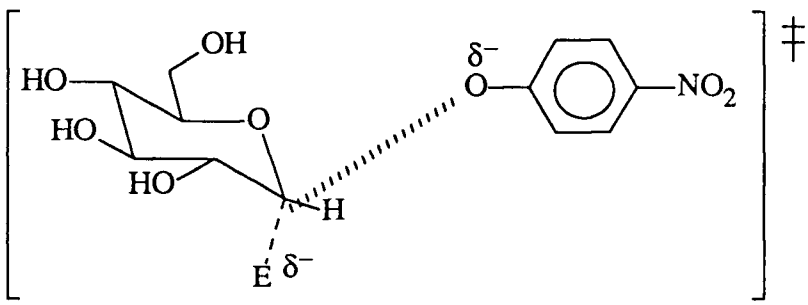

Scheme 14. Transition state structure of glucoside hydrolysis[59].

6. Modified Sugars as Transition State Probes

The earlier linear free energy discussion describes the insights which can be gained into the mechanism of glycosyl transfer enzymes through changes in the glycoside leaving group. Additional information regarding these mechanisms can be obtained from structural modification of the glycone, or sugar, portion of the substrate. Specifically, such modifications can provide evidence for:

1. specific interactions between the sugar ring and the enzyme active site, and

2. the electronic nature of the transition state.

Changes in the glycone must, of course, be sterically quite conservative, to avoid large repulsive interactions within the enzyme active site. The only substitutions for a sugar hydroxyl group which do not introduce possible repulsions are hydrogen and fluorine (Table 9).

Table 9. Comparison of Size of Several Functional Groups[60].

Group	Bond Length (A)	Van der Waals Radius (A)	Total (A)
C-H	1.09	1.20	2.29
C-F	1.39	1.35	2.74
C-O(H)	1.43	1.40	2.83
C-OH	1.43	2.10	3.53

Deoxy- and deoxyfluoro-sugars are particularly important to the study of glycosyl transfer mechanisms because they provide a useful means for investigating the interactions between enzyme and substrate. Recall that non-covalent interactions of the enzyme with its substrate at the transition state are suggested to be responsible for most of the rate enhancement of the enzymatic reaction[61]. In glycosyl transferases, this non-covalent stabilization is believed to arise primarily from hydrogen-bonding between the enzyme and

the glycone hydroxyl groups. Now consider the hydrogen-bonding capability of the series of hydroxy-, deoxy-, and deoxyfluoro-compounds. (In a hydrogen-bond, the functional group which contains the interacting hydrogen atom is called the "donor", and this hydrogen interacts with the lone-pair electrons of the "acceptor" atom, e.g. F, N, O.) The hydroxyl group of the natural sugar can both donate and accept a hydrogen-bond, while the hydrogen of the deoxy-sugar cannot participate at all in significant hydrogen-bonding. The fluorine of the deoxyfluoro-sugar cannot donate a hydrogen-bond, but could act as an acceptor (albeit probably a weaker acceptor than oxygen, since fluorine's lone pair electrons are more tightly held by the nucleus). Therefore, if a hydrogen-bond exists between the enzyme and a particular hydroxyl of the substrate, the enzyme should show a markedly decreased affinity for the corresponding deoxy analogue, where no such interaction is possible. The corresponding deoxyfluoro analogue can provide evidence on the polarity of the hydrogen-bond as follows. If the substrate hydroxyl is the donor, then this hydrogen-bond will be lost in the complex with the fluorinated sugar, resulting in poor binding. If, however, the sugar accepts the hydrogen-bond, the fluorine can still participate, and the deoxyfluoro analogue may bind with a similar affinity to that of the normal sugar. This has been probed in detail in the enzyme glycogen phosphorylase, which catalyzes the reversible phosphorolysis of glycogen to produce α-D-glucopyranosyl phosphate (glucose-1-phosphate, or G1P) (Scheme 15).

$$(\text{glycogen})_n + P_i \rightleftharpoons \text{glucose-1-phosphate} + (\text{glycogen})_{n-1}$$

Scheme 15. Reaction catalyzed by glycogen phosphorylase.

Withers and co-workers investigated glycogen phosphorylase binding interactions with deoxy- and deoxy-fluoro-glucose analogues[62] (glucose is known to bind as an inhibitor to an inactive form of the enzyme). The strength and polarity of hydrogen-bonds to each of the glucose hydroxyls were determined from the differences in the affinity of the enzyme

for the various inhibitors, and it was found that the strongest enzyme-sugar interactions occurred at the 3 and 6 positions, with estimated hydrogen-bond energies of 3.2 and 2.6 kcal/mol, respectively. A weaker interaction of 1.5 kcal/mol was identified at the 4 position.

This work was extended to investigate the effects of deoxy and deoxyfluoro modifications on transition state stabilization. Since better stabilizing interactions at the transition state lead to greater rate enhancement, it was proposed that, on the basis of the hydrogen-bonding capabilities of the various sugars, the deoxyfluoro compounds should generally be better substrates than the deoxy analogues, although both will probably be slower than the natural substrate. Further, the difference in affinities of the analogues versus the natural sugar can provide an estimate of the effective strength of the hydrogen-bonds at each position at the transition state.

Replacement of the sugar hydroxyl by hydrogen or fluorine will also produce differences in the intrinsic electronic nature of the transition state, and will thus affect the relative rates of reaction of the deoxy and deoxyfluoro analogues. Glycoside hydrolysis is slowed by nearby electron-withdrawing substituents on the sugar ring, since these destabilize the positive charge which is generated at the anomeric center of the transition state. On this basis, the order of hydrolysis rates should be deoxy > hydroxy > deoxyfluoro. (This is different from the relative rates predicted from the above analysis of binding, i.e. hydroxy > deoxyfluoro > deoxy). In reality the effects will both be in operation during hydrolysis, and it is difficult to quantify them individually.

In order to investigate the effects of glycone substitution on binding and catalysis, a series of deoxy- and deoxyfluoro-α-D-glucopyranosyl phosphates was synthesized, and each compound tested as a substrate for rabbit muscle glycogen phosphorylase[63]. The reaction (see Scheme 16, above) is believed to proceed via a double displacement mechanism similar to that for a retaining α-glucosidase, with a glucosyl-enzyme

intermediate (of uncertain nature), and an oxocarbonium-ion-like transition state. The kinetic data are presented in Table 10.

Note that the deoxyfluoro compounds react 3 to 40 times slower than the deoxy analogues. This provides excellent evidence for oxocarbonium character in the transition state, since these differences can only be explained by the electron-withdrawing effect of fluorine, which destabilizes the positive charge: binding effects alone cannot account for this rate decrease. Also, a good linear free energy correlation was found between $\log(V_{max})$ of the enzyme catalyzed process and log(k) of the acid-catalyzed hydrolysis of these same compounds[63]. Since the acid-catalyzed process is known to proceed *via* an oxocarbonium-ion intermediate, this further supports the proposal that the enzymatic transition state carries substantial positive charge.

Table 10. Kinetic Parameters for Glycogen Phosphorylase-Catalyzed Hydrolysis of α-D-Glucopyranosyl Phosphate (G1P) Analogues[63].

Compound	$V_{max}/K_m \times 10^{-4}$ (L/min/mg enzyme)	$\Delta\Delta G^{\ddagger}$ (kcal/mol)
G1P	187500	--
2-fluoro G1P	1.08	7.3
3-fluoro G1P	2.2	6.8
4-fluoro G1P	37	5.1
6-fluoro G1P	0.26	8.1
2-deoxy G1P	n.d.	n.d.
3-deoxy G1P	5.8	6.3
4-deoxy G1P	400	3.7
6-deoxy G1P	11.1	5.9

$\Delta\Delta G^{\ddagger}$ represents the difference in activation free energies of enzyme-catalyzed reaction of glucose-1-phosphate and the respective analogue (calculated from Equation 4).

A minimum estimate of the hydrogen-bond strength at each position can be calculated from V_{max}/K_m values for the deoxy sugars. Since electronic effects due to

removing the electronegative oxygen should accelerate the reaction relative to the parent sugar, any decrease in rate relative to α-D-glucopyranosyl phosphate must arise solely from poorer binding interactions at the transition state. The corresponding increases in activation energy, $\Delta\Delta G^{\ddagger}$, are presented in Table 10, and have been calculated from Equation 4.

$$\Delta\Delta G^{\ddagger} = RT \ln \frac{(V_m/K_m)_2}{(V_m/K_m)_1} \qquad (4)$$

These values therefore represent minimum estimates of the hydrogen-bond strengths to each hydroxyl in the transition state. The order of bond strengths, 3 > 6 > 4, is consistent with the earlier study of ground state binding of glucose analogues. While the order of bond strengths is the same in both experiments, a comparison of the estimated bond energies reveals that the interactions are substantially larger for the reaction of the α-D-glucospyranosyl phosphate analogues. This is consistent with a basic principle of enzyme catalysis, i.e. that an enzyme should bind preferentially to the transition state rather than the ground state.

The hydrolysis of glycosides by glycosyl transfer enzymes (e.g. lysozyme, β-glucosidase) is believed to proceed *via* a covalent glycosyl-enzyme intermediate, where the transition states for both formation and hydrolysis of this intermediate have substantial oxocarbonium ion character (Scheme 3, mechanism for a β-glucosidase). If this is indeed correct, then according to the electronic effects discussed above, substitution of fluorine for hydroxyl at the C(2) position of a glycoside sugar ring should significantly destabilize the transition state for both steps, thus decreasing the rate of glycosylation and deglycosylation. If a highly reactive leaving group is incorporated into a 2-deoxy-2-fluoroglycoside, it may increase the glycosylation step sufficiently to trap the covalent 2-fluoroglycosyl-enzyme intermediate. This has been shown to be the case in the β-

glucosidase-catalyzed reaction of 2',4'-dinitrophenyl 2-deoxy-2-fluoro-β-D-glucopyranoside, as was described in Section 2.2[12].

It is proposed that substitution of fluorine at the C(2) postion in β-glucosides should perturb the normal mechanism in the following two ways:

1. Increase the S_N2 (concerted) nature of the reaction, since the fluorine destabilizes any oxocarbonium ion character.
2. Slow the hydrolysis of the glucosyl-enzyme intermediate such that the rate of the glucosylation step can be determined, even with highly activated leaving groups.

The extent to which the normal mechanism is altered can be investigated through structure-reactivity studies of substituted aryl 2-deoxy-2-fluoro-glucosides, and by determination of the α-secondary kinetic isotope effect.

7. The Aims of This Study

It was proposed to investigate the mechanism of glucoside hydrolysis by pABG-5 β-glucosidase using the following techniques:

1. Linear free energy correlation -- Determination of the kinetic parameters for hydrolysis of several substituted phenyl glucosides may reveal a relationship between substrate structure and reactivity in this enzyme system, and thus provide evidence concerning the rate-determining step of the reaction and the extent of bond cleavage at the transition state.

2. α-Secondary kinetic isotope effects -- The value of k_H/k_D for enzymic hydrolysis of several substituted phenyl glucosides should provide information on the degree of oxocarbonium-ion character at the transition state. This will give insight into the identity of the rate-limiting step, the degree of bond cleavage at the transition state, and possible preassociation of the enzymic nucleophile.

3. Inactivation by aryl 2-deoxy-2-fluoro glucosides -- The nature of the inactivation of β-glucosidase by the 2-deoxy-2-fluoro compounds offers an unusual opportunity to perform a structure-reactivity study of enzyme inactivation by several substituted phenyl 2-deoxy-2-fluoro glucosides, which may provide evidence for any linear free energy relationship between the inactivator structure and inactivation kinetics. Also, determination of the α-secondary kinetic isotope effect on the inactivation will give further indication of the degree of bond cleavage and amount of rehybridization at the transtion state of the reaction of enzyme with the 2-deoxy-2-fluoro sugars. A comparison of these structure-reactivity and kinetic isotope effect data with the results for the parent glucosides can then provide insight into the nature of the mechanistic changes caused by fluorine substitution at C(2) of the glycone.

CHAPTER II

RESULTS AND DISCUSSION

1. Synthesis

All protected glucosides were synthesized according to the Koenigs-Knorr method from 2,3,4,6-tetra-O-acetyl α-D-glucopyranosyl bromide and the corresponding phenol[64]. In general the yields were low due to a major hydrolytic side reaction giving 2,3,4,6-tetra-O-acetyl D-glucopyranose. The isotopic purity of the C(1)-deuterated glucosides was determined by ^{1}H-nmr spectroscopy, and all were found to have approximately 2% contamination of protio material. This very small contamination does not significantly affect reaction rates.

Glucosides containing leaving groups of high pK_a (> 6) were deacetylated according to the method of Zemplen, using sodium methoxide in dry methanol[55]. This reaction was quite convenient and gave good yields of the free glucoside. Those compounds with leaving groups of low pK_a (< 6) were deprotected using HCl in dry methanol[65]. 2',4',6'-Trichlorophenyl β-D-glucopyranoside was deacetylated using AG1-X8 ion exchange resin (OH^- form), according to a method reported by Reed et al[66]. It was hoped that this would be a more convenient alternative to the HCl deprotection for glucosides with highly activated leaving groups, but the protocol proved not to be generally applicable.

2. Extinction Coefficients

Values of ε for all glucosides and phenols were determined under the standard assay conditions for this study. The assay wavelength was chosen as the point of maximal phenol absorbance, or the point of maximal absorbance difference between phenol and glucoside if the glucoside absorbed significantly at the phenol λ_{max}. The extinction coefficients and assay wavelengths are presented in Table 11.

The glucoside extinction coefficients given are those determined by the method of total enzymic hydrolysis of a glucoside solution of known absorbance (see Methods section 2.2).

Table 11. Extinction Coefficients of Substituted Phenols and Phenyl Glucosides.

Phenol Substituent	Assay Wavelength (nm)	ε_{phenol} x 10^{-3} (M^{-1} x cm^{-1})	$\varepsilon_{glucoside}$ x 10^{-3} (M^{-1} x cm^{-1})
2,4-dinitro	400	10.91	0.000
2,5-dinitro	440	4.295	0.007
3,4-dinitro	400	11.05	0.041
4-chloro-2-nitro	425	3.561	0.015
2,4,6-trichloro	312	3.204	0.468
4-nitro	400	7.280	0.000
2-nitro	400	2.170	0.000
3,5-dichloro	280	1.315	0.583
3-nitro	380	0.478	0.093
4-cyano	270	4.276	1.175
4-bromo	288	1.120	0.440
4-chloro	278	1.344	0.764
β-naphthyl	325	1.473	0.657
H	277	1.063	0.285
4-*t*-butyl	272	1.486	0.761

3. Hydrolysis of Phenyl β-D-Glucosides by pABG-5 β-Glucosidase

Linear free energy studies of several glycosidase systems have demonstrated that structure-reactivity relationships can provide a good deal of insight into the mechanism of catalysis[19,52,56]. In order to investigate the relationship between substrate electronic structure and reactivity in the pABG-5 β-glucosidase system, a Hammett-type investigation was undertaken in which K_m and k_{cat} values for fifteen substituted phenyl glucosides were determined. The enzymic hydrolysis rates were measured by spectrophotometric detection of phenol release, under the standard assay conditions described in Methods section 2.3. The enzyme concentration was adjusted with each substrate to ensure that:

1. a sufficient absorbance change was observed to enable accurate calculation of rate, and
2. the reaction course could be followed for several minutes without exceeding 10% substrate usage, thus ensuring linear dependence of product release *vs.* time.

This was sometimes difficult, particularly with slow substrates and those which have a relatively small difference in extinction coefficient between glucoside and free phenol. In such cases, the linear portion of the reaction was often exceeded, and rates were calculated from the initial slopes of observed phenol release. Substrate concentrations employed ranged from at least one-sixth the value of K_m to six times K_m.

The data so obtained were fitted to the standard Michaelis-Menten equation using the weighted least squares regression computer program Curvefitter, written by I. P. Street for an Apple IIe computer[67], and the constants K_m and k_{cat} were thus determined. The data are presented graphically in Appendix III according to the method of Lineweaver and Burk[68], a convenient format for visual inspection; lines presented on these graphs were obtained by simple linear least squares analysis. This method was not used for calculation of kinetic constants, however, due to errors inherent in the double-reciprocal analysis (i.e. a nonlinear error span[69]). The kinetic constants are given in Table 12.

These rate data were plotted according to Hammett and analyzed for trends which could provide evidence concerning the rate-determining step and possible reaction intermediate. Figure 13 shows a concave downward plot of $\log(k_{cat})$ *vs.* leaving group pK_a; above pK_a 8, $\log(k_{cat})$ shows a linear dependence upon leaving-group ability, while below this point the rate is essentially independent of aglycone structure.

Table 12. Kinetic Parameters for Hydrolysis of β-Glucosides by pABG-5 β-Glucosidase.

Phenol Substituent	pK_a†	k_{cat} (s^{-1})	K_m (mM)	k_{cat}/K_m (s^{-1} x mM^{-1})
2,4-dinitro	3.96	87.9	0.031	2800
2,5-dinitro	5.15	120	0.045	2700
3,4-dinitro	5.36	185	0.033	5600
2,4,6-trichloro	6.39	240	0.0092	26000
4-chloro-2-nitro	6.45	144	0.013	11000
4-nitro	7.18	169	0.078	2200
2-nitro	7.22	111	0.033	3400
3,5-dichloro	8.19	159	0.13	1200
3-nitro	8.39	108	0.19	570
4-cyano	8.49	129	0.21	600
4-bromo	9.34	28.8	0.56	52
4-chloro	9.38	29.6	0.64	46
2-naphthyl	9.51	25.3	0.16	160
H	9.99	5.44	2.12	2.6
4-*t*-butyl	10.37	5.13	0.069	74

†Phenol pK_a values were taken from the following references: 37, 69, 70, 71.

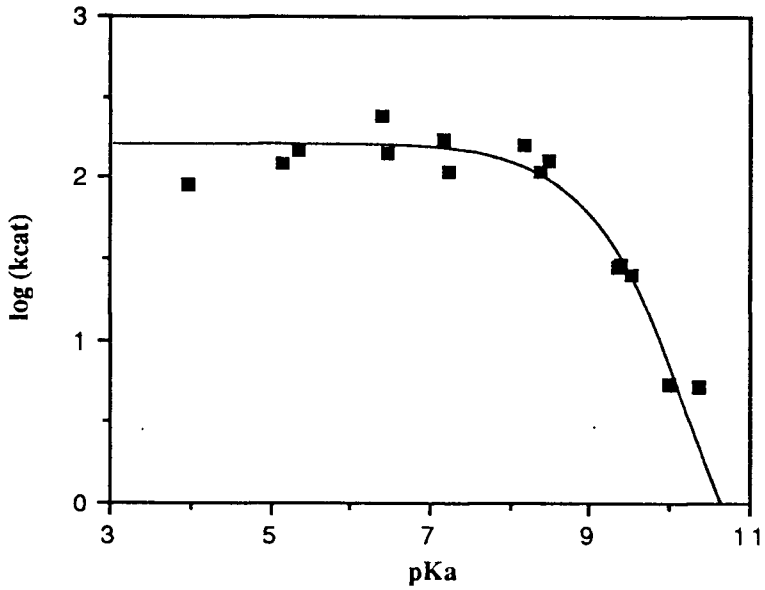

Figure 13. Hammett correlation of rate of glucoside hydrolysis and leaving group pK_a.

Recall that the proposed mechanism for hydrolysis by β-glucosidase involves two distinct catalytic steps (glucosylation and deglucosylation), and that Hammett plots such as that in Figure 13 are indicative of a change of rate-determining step in a multistep reaction[42]. In this case, it appears that, for the faster substrates (leaving group $pK_a < 8$), deglucosylation of the enzyme is rate-limiting, since the rate is independent of the specific electronic nature of the leaving group. Around pK_a 8, glucosylation becomes the rate-determining step. The slope of the line containing the eight points from substrates containing phenols of high pK_a (> 8) is -0.73, corresponding to a Hammett constant ρ = 1.6. This reaction constant is quite comparable to values for similar glycosidase systems; for example, Nath and Rydon observed a ρ value of 1.16 when $\log(V_{max})$ was correlated with σ for hydrolysis of phenyl glucosides by almond β-glucosidase[52], and a similar value of ρ, 1.20, was determined for the hydrolysis of phenyl β-di-(N-acetylchitobiosides) by lysozyme[56].

Although one cannot make specific conclusions about the degree of bond breakage at the transition state based upon the value of ρ, since the amount of proton donation to the departing phenol is not known, such ρ values indicate a large amount of charge separation at the transition state for glycoside hydrolysis[15]. Thus it can be inferred that in the reaction catalyzed by pABG-5 β-glucosidase, cleavage of the sugar-aglycone bond is well advanced at the transition state.

The dependence of $\log(k_{cat}/K_m)$ upon pK_a (Figure 14) shows a concave downward curve quite similar to the $\log(k_{cat})$ data, although there is considerably more spread in the points than in the $\log(k_{cat})$ values. The break point in this curve occurs between pK_a 7 and 8.

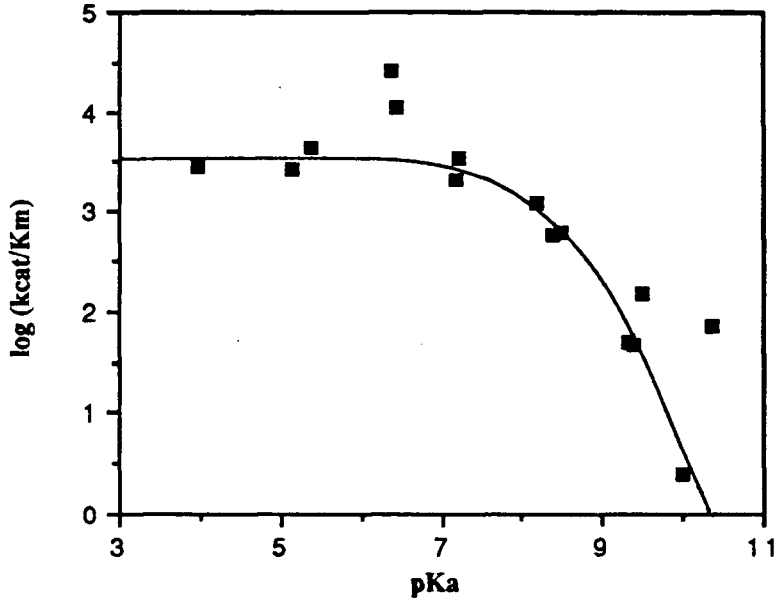

Figure 14. Hammett correlation of log(k_{cat}/K_m) and leaving group pK_a.

The differences between the meanings of k_{cat} and k_{cat}/K_m should be emphasized here. The following discussion will show that k_{cat} is the rate constant for the rate-determining-step of the reaction (the step which contains the highest transition state on the reaction pathway). On the other hand, k_{cat}/K_m will be shown to be the rate constant which reflects the energy difference between the initial ground state (free enzyme and substrate) and the transition state for the first irreversible step of the reaction. Consider the following mechanism:

$$E + S \underset{k_{-1}}{\overset{k_1}{\rightleftharpoons}} ES \underset{k_{-2}}{\overset{k_2}{\rightleftharpoons}} EP \xrightarrow{k_3} E + P$$

This could represent the hydrolysis of β-glucosides by β-glucosidase, in which case ES is the Michaelis complex and EP is the covalent glucosyl-enzyme intermediate. The free energy diagram for this reaction is shown below (the energy levels are arbitrary).

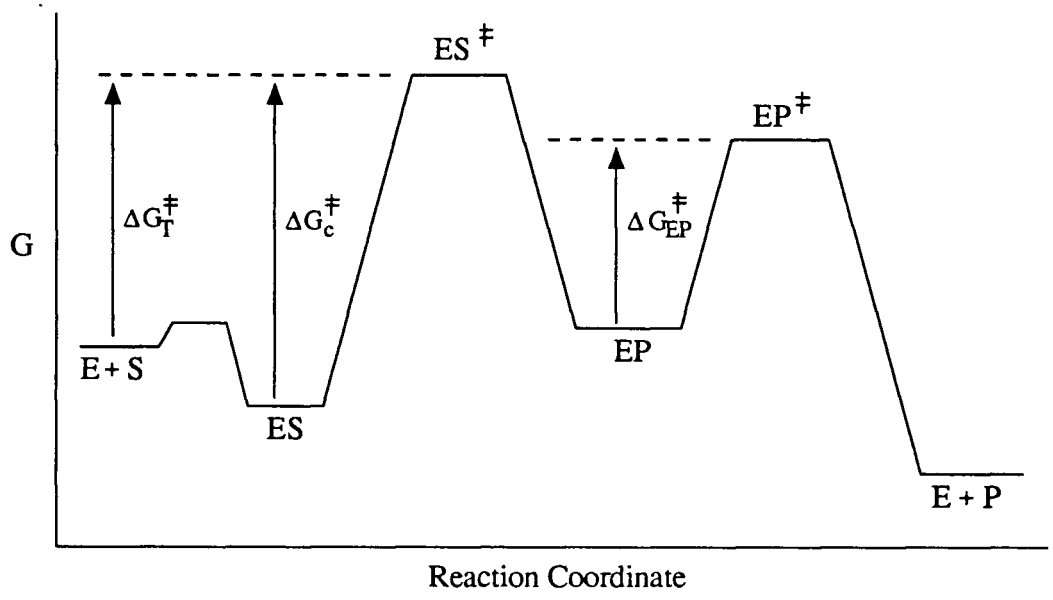

Figure 15. Free energy diagram for an enzymic reaction involving interconversion of intermediate species.

It can be shown that the kinetic parameters for this mechanism are given by:

$$k_{cat} = \frac{k_2 k_3}{k_{-2} + k_2 + k_3} \qquad (5)$$

$$K_m = \frac{k_3(k_{-1} + k_2) + k_{-1}k_{-2}}{k_1(k_3 + k_{-2} + k_2)} \qquad (6)$$

$$k_{cat}/K_m = \frac{k_1 k_2 k_3}{[k_3(k_{-1} + k_2) + k_{-1}k_{-2}]} \qquad (7)$$

The formation of ES will be referred to as the association step, interconversion of ES and EP as the chemical step, and the final step is termed product release.

First consider a reaction wherein there is a *rapid, reversible association*, followed by a *rate-determining irreversible chemical step*. Such is proposed to be the case in this work for the hydrolysis of slow substrates (leaving group $pK_a > 8$), where glucosylation is the rate-determining step. The following kinetic relationships will apply: $k_{-1} \gg k_2$, $k_3 \gg k_{-2}$, and $k_3 \gg k_2$. The rate constants from Equations 5 and 7 are now reduced to:

$$k_{cat} = k_2 \qquad (8)$$

$$k_{cat}/K_m = \frac{k_1 k_2}{k_{-1}} \qquad (9)$$

The Eyring equation relates these rate constants to the energy level differences of the various species on the reaction pathway:

$$k_{cat} = (\mathbf{k}T/h) \exp\{-(G_{ES}^{\ddagger} - G_{ES})/RT \qquad (10)$$

$$= (\mathbf{k}T/h) \exp\{-\Delta G_c^{\ddagger}/RT\} \qquad (11)$$

$$k_{cat}/K_m = (\mathbf{k}T/h) \exp\{-(G_{ES}^{\ddagger} - G_{E+S})/RT\} \qquad (12)$$

$$= (\mathbf{k}T/h) \exp\{-\Delta G_T^{\ddagger}/RT\} \qquad (13)$$

In this case, both k_{cat} and k_{cat}/K_m provide information about the same transition state, $ES^{\ddagger}$, but the initial reference point for k_{cat} is the Michaelis complex, while k_{cat}/K_m refers to free enzyme and free substrate.

Alternatively, the reaction could consist of *rapid reversible association*, followed by an *irreversible chemical step*, then *rate-determining product release*. (This is essentially the kinetic scheme proposed for the hydrolysis of the faster substrates in this study, i.e. rate-limiting deglucosylation). The kinetic relationships in this case are: $k_{-1} \gg k_2$, $k_3 \gg k_{-2}$, and $k_2 \gg k_3$. Applying this to Equations 5 and 7, and converting k_{cat} and k_{cat}/K_m to Eyring form:

$$k_{cat} = k_3 = (\mathbf{k}T/h) \exp\{-(G_{EP}^{\ddagger} - G_{EP})/RT \qquad (14)$$

$$= (\mathbf{k}T/h) \exp\{-\Delta G_{EP}^{\ddagger}/RT\} \qquad (15)$$

$$k_{cat}/K_m = \frac{k_1 k_2}{k_{-1}} = (\mathbf{k}T/h) \exp\{-(G_{ES}^{\ddagger} - G_{E+S})/RT \qquad (16)$$

$$= (\mathbf{k}T/h) \exp\{-\Delta G_T^{\ddagger}/RT\} \qquad (17)$$

Now, k_{cat} and k_{cat}/K_m are associated with different transition states. The value of k_{cat} reflects the transition state for product release (with respect to EP), while k_{cat}/K_m is, as above, the overall rate constant for free enzyme and free substrate proceeding to the transition state of the chemical step, $ES^{\ddagger}$.

It can be further shown that k_{cat} will always be associated with the transition state for the rate-determining step of the reaction, while k_{cat}/K_m will always be the apparent second-order rate constant for free enzyme and free substrate proceeding to the transition state of the first irreversible step on the reaction pathway, regardless of which is the rate-determining step[73].

In light of this discussion, the shape of the graph in Figure 14 is difficult to understand. If glucosylation is considered to be irreversible because the aglycone immediately diffuses away from the active site after cleavage of the glucosidic bond, k_{cat}/K_m should always denote the rate of free enzyme plus free substrate proceeding to the transition state for glucosylation, and the concave-downward plot of $\log(k_{cat}/K_m)$ *vs.* pK_a cannot be simply interpreted as an indication of a change from rate-limiting deglucosylation to glucosylation [as in the plot of $\log(k_{cat})$ *vs.* pK_a]. Indeed, one would expect to see no break in this curve, presuming that the rate of glycone-aglycone bond-fission continues to increase as phenol pK_a decreases. Such results have, however, been found previously in a similar system, almond β-glucosidase, where Dale et al. observed a break in $\log(V_{max}/K_m)$ *vs.* pK_a for enzymic hydrolysis of substituted phenyl glucosides (Figure 12, p. 30), which they have attributed to a change in rate-determining step[19].

There are several alternate hypotheses which may explain these results. First, one can see from Equation 12, above, that k_{cat}/K_m will be lower than expected if free substrate is unusually stable or if the transition state for glucosylation is unusually unstable, or both (increased $\Delta G_T^{\ddagger}$). It is, however, difficult to accept that the stabilities of the reactants or transition state would be changed so drastically as to produce the break seen in the plot in Figure 14.

Another proposed cause of the observed results is that the first irreversible step of the reaction may change as the leaving group pK_a changes. If glucosylation becomes reversible for the fastest substrates, and deglucosylation is rate-limiting, Equation 7 becomes:

$$k_{cat}/K_m = \frac{k_1 k_2}{k_{-1} k_{-2}} k_3 \quad \text{(faster substrates)} \qquad (18)$$

$$= (\mathbf{k}T/h)\ \exp\{-(G_{EP}^{\ddagger} - G_{E+S})/RT\} \qquad (19)$$

The value of k_{cat}/K_m is then the apparent second order rate constant for free enzyme and substrate proceeding to the transition state for deglucosylation. If for the slower substrates glucosylation is still considered to be irreversible,

$$k_{cat}/K_m = \frac{k_1 k_2}{k_{-1}} \quad \text{(slower substrates)}$$

$$= (\mathbf{k}T/h)\ \exp\{-(G_{ES}^{\ddagger} - G_{E+S})/RT$$

Now, k_{cat}/K_m refers to the transition state for the glucosylation step for the slower substrates, and to the deglucosylation transition state for the faster substrates. This change in the first irreversible step of the reaction could result in the observed break in the plot of $\log(k_{cat}/K_m)$ *vs.* pK_a.

The glucosylation step could become reversible for the faster substrates if the phenol does not immediately diffuse away from the active site after cleavage of the glucosidic bond, and two hypotheses can be proposed to account for such an occurrence. First, all of these substrates have one or more highly polar substituents on the phenyl ring, which could perhaps interact strongly with polar groups within the enzyme's secondary binding site. These interactions might hold the phenol within the active site, allowing phenol and sugar to recombine to give the original glucoside. A second possible force that could maintain the phenol within the active site is formation of an ion pair between a negatively charged phenolate ion and positively charged enzyme residue, perhaps the

general acid catalyst. A likely candidate for the general acid in this enzyme is a histidine residue, which in its protonated state bears a positive charge. A histidine has been suggested as the general acid group in other glycosidase systems, e.g. yeast α-glucosidase[27], and also the pK_a of the general acid moiety in pABG-5 β-glucosidase has been determined through pH-activity studies to be approximately 8.5, which is within a reasonable range for a histidine. If the acid group does not donate its proton to the phenolate oxygen during cleavage of the glucosidic bond, the negatively-charged phenolate will be in very close proximity to the positively-charged histidine, and an ion pair may be formed (Figure 16). This hypothesis seems quite plausible for the substrates which exhibit rate-limiting deglucosylation, as these glucosides have leaving-group pK_a's lower than that of the general acid, thus decreasing the likelihood that the proton will be transferred from the acid to the phenolate.

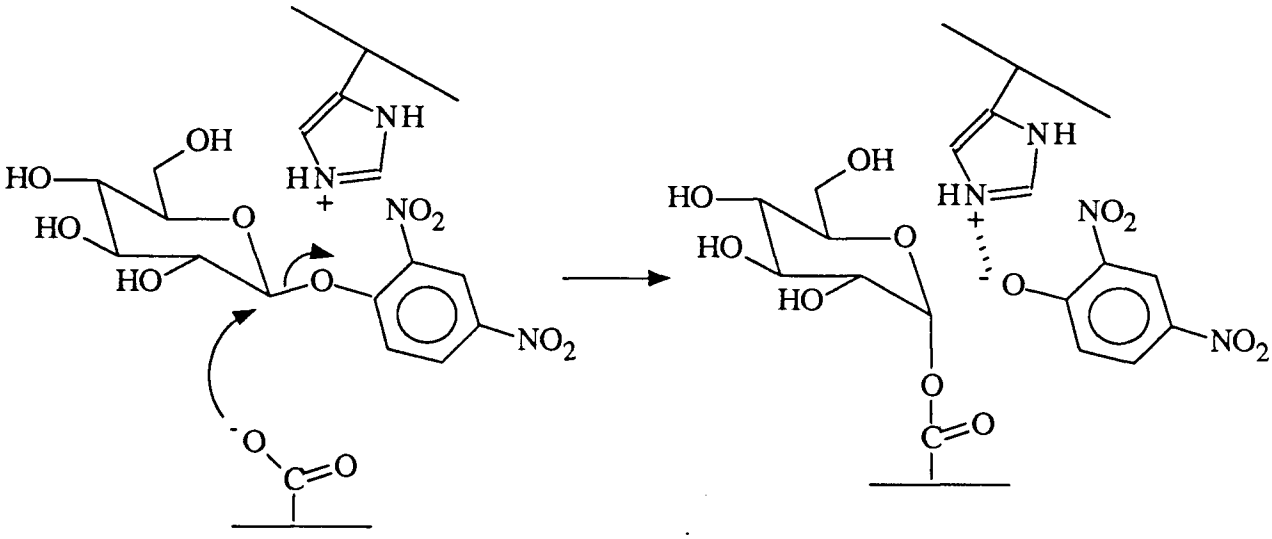

Figure 16. Formation of an ion pair between an enzymic histidine and a dinitrophenolate ion.

In Figure 14, it would appear that three glucosides exhibit substantial positive deviations from the curve of $\log(k_{cat}/K_m)$ vs. pK_a; 2',4',6'-trichlorophenyl β-D-

glucopyranoside (pK_a 6.39), 4'-chloro-2'-nitrophenyl β-D-glucopyranoside (pK_a 6.45), and 4'-*t*-butylphenyl β-D-glucopyranoside (pK_a 10.34). Since k_{cat}/K_m reflects the difference in energy levels between free enzyme and substrate and the transition state for the first irreversible step, a higher than predicted value of k_{cat}/K_m indicates an unusually unstable free substrate, an unusually stable transition state, or both. In 4'-*t*-butylphenyl β-D-glucopyranoside, it is possible that hydrophobic repulsions caused by the large alkyl group make this substrate relatively unstable in the polar buffer medium, thus raising the energy level of free reactants closer to the level of the transition state. 2',4',6'-trichlorophenyl β-D-glucopyranoside has two relatively large substituents *ortho* to the phenol oxygen, and such groups could cause severe steric crowding and thus destabilize the free substrate. Similar deviations with substrates containing large *ortho* groups and/or bulky alkyl substituents have been noted in comparable enzyme systems[52]. In the pABG-5 β-glucosidase system, however, *ortho* substituents on the aryl aglycone do not consistently perturb the system, as evidenced by the plots in Figure 17, which differentiate each data point according to the position of substitution on the phenyl ring. (When the substrate contains a polysubstituted aglycone, it has been classed according to the substitution position closest to the phenol oxygen; for example, 3',4'-dinitrophenyl β-D-glucopyranoside is considered to be *meta*-substituted).

4. α-Secondary Kinetic Isotope Effects on Glucoside Hydrolysis by pABG-5 β-Glucosidase

Use of isotopically-labelled compounds has been shown to be of great value in elucidation of enzyme mechanism, because the normal binding interactions of the substrate are not perturbed by the isotopic substitution. The particularly facile synthesis of 2,3,4,6-

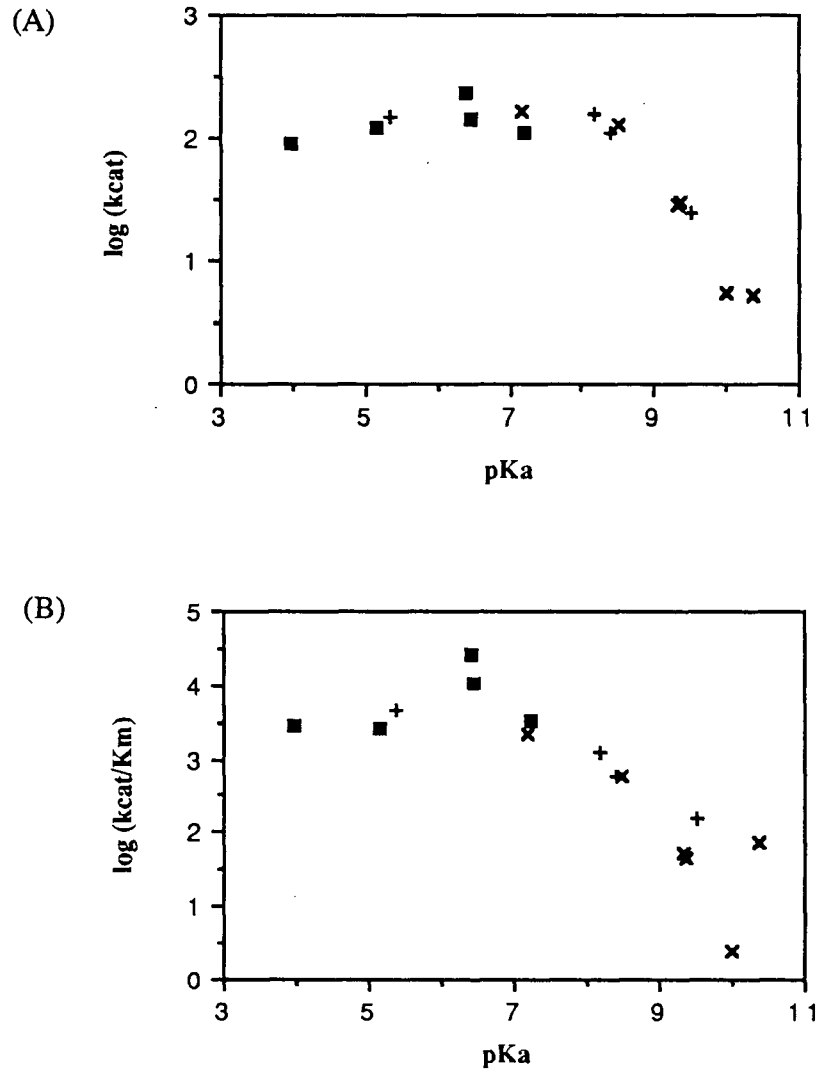

Figure 17. Hammett correlations of hydrolysis of ortho-, meta-, and para-substituted phenyl β-D-glucopyranosides by pABG-5 β-glucosidase.

■, *ortho*-substituted glucosides; +, *meta*-substituted glucosides; x, *para*-substituted glucosides.

tetra-O-acetyl {1-^{2}H}-glucose *via* sodium borodeuteride reduction of 2,3,4,6-tetra-O-acetyl glucono-(1,5)-lactone[74] provides an easy route to the C(1)-deuterated phenyl glucosides, and thus it is possible to determine the effect of deuterium substitution on glucoside hydrolysis by β-glucosidases.

Five glucosides with wide-ranging leaving-group pK_a's were chosen to measure the kinetic isotope effect on glucoside hydrolysis by pABG-5 β-glucosidase, and the isotope effects were determined in the following manner. Nine or ten rates of hydrolysis of both protio and deuterio substrates at were determined concentrations approximately ten times the value of K_m, and the values of k_H and k_D were calculated as the mean of the nine or ten individual rates. This measures the kinetic isotope effect on k_{cat}. In each case, the kinetic isotope effect was verified at higher substrate concentration to ensure that the observed effect was not due to any contamination by an inhibitor in either substrate stock. The kinetic isotope effect values are presented in Table 13.

Table 13. Kinetic Isotope Effects on Glucoside Hydrolysis by pABG-5 β-Glucosidase.

Aglycone	pK_a	k_H/k_D
2',4'-dinitrophenyl	3.96	1.10 ± 0.02
4'-nitrophenyl	7.18	1.12 ± 0.02
3'-nitrophenyl	8.39	1.07 ± 0.02
4'-bromophenyl	9.34	1.06 ± 0.02
β-naphthyl	9.51	1.05 ± 0.02

These kinetic isotope effect values fall within the range of normal α-secondary isotope effects, and are quite similar to values found in isotope effect studies of other glycosidase systems. For example, Legler et al. observed k_H/k_D values in the range of 1.08 to 1.14 for hydrolysis of aryl O-glucosides by *A. wentii* β-glucosidase[15]. Also, Van Doorslaer found isotope effects of 1.11 to 1.15 for glucoside hydrolysis by *S. atra* β-

glucosidase[16], and the hydrolysis of phenyl 4-O-(2-acetamido-2-deoxy-β-D-glucopyranosyl)-β-D-glucopyranoside by lysozyme exhibited an isotope effect of 1.11[57]. Such kinetic isotope effects are indicative of a rate-determining step which involves a change in hybridization from sp^3 toward sp^2 at the transition state, which is of course consistent with the proposed glucosidase mechanism.

Interestingly, the isotope effects in this study appear to be segregated into two groups, with the faster substrates exhibiting an average isotope effect of 11%, while the isotope effect for the slower substrates is around 6%. These data provide supportive evidence for the hypothesis that the rate-determining step of the reaction changes as leaving group pK_a changes, which was proposed on the basis of the linear free energy investigation discussed above. It is not possible to determine from these data whether 3'-nitrophenyl glucoside is proceeding *via* rate-limiting glucosylation or deglucosylation; it exhibits an intermediate value of k_H/k_D and could be associated with either the faster or slower substrates. Indeed, both steps probably contribute to the observed rate.

The magnitude of the isotope effect for the glucosylation step, although significantly different from zero, is nevertheless quite small. There are several possible explanations for this small observed effect. First, there may be only a small degree of C(1)-O bond cleavage at the transition state. This hypothesis is refuted, however, by the relatively large ρ value for this process, which indicates that bond cleavage is fairly advanced at the transition state. Secondly, the bond-cleavage step may be only partially rate-determining; for example, Sinnott and Souchard proposed a rate-limiting conformational change to explain the low isotope effect for β-galactosidase-catalyzed hydrolysis of phenyl galactoside[55]. This is unlikely to be the case in this study, however, in light of the good Hammett correlation, which suggests that bond cleavage is indeed the rate-determining-step for the slower substrates. A more reasonable explanation for the relatively low kinetic isotope effect for glucosylation is a relatively large degree of preassociation of the nucleophilic enzyme carboxylate at the transition state. This has been

suggested as the cause of the similarly low isotope effect value of 1.015 for hydrolysis of phenyl glucoside by sweet almond β-glucosidase[57].

The kinetic isotope effect for the faster substrates, where deglucosylation is believed to be rate-limiting (2',4'-dinitrophenyl β-D-glucopyranoside and 4'-nitrophenyl β-D-glucopyranoside), is larger than that for the substrates which exhibit rate-limiting glucosylation (4'-bromophenyl β-D-glucopyranoside and β-naphthyl β-D-glucopyranoside). This suggests that there is somewhat more oxocarbonium ion character at the transition state for deglucosylation than for glucosylation, and one possible rationale for this result is that there is less preassociation of a nucleophile at the deglucosylation transition state. This seems reasonable, since the nucleophile in the glucosylation step, carboxylate, is probably substantially ionized, and this negative charge will be strongly attracted to any positive charge buildup at the sugar anomeric center. In deglucosylation, the attacking moiety, water, is not substantially charged, and hence is less likely to preassociate with the developing positive charge at the reaction center. An alternative explanation might be that the leaving group for rate-limiting deglucosylation, the enzymic carboxylate, has a lower pK_a than the leaving group for rate-determining glucosylation, e.g. naphthol. The carboxylate is thus a better leaving group than the high pK_a phenols, and so deglucosylation may require less nucleophilic assistance than glucosylation. This would likely result in more buildup of positive charge at the transition state for deglucosylation, and a higher kinetic isotope effect, as observed.

5. Inactivation of pABG-5 β-Glucosidase with 2-Deoxy-2-Fluoro Glucosides

Recent experimentation[12,13] has shown that incubation of pABG-5 β-glucosidase with 2',4'-dinitrophenyl 2-deoxy-2-fluoro-β-D-glucopyranoside or 2-deoxy-2-fluoro-β-D-glucopyranosyl fluoride results in a rapid first-order inactivation of the enzyme. It has been proposed that the electronegative fluorine at C(2) slows both the glucosylation and

deglucosylation steps, and that incorporation of a highly-activated leaving group such as 2,4-dinitrophenolate or fluoride ion results in a sufficient rate of glucosylation to cause accumulation of the covalent 2-deoxy-2-fluoroglucosyl-enzyme intermediate (see Scheme 6, p. 5).

Recall from Figure 13 that, as the leaving group pK_a of the phenyl glucoside decreases, deglucosylation becomes rate-limiting, and below pK_a 8 one can no longer determine (by steady state methods) the effect of aglycone structure on the rate of glucosylation. However, since fluorine substitution at C(2) essentially prevents turnover of the glucosyl-enzyme intermediate, the rate of the glucosylation step, and the effect of aglycone modification on that rate, can be determined, even with highly activated leaving groups.

In order to investigate the structure-reactivity relationship in the inactivation of β-glucosidase by 2-deoxy-2-fluoro-glucosides, inactivation kinetics were studied with six different aryl 2-deoxy-2-fluoro-β-D-glucopyranosides whose leaving group pK_a's ranged from 3.96 to 7.18. Within this range, inactivation rates varied widely, from extremely slow to extremely fast, and this wide disparity in rates necessitated the use of four different methods for determination of kinetic parameters of inactivation.

The kinetics of inactivation of pABG-5 β-glucosidase by 2',4'-dinitrophenyl 2-deoxy-2-fluoro-β-D-glucopyranoside had been studied previously by the method of time-dependent inactivation (Methods, Section 2.4.3). However, because the inactivation by this glucoside is extremely rapid, measurement of the rate was impossible at concentrations approaching saturation[75]. This compound has now been reinvestigated using stopped flow techniques which can measure reactions with half-lives on the order of milliseconds, and allows direct and rapid observation of the phenolate release during inactivation. Highly concentrated enzyme (~1 μM) was used to produce a detectable absorbance change, since each molecule of enzyme releases only one molecule of 2,4-dinitrophenolate ion during the

inactivation. (This experiment was performed by another worker in this laboratory, M. Namchuk).

Incubation of β-glucosidase with 4'-nitrophenyl 2-deoxy-2-fluoro-β-D-glucopyranoside resulted in very slow inactivation of the enzyme, and thus the reaction could be followed in a normal spectrophotometer by observing the absorbance increase due to released 4-nitrophenolate ion over a period of 16-18 hours. Inactivation rates were determined from initial slopes of absorbance *vs.* time, and K_i and k_i were calculated by weighted linear regression analysis of rate *vs.* inactivator concentration (see Methods section 2.4.1). The phenolate release indicated a first-order inactivation of enzyme at all concentrations of 4'-nitrophenyl 2-deoxy-2-fluoro-β-D-glucopyranoside during the initial part of the reaction, but at high concentrations of inactivator (near K_i), a steady-state was reached after approximately four hours, and no further inactivation was observed (Figure 18). This low steady state level of activity (~14% of the initial rate of phenolate release) is believed to arise from reactivation of β-glucosidase *via* a transglucosylation reaction (Scheme 8, p. 8). Earlier studies on the enzyme inactivated by 2',4'-dinitrophenyl 2-deoxy-2-fluoro-β-D-glucopyranoside found that the covalently-bound 2-deoxy-2-fluoro-glucosyl-enzyme was extremely stable ($t_{1/2}$ = 500 h)[12] except when incubated with a glucoside which could act as an acceptor. When such an acceptor is present, full enzymic activity is rapidly restored, and a disaccharide product can be isolated. It is likely that, since the rate of inactivation by 4'-nitrophenyl 2-deoxy-2-fluoro-β-D-glucopyranoside is relatively slow, reactivation by transglucosylation becomes significant at high inactivator concentrations, and eventually the inactivation and transglucosylation rates become equal. This observation confirms results of an earlier investigation of this inactivator which used the method of time-dependent inactivation to determine k_i and K_i and which also observed first-order inactivation followed by a steady-state level of enzyme activity at high inactivator concentration[76].

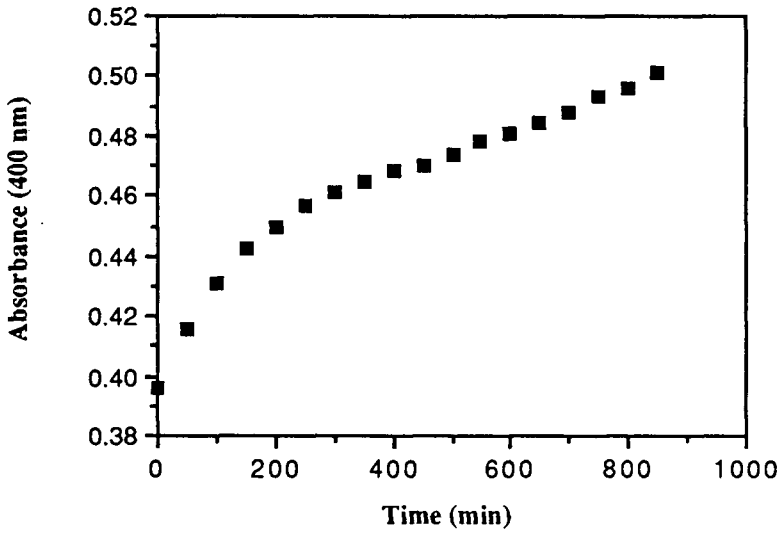

Figure 18. Absorbance at 400 nm due to reaction of β-glucosidase with 4'-nitrophenyl 2-deoxy-2-fluoro-β-D-glucopyranoside. Inactivator concentration = 1.281 mM, enzyme concentration = 9.2 μM.

When the rate of inactivation was neither extremely fast nor extremely slow, the method of time-dependent inactivation was used to determine the kinetic parameters. Such was the case for 3',4'-dinitrophenyl, 4'-chloro-2'-nitrophenyl, and 2',4',6'-trichlorophenyl 2-deoxy-2-fluoro-β-D-glucopyranoside. Enzyme was incubated at 37°C in the presence of inactivator, and at appropriate time intervals aliquots of this mixture were diluted into saturating concentration of PNPG and assayed for residual enzyme activity. (This procedure prevents further inactivation by diluting the inactivator and by providing an excess of a competing ligand.) The observed rate constant for the first-order inactivation, k_{obs}, at each inactivator concentration is calculated using a computer fitting program. The overall K_i and k_i were determined by fitting the rate constants to Equation 20, a variation of the Michaelis-Menten equation, using a weighted regression program.

$$k_{obs} = \frac{k_i[I]}{K_i + [I]} \qquad (20)$$

The kinetics of inactivation of β-glucosidase by 4'-chloro-2'-nitrophenyl- and 2',4',6'-trichlorophenyl 2-deoxy-2-fluoro-β-D-glucopyranosides were also determined by "burst" techniques, i.e. direct observation of release of phenolate ion during the inactivation, as with 2',4'-dinitrophenyl 2-deoxy-2-fluoro-β-D-glucopyranoside. However, since these compounds react significantly more slowly than the 2',4'-dinitrophenyl derivative, it was possible to follow the events on a traditional spectrophotometer. The rate of phenol release decreases exponentially with time as the concentration of active enzyme decreases, and k_{obs} at each concentration of inactivator is calculated by fitting absorbance *vs.* time data to an exponential decay function with the aid of a computer program. The constants K_i and k_i were then determined using the Curvefitter weighted regression program. The kinetic parameters thus determined were found to be comparable to those from the time-dependent inactivation studies.

The kinetic parameters of inactivation of β-glucosidase by 2',5'-dinitrophenyl 2-deoxy-2-fluoro-β-D-glucopyranoside were determined using "burst" techniques. However, the inactivation was quite rapid, and accurate rate determinations could not be made at concentrations approaching saturation (maximum concentration measurable = 0.014 mM), and extrapolation of these low concentration data to obtain values of k_i and K_i may result in large inaccuracies in the kinetic constants. An assessment of these errors may be drawn from results of experiments with 2',4'-dinitrophenyl 2-deoxy-2-fluoro-β-D-glucopyranoside. Time-dependent inactivation studies of that glucoside at very low inactivator concentrations (maximum concentration measurable = 0.005 mM) yielded values of $k_i = 25$ min^{-1} and $K_i = 0.05$ mM[13], whereas stopped flow determinations at concentrations up to 0.305 mM gave more reliable values of $k_i = 123$ min^{-1} and $K_i = 0.245$ mM. The value of k_i/K_i is, however, identical in both experiments. Based on these results, it is suggested that the value of k_i/K_i for the 2',5'-dinitrophenyl derivative is reasonably accurate, but the individual constants k_i and K_i are not.

The data are listed in Table 14 and plotted according to Hammett in Figure 19.

Table 14. Inactivation Parameters of β-Glucosidase by 2-Deoxy-2-Fluoro-β-D-Glucopyranosides.

Phenol Substituent	pK_a	K_i (mM)	k_i (min^{-1})	k_i/K_i ($mM^{-1}min^{-1}$)
2,4-dinitro	3.96	0.245	120	500
2,5-dinitro	5.15	0.035	5.0	140
3,4-dinitro	5.36	0.718	0.65	0.91
2,4,6-trichloro	6.39	0.143*	2.1*	15*
		0.077†	0.95†	12†
4-chloro-2-nitro	6.45	1.38*	2.3*	1.6*
		1.82†	2.9†	1.6†
4-nitro	7.18	1.67	0.017	0.0099

* Determined using phenolate burst method
† Determined using time-dependent inactivation method

Recall that the proposed kinetic scheme for hydrolysis of the 2-deoxy-2-fluoro-β-D-glucopyranosides is:

$$E + GX \underset{k_{-1}}{\overset{k_1}{\rightleftharpoons}} E \cdot GX \xrightarrow{k_2} E\text{-}G \xrightarrow{k_3} E + GOH$$

with HX released at the k_2 step and H_2O at the k_3 step.

Equations 5 and 7, above, define k_{cat} and k_{cat}/K_m in terms of the individual rate constants. Since k_3 is essentially zero in the reaction of the 2-deoxy-2-fluoro substrates with β-glucosidase,

$$k_i = k_2 = (kT/h) \exp\{-\Delta G_{ES}^{\ddagger}/RT\} \qquad (21)$$

$$k_i/K_i = \frac{k_1 k_2}{k_{-1}} = (kT/h) \exp\{-\Delta G_T^{\ddagger}/RT\} \qquad (22)$$

Both k_i and k_i/K_i are associated with the energy barrier to the transition state for glucosylation, but k_i is referenced with respect to the Michaelis complex, while k_i/K_i is referenced with respect to free enzyme and inactivator (see Figure 15).

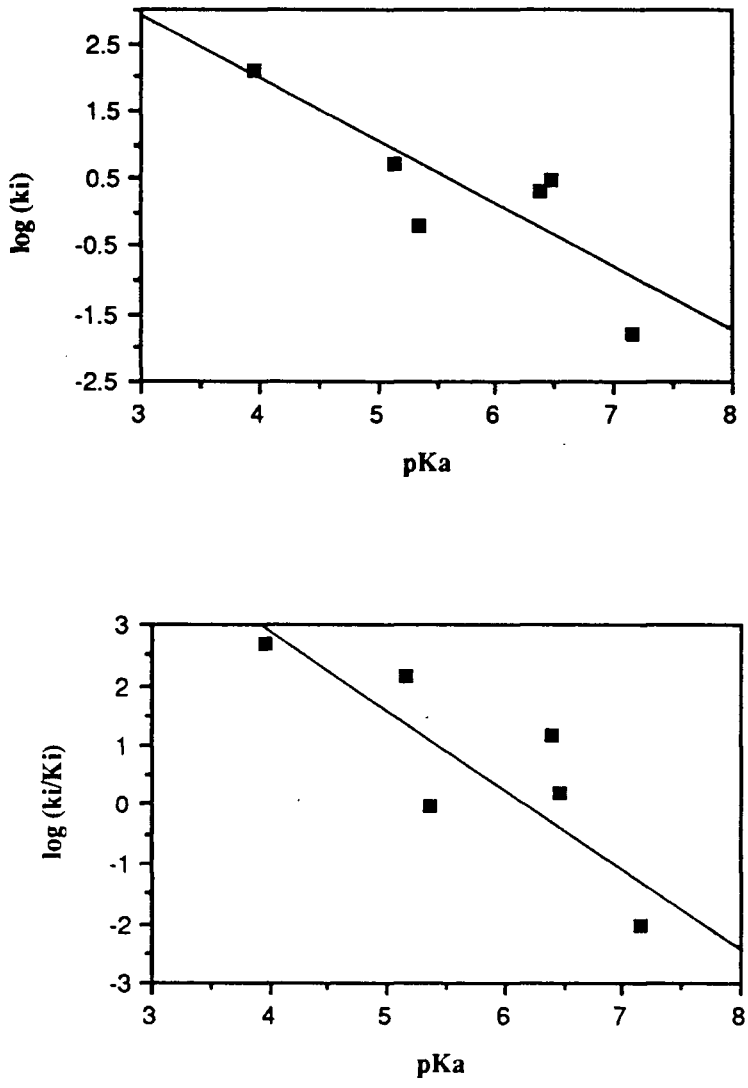

Figure 19. Hammett correlations of inactivation rates of pABG-5 β-glucosidase by 2-deoxy-2-fluoro-β-D-glucopyranosides.

The plots in Figure 19 show a definite relationship between the rate of inactivation and the pK_a of the leaving group of the inactivator. This is in sharp contrast to the data presented in Figures 13 and 14 for the parent glucosides in this pK_a range, where virtually no dependence of rate upon leaving group ability was observed. Clearly, when the rate of glucosylation is determined, a reasonable correlation can be found between reaction rate

and substrate structure. The slopes of $\log(k_i)$ *vs.* pK_a and $\log(k_i/K_i)$ *vs.* pK_a are -0.92 and -1.2, respectively, which correspond to ρ values of 2.0 and 2.7. These values indicate a large amount of charge separation at the transition state and thus it can be inferred that cleavage of the sugar-aglycone bond is well-advanced.

Although there appears to be a definite trend in the data, there is, also a good deal of scatter, which might be attributable to effects of the substituents on the aglycone, i.e. the nature of the substituent groups and their positions on the phenyl ring. Although substituents *ortho* to the phenyl oxygen did not appear to perturb the enzyme system in hydrolysis of the parent glucosides (Figure 17, p. 54), all glucosides which have *ortho* substituents in that study exhibit rate-limiting deglucosylation, so it is not possible (through steady-state kinetics) to observe any effect those *ortho* groups might have on the rate of glucosylation. In similar enzyme systems, *ortho* substituents, particularly nitro groups, have been observed to cause deviations from predicted structure-reactivity behavior[52], perhaps by destabilizing the ground state through steric crowding. In this study, the plot of $\log(k_i/K_i)$ *vs.* pK_a might be considered to consist of two separate lines of similar slope ($\cong -1$), the upper line representing those inactivators containing one or more *ortho* groups on the aglycone ring and the lower line representing the *meta-* and *para-* substituted compounds (Figure 20).

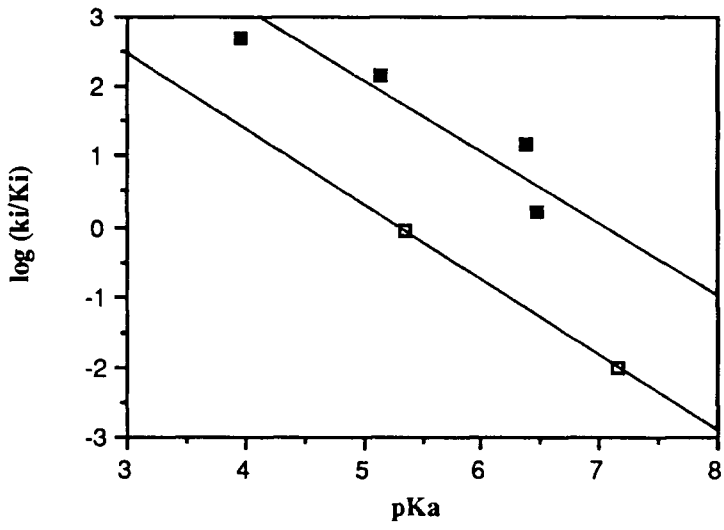

Figure 20. Hammett correlations of inactivation of β-glucosidase by ortho-substituted (■) *or meta- and/or para-substituted* (❑)*phenyl 2-deoxy-2-fluoro-β-D-glucopyranosides.*

An assessment of the effects of the fluorine substitution at C(2) on reaction rate and binding can be made by comparison of the kinetic parameters of the aryl 2-deoxy-2-fluoro-β-D-glucopyranosides with their corresponding parent glucosides. Care must be taken, however, because for the respective glucosides, k_{cat} reflects k_3 (rate-limiting deglucosylation), while k_i measures k_2*. In order to make a meaningful comparison between the two sets of data, theoretical values of k_2 were calculated for the parent glucosides by extrapolating the line containing the high pK_a (> 8) points in Figure 13, which enables one to estimate the effect of the fluorine substitution on the glucosylation step. The pertinent data are summarized in Table 15.

---

*Although the rate of deglucosylation (*via* transglucosylation) is relatively significant in the reaction of 4'-nitrophenyl 2-deoxy-2-fluoro-β-D-glucopyranoside, the value of k_i was calculated from the initial portion of the reaction only, and k_i can be considered equivalent to k_2.

Table 15. Comparison of Kinetic Parameters for β-D-Glucosides and 2-Deoxy-2-Fluoro-β-D-Glucosides.

Phenol Substituent	Glucosides K_m (mM)	Glucosides k_2† (min^{-1})	2-Deoxy-2-Fluoroglucosides K_i (mM)	2-Deoxy-2-Fluoroglucosides k_i (min^{-1})
2,4-dinitro	0.031	11 700 000	0.245	120
2,5-dinitro	0.045	1 600 000	0.035	5.0
3,4-dinitro	0.033	1 100 000	0.718	0.65
2,4,6-trichloro	0.0092	197 000	0.143	2.1
4-chloro-2-nitro	0.014	178 000	1.38	2.3
4-nitro	0.078	52 200	1.67	0.017

†Estimated values obtained by extrapolation of plot in Figure 13.

Several interesting points of comparison can be noted. First, the fluorine substitution does not appear to greatly affect substrate binding, since the K_i values for the 2-deoxy-2-fluoro glucosides are only ten to twenty times higher than the corresponding K_m values except in the case of the 4'-chloro-2'-nitrophenyl derivative. In fact, the 2-deoxy-2-fluoro substrates bind better than some of the parent glucosides in the linear free energy study (see Table 12). However, as predicted, the reaction rates have been substantially reduced by the presence of the fluorine adjacent to the reaction center, as the ratio of k_2 to k_i ranges from 10^5 to 10^6. Clearly, the energy barrier between free enzyme plus substrate and the transition state has been greatly increased by the introduction of the fluorine atom.

One possible cause of these tremendous rate reductions is altered binding interactions between enzyme and the 2-deoxy-2-fluoro substrates as compared with the parent glucosides. It is quite likely that an interaction between the C(2) hydroxyl and the enzyme active site is crucial for stabilization of the transition state relative to the ground state of the substrate. For example, an enzymic group might be positioned to hydrogen-bond with the C(2) hydroxyl in the oxocarbonium ion half-chair conformation but not in

the full chair conformation of the ground state. If this is so, and this stabilizing interaction is lost as a result of substituting fluorine for the hydroxyl, the transition state for reaction of the 2-deoxy-2-fluoro glucoside will be much higher in energy than that for the parent glucoside, and the reaction rate will be significantly decreased. Also, it is conceivable that an enzyme-substrate interaction at C(2) is important for positioning the substrate correctly with respect to the nucleophilic enzyme carboxylate, and if that interaction was lost the 2-deoxy-2-fluoro compound would not be positioned ideally within the active site. However, the similarities between the values of K_m and K_i indicate that binding of the 2-deoxy-2-fluoro substrates is not severely disrupted. While changes in binding orientation may indeed contribute to the rate reductions, it is unlikely that this is the sole cause of the large observed effects.

A probable cause of much of the rate reduction is destabilization of an oxocarbonium-ion-like transition state by the electronegative fluorine. Such a transition state is proposed for the hydrolysis of aryl β-D-glucosides by β-glucosidase, and is supported by the kinetic isotope effect data discussed above. Any buildup of positive charge at C(1) of the sugar will be greatly destabilized by the adjacent fluorine, thus slowing the rate of hydrolysis. These findings are quite comparable to effects observed in the hydrolysis of α-D-glucopyranosyl phosphate by glycogen phosphorylase. A reduction in V_{max}/K_m of ~10^5 was seen when fluorine was substituted for the C(2) hydroxyl of α-D-glucopyranosyl phosphate, and a combination of binding effects and destabilization of an oxocarbonium-ion-like transition state were proposed to account for the decrease in rate[63].

There is additional evidence that the tremendous reductions seen in hydrolysis rates when fluorine is substituted for the C(2) hydroxyl result from a combination of the electron-withdrawing effect of the highly electronegative fluorine and perturbed binding interactions between the enzyme and substrate. Table 16 contains a comparison of kinetic parameters for the series of substrates 4'-nitrophenyl β-D-glucopyranoside (PNPG), 4'-

nitrophenyl 2-deoxy-β-D-glucopyranoside (2d-PNPG), and 4'-nitrophenyl 2-deoxy-2-fluoro-β-D-glucopyranoside (2F-PNPG).

Table 16. Effect of Hydroxyl, Hydrogen, and Fluorine Substituents at C(2) on Kinetic Parameters of Hydrolysis by pABG-5 β-Glucosidase.

Substrate	K_m (mM)	k_{cat} (min^{-1})	k_{cat}/K_m ($mM^{-1}min^{-1}$)
PNPG	0.078	10 100	129 000
2d-PNPG[12]	0.016	1.5	93
2F-PNPG	1.67	0.0165	0.0099

Note that 4'-nitrophenyl 2-deoxy-β-D-glucopyranoside was hydrolyzed more slowly by β-glucosidase than was the parent glucoside, but faster than the corresponding 2-deoxy-2-fluoro analogue. If the effect of the various substituents at C(2) were solely inductive, the 2-deoxy species would be expected to be hydrolyzed faster than the parent glucoside. It appears that some interaction between the enzyme active site and the hydroxyl group at C(2) must be essential for the enzyme to operate efficiently.

In order to further investigate the effect of the fluorine atom at C(2) on the transition state for glucosylation, it was proposed that the α-secondary kinetic isotope effect of inactivation by 2',4'-dinitrophenyl 2-deoxy-2-fluoro-β-D-glucopyranoside be determined. However, several restrictions of the system made it impossible to use the same technique described previously for determination of the isotope effect of hydrolysis of the parent glucosides, i.e. multiple determinations of rate at saturating substrate concentration. First, the maximum concentration of this glucoside achievable in phosphate buffer at pH 6.8 is approximately 1.6 mM, so concentrations of ten times the value of K_i (K_i = 0.245 mM) are not possible. Second, the inactivation of the enzyme by this compound is extremely rapid and stopped flow techniques must be employed for accurate determination of the rate constants, and this makes it impractical to measure the rates of reaction of the protio and

deutero compounds alternately because large amounts of substrate solution would be required to thoroughly rinse the apparatus between samples. Thus it was decided to determine k_H and k_D by measuring the inactivation rates at several different inactivator concentrations and fitting the data to Equation 20, above. Figure 21 depicts the double-reciprocal plot of inactivation rate *vs.* inactivator concentration for both the protio and deutero material.

Several difficulties were encountered in this experiment, and it proved difficult to obtain an accurate value for k_H/k_D using this method. A shortage of deutero material permitted rate determinations at only four inactivator concentrations, and the enzyme was not stable over the several hours required to complete the determinations. However, the data do suggest that the isotope effect on the inactivation is extremely small, probably between 0 - 5%.

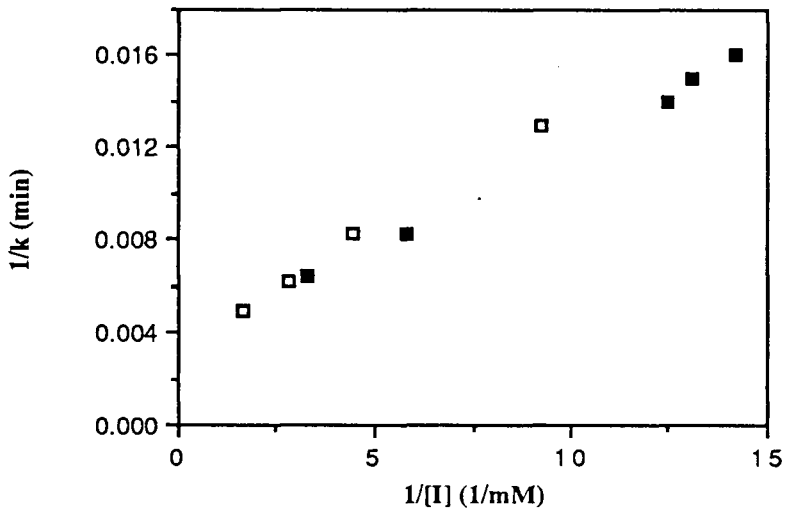

Figure 21. Double-reciprocal plot of inactivation rate vs. inactivator concentration for 2',4'-dinitrophenyl 2-deoxy-2-fluoro-β-D-glucopyranoside (■) *and 2',4'-dinitrophenyl {1-^{2}H}-2-deoxy-2-fluoro-β-D-glucopyranoside* (❑).

This isotope effect data, taken together with the slopes of the Hammett plots in Figure 19, suggest a very late transition state for the inactivation of pABG-5 β-glucosidase by the 2-deoxy-2-fluoro inactivators, wherein the sugar-aglycone bond is essentially fully broken and the covalent bond between the enzyme carboxylate and 2-deoxy-2-fluoro-glucose is nearly fully formed. It appears that full nucleophilic participation is required for cleavage of the glucosidic bond when a fluorine atom is present at C(2) of the sugar. This is a very reasonable result, since the electron-withdrawing nature of the fluorine would greatly destabilize any positive charge buildup at the anomeric center and thus force the mechanism of inactivation to be more concerted than that for the hydrolysis of the parent glucosides.

6. Conclusions

The results of the experiments presented in this thesis help to characterize several mechanistic aspects of glucoside hydrolysis catalyzed by *Agrobacterium* β-glucosidase. The relationship between electronic structure of the substituted phenyl glucosides and the rate of enzymic hydrolysis provides strong supportive evidence for a two-step mechanism which proceeds *via* a covalent glucosyl-enzyme intermediate. The concave-downward plot of $\log(k_{cat})$ *vs.* leaving group pK_a indicates that glucosylation is the rate-determining step for the phenyl glucosides with poor leaving groups while deglucosylation is rate-limiting when the leaving group is highly activated. The value of ρ for the glucosylation step, 1.61, suggests that the glycone-aglycone bond is substantially cleaved at the transition state, while the small secondary kinetic isotope effect (6%) for this step indicates that nucleophilic participation of the enzymic carboxylate is significantly advanced. These results suggest a transition state quite similar to that proposed by Rosenberg and Kirsch for almond β-glucosidase (see Scheme 14, p. 34). Hydrolysis of the glucosyl-enzyme

intermediate to yield free glucose appears to require less preassociation of the nucleophilic water, as evidenced by an isotope effect of approximately 11% which indicates substantial oxocarbonium ion character at the transition state.

Investigation of the inactivation of β-glucosidase by substituted phenyl 2-deoxy-2-fluoro glucosides indicates that there is a correlation between the structure of the inactivator aglycone and the rate of inactivation, which suggests that the fundamental enzyme-glucoside interactions are probably not severely altered by the fluorine substitution. Observation of such a linear free energy relationship in enzyme inactivation has rarely been accomplished. The large ρ value and small kinetic isotope effect measured for inactivation by the 2-deoxy-2-fluoro compounds suggest that at the transition state there is nearly complete departure of the aglycone and essentially full participation of the enzymic nucleophile. The presence of the fluorine at C(2) of the sugar causes tremendous reductions in the rate of cleavage of the glucosidic bond as compared to the hydrolysis rates for the parent glucosides. These results provide good evidence that the normal enzymic hydrolysis reaction proceeds *via* a transition state with oxocarbonium ion character and that the fluorine substitution destabilizes the buildup of positive charge and thus greatly increases the energy barrier for glucosylation.

CHAPTER III

MATERIALS AND METHODS

1. Synthesis

1.1. General Procedures and Materials

Melting points (m.p.) were determined using a Laboratory Devices Mel-temp II melting-point apparatus, and are uncorrected.

^{1}H-nuclear magnetic resonance (nmr) spectra were recorded on a 300 MHz Varian XL-300 instrument. Chemical shifts are listed in the delta (δ) scale. Compounds run in $CDCl_3$ and CD_3OD are referenced against internal tetramethyl silane (TMS) (δ = 0.00 ppm). ^{19}F nmr spectra were recorded on a 200 MHz Bruker AC-200 instrument, and chemical shift values (δ) are referenced against external trifluoroacetic acid (δ = 76.53 ppm).

Micro-analyses were performed by Mr. P. Borda, Micro-analytical laboratory, University of British Columbia, Vancouver.

Solvents and reagents used were either reagent grade, certified, or spectral grade. Dry methanol was distilled from magnesium methoxide prepared *in situ* by reaction of methanol with magnesium turnings in the presence of iodine. Acetyl chloride was dried by refluxing for several hours over PCl_5, followed by distillation.

Substituted phenols were obtained from the following sources: Aldrich chemicals; 4-chloro, 3,5-dichloro, 4-cyano, 3-nitro, and 2-nitro-4-chloro: Fluka Chemical Co.; 3,4-dinitro, 2,5-dinitro: Eastman Organic Chemicals; 2,4,6-trichloro: B. D. H. Co.; 2-naphthol. All chemicals were used as supplied without further purification.

Thin-layer-chromatography (tlc) separations were performed using Merck Kieselgel 60 F-254 analytical plates. Compounds were detected visually (when possible) under U.V. light, or by charring with 5% sulfuric acid in methanol. Acetylated compounds were separated with the solvent system of 1:1 ethyl acetate/petroleum ether. Deprotected

glucosides were run in 1:20 methanol/ethyl acetate. Preparative tlc plates were prepared as follows. An aqueous slurry of Merck GF254 silica gel was applied to glass plates (20 cm x 20 cm) to give a 1 mm thickness of gel, the plates air dried, then baked for 1 hour (100°C). Column chromatography was performed according to the method of Still et al.[77], using a silica gel column of Kieselgel 60 (180-230 mesh).

Several compounds used in this work were synthesized by others in this laboratory: From Leise Berven; 2',5'-dinitrophenyl 2,3,4,6-tetra-O-acetyl-β-D-glucopyranoside, phenyl 2,3,4,6-tetra-O-acetyl-β-D-glucopyranoside, 1,2,3,4,6-penta-O-acetyl {1-^{2}H}-α-D-glucopyranoside, 2',4'-dinitrophenyl 2,3,4,6-tetra-O-acetyl 2-deoxy-2-fluoro-{1-^{2}H}-β-D-glucopyranoside. From Adam Becalski; 2',4'-dinitrophenyl β-D-glucopyranoside: from Paul Bird; 1,2,3,4,6-penta-O-acetyl 2-deoxy-2-fluoro-α-D-glucopyranose: from Mark Namchuk; 2',4'-dinitrophenyl 2-deoxy-2-fluoro-β-D-glucopyranoside.

1.2. General Compounds

1,2,3,4,6-Penta-O-acetyl α-D-glucopyranose (1)

Compound (**1**) was prepared by the method of Wolfrom and Thompson[78]. Acetic anhydride (53 mL) was heated to 40°C in a water bath, concentrated sulfuric acid (0.4 mL) was added dropwise. α-D-Glucose (10 g, 0.0558 mmol) was added, with stirring, over a 30-minute period so that the temperature of the system did not exceed 45°C, and the reaction stirred for an additional 30 min at 35-45°C. The reaction mixture was then poured into 400 mL of ice water and stirred vigorously for 30 min when 1,2,3,4,6-penta-O-acetyl-α-D-glucopyranose precipitated as a sticky white solid. The product was collected by vacuum filtration and washed with water (20 mL) and 5% sodium bicarbonate solution (2 x 20 mL), then again with water until the washings were neutral. The product was recrystallized from 95% ethanol and dried *in vacuo* over P_2O_5 to produce a white powder (17.81 g, 0.0458 mmol, 82%). M.p. 109-110°C (lit.[76] m.p. 112-113°C).

2,3,4,6-Tetra-O-acetyl α-D-glucopyranosyl bromide (Acetobromoglucose, 2)

Compound (**1**) was brominated by the method of Haynes and Newth[79]. Finely powdered (**1**) (10 g, 25.6 mmol) was added to a solution of 45% HBr in acetic acid (10 mL) and acetic anhydride (1 mL), stirred until homogeneous (approximately 10 minutes), then for an additional 35 minutes until the reaction was complete by tlc. The solution was diluted with $CHCl_3$ (40 mL), poured quickly into 200 mL ice water, and stirred vigorously for 5 minutes. The two phase mixture was transferred to a separatory funnel, the organic layer withdrawn, and the aqueous layer extracted with cold $CHCl_3$ (2 x 20 mL). The combined organic extracts were washed with cold saturated sodium bicarbonate (2 x 100 mL) until the aqueous layer remained basic, then washed with cold H_2O (100 mL). The organic phase was dried over $MgSO_4$, filtered, and the solvent evaporated *in vacuo*. The resulting gum was dissolved in a minimum volume of anhydrous ether, low-boiling petroleum ether added to produce turbidity, and the product (**2**) crystallized as white needles on standing at -5°C. M.p. 88-90° (lit.[78] m.p. 88-89°). Acetobromoglucose could be stored under petroleum ether at -5°C for several months.

2,3,4,6-Tetra-O-acetyl {1-^{2}H}-α-D-glucopyranosyl bromide (D-Acetobromoglucose, 3)

This compound was prepared according to the same method as **2**, above, using 1,2,3,4,6-penta-O-acetyl {1-^{2}H}-α-D-glucopyranose (5 g, obtained from Leise Berven), and the white crystalline product was stored under petroleum ether at -5°C. M.p. 87-89°C. ^{1}H-nmr showed approximately 2% contamination of 1,2,3,4,6-penta-O-acetyl-α-D-glucopyranose.

2,3,4,6-Tetra-O-acetyl 2-deoxy-2-fluoro-α-D-glucopyranosyl bromide (2F-acetobromo-glucose, 4)

This compound was prepared according to the same method as acetobromoglucose (2), above, using 1,2,3,4,6-penta-O-acetyl-2-deoxy-2-fluoro-α-D-glucopyranose (3 g, obtained from Paul Bird). The product bromide crystallized as white needles and was stored under petroleum ether at -5°C. M.p. 77-79°C (lit.[80] m.p. 79-80°C).

1.3. Aryl 2,3,4,6-Tetra-O-Acetyl β-D-Glucopyranosides

The Koenigs-Knorr procedure of glucoside synthesis[64] was used for all glucosides. The appropriately substituted phenol is suspended in 1N NaOH (1 mmol phenol/mL base), acetobromoglucose dissolved in acetone (~0.4 mmol acetobromoglucose/mL) added to the phenol solution, and the mixture stirred for 16-24 hours at room temperature. After evaporation of the solvent the resulting aqueous slurry was diluted with water and extracted with dichloromethane (3 x 50 mL), the combined organic extracts washed twice with base (2N NaOH or saturated sodium bicarbonate), dried over $MgSO_4$, filtered, and solvent evaporated *in vacuo* to give a colorless gum. Most products crystallized immediately upon addition of ethanol. C(1)-deuterated and 2-deoxy-2-fluoro glucosides were formed in the same manner.

1.4. Aryl β-D-Glucopyranosides

Three procedures were used to deacetylate the aryl β-D-glucopyranosides. Compounds with leaving group pK_a's of 6 or higher were deacetylated by a modified Zemplen method[55], using sodium methoxide in dry methanol. Glucosides with highly activated leaving groups ($pK_a < 6$) were deacetylated with HCl in dry methanol, according to Ballardie et al[65]. 2',4',6'-trichlorophenyl-β-D-glucopyranoside was deprotected using AG1-X8 (OH^-) resin in dry methanol[66].

1.4.1. Deacetylation with Sodium Methoxide/Methanol[55]

The protected glucoside was suspended in dry methanol (~0.2 mmol/10 mL), and an appropriate volume of sodium methoxide in methanol (generated by adding ~0.22 g sodium metal (10 mmol) to 10 mL dry methanol and allowing the sodium to react completely) added to give a final methoxide ion concentration of 0.1M. The reaction was stirred at room temperature until complete, usually 1 to 2 hours, then excess base was neutralized by addition of Dowex 50W (H^+) cation exchange resin, the resin removed by gravity filtration and washed several times with methanol. The methanol was evaporated *in vacuo* to give a crystalline product, which was then recrystallized from an appropriate solvent.

1.4.2. Deacetylation with HCl/Methanol[65]

The protected glucoside was suspended in dry methanol (16 mg/mL), cooled to 0°C, and sufficient freshly distilled acetyl chloride added to generate a final HCl concentration of 3-5% (w/v). The reaction mixture was stored at 4°C until reaction was complete (36-48 hours), then the solvent was removed *in vacuo*, and the product washed several times with anhydrous diethyl ether to remove residual acid. The resulting gum was dissolved in a polar solvent (methanol or acetone), then triturated with methylene chloride and acetone or hexane to induce crystallization of the product glucoside.

1.4.3. Deacetylation with AG1-X8 (OH^-) Resin/Methanol[66]

The resin was converted to its basic form by washing with several volumes of 5N sodium hydoxide, followed by repeated rinsing with dry methanol and air drying.

The protected glucoside was suspended in dry methanol, resin (~0.1 g resin/mmol glucoside) added and the mixture stirred at room temperature for 18 hours. The resin was then removed by gravity filtration, washed several times with methanol, and the methanol

evaporated *in vacuo*. Glucoside product was crystallized from the resulting gum using an appropriate solvent system.

Phenyl β-D-glucopyranoside (6)

The acetylated compound (**5**, obtained from Leise Berven, 0.840 g, 1.98 mmol), was deacetylated with sodium methoxide/methanol, and (**6**) was recrystallized from ethanol to produce fine white needles (0.362 g, 1.41 mmol, 71%). M.p. 170-171°C (lit.[52] m.p. 171-172°C); Rf 0.17; ^{1}H nmr (D_2O): δ 7.41 (m, 2 H, H(2'), H(6')), 7.15 (m, 3 H, H(3'), H(4'), H(5')), 5.15 (d, 1 H, $J_{1,2}$ 7 Hz, H(1)), 3.94 (dd, 1 H, $J_{3,4}$ 12, $J_{4,5}$ 2 Hz, H(4)), 3.75 (dd, 1 H, $J_{2,3}$ 5, $J_{3,4}$ 12 Hz, H(3)), 3.66-3.45 (4 H, H(2), H(5), H(6), H(6')). Anal calc. for $C_{12}H_{16}O_6$: C, 56.24; H, 6.31%. Found: C, 56.25; H, 6.38%.

4'-Nitrophenyl β-D-glucopyranoside (8)

The acetylated compound (**7**) was prepared according to Koenigs and Knorr from acetobromoglucose (1.022 g, 2.49 mmol) and 4-nitrophenol (0.710 g, 5.10 mmol), and was recrystallized from ethanol to give white needles (0.404 g, 0.861 mmol, 35%). This material (0.355 g, 0.756 mmol) was deacetylated with sodium methoxide/methanol, and the product (**8**) crystallized after 2 hours, and was recrystallized from ether to produce fine white needles (0.156 g, 0.518 mmol, 68%). M.p. 164-166°C (lit.[52] m.p. 164-165°C); Rf 0.25; ^{1}H nmr (D_2O): δ 8.20 (d, 2 H, J 9 Hz, H(3'), H(5')), 7.10 (d, 2 H, J 9 Hz, H(2'), H(6')), 5.20 (d, 1 H, $J_{1,2}$ 8 Hz, H(1)), 3.95 (dd, 1 H, $J_{3,4}$ 13, $J_{4,5}$ 2 Hz, H(4)), 3.70 (dd, 1 H, $J_{2,3}$ 6, $J_{3,4}$ 13 Hz, H(3)), 3.65-3.40 (4 H, H(2), H(5), H(6), H(6')).

4'-Chlorophenyl β-D-glucopyranoside (10)

The acetylated compound (**9**, obtained from Leise Berven, 0.222 g, 0.480 mmol) was deacetylated with sodium methoxide/methanol, and the product glucoside (**10**) was recrystallized from methanol to produce fine white needles (0.070, 0.241 mmol, 50%).

M.p. 172-174°C (lit.[52] m.p. 173-175°C); Rf 0.27; ^{1}H nmr (CD_3OD): δ 7.40 (d, 2 H, J 9 Hz, H(3'), H(5')), 7.10 (d, 2 H, J 9 Hz, H(2'), H(6')), 5.10 (d, 1 H, $J_{1,2}$ 8 Hz, H(1)), 3.95 (dd, 1 H, $J_{3,4}$ 14, $J_{4,5}$ 3 Hz, H(4)), 3.75 (dd, 1 H, $J_{2,3}$ 5, $J_{3,4}$ 14 Hz, H(3)), 3.65-3.40 (4 H, H(2), H(5), H(6), H(6')). Anal. calc. for $C_{12}H_{15}O_6Cl+1/2H_2O$; C, 48.10; H, 5.39%; Found: C, 47.70; H, 5.41%.

4'-Bromophenyl β-D-glucopyranoside (12)

The acetylated compound (**11**) was prepared according to Koenigs and Knorr from acetobromoglucose (2.532 g, 6.16 mmol) and 4-bromophenol (1.741 g, 10.1 mmol), and was recrystallized from ethanol to give white needles (0.710 g, 1.42 mmol, 23%). This material (0.494 g, 0.980 mmol) was deacetylated with sodium methoxide/methanol, and the product glucoside (**12**) was recrystallized from ethanol to produce fine white needles (0.132, 0.390 mmol, 40%). M.p. 175-176°C ; Rf 0.31; ^{1}H nmr (D_2O): δ 7.55 (d, 2 H, J 9 Hz, H(3'), H(5')), 7.05 (d, 2 H, J 9 Hz, H(2'), H(6')), 5.10 (d, 1 H, $J_{1,2}$ 8 Hz, H(1)), 3.95 (dd, 1 H, $J_{3,4}$ 14, $J_{4,5}$ 2 Hz, H(4)), 3.70 (dd, 1 H, $J_{2,3}$ 7, $J_{3,4}$ 14 Hz, H(3)), 3.60-3.40 (4 H, H(2), H(5), H(6), H(6')). Anal. calc. for $C_{12}H_{15}O_6Br$; C, 43.00; H, 4.52%; Found: C, 42.61; H, 4.71%.

4'-t-Butylphenyl β-D-glucopyranoside (14)

The acetylated compound (**13**) was prepared according to Koenigs and Knorr from acetobromoglucose (2.518 g, 6.13 mmol) and 4-*t*-butylphenol (1.510 g, 10.1 mmol), and was recrystallized from 1:1 ether/petroluem ether to give white needles (0.508 g, 1.06 mmol, 17%). This material (0.247 g, 0.510 mmol) was deacetylated with sodium methoxide/methanol. An opalescent white solid formed on trituration with water, and the product (**14**) was recrystallized from ethyl acetate/hexane to produce white crystals (0.122 g, 0.391 mmol, 77%). M.p. 145-147°C (lit.[52] m.p.145-146°C); Rf 0.31; ^{1}H nmr (D_2O): δ 7.30 (d, 2 H, J 9 Hz, H(2'), H(6')), 6.90 (d, 2 H, J 9 Hz, H(3'), H(5')), 5.15 (d, 1 H,

$J_{1,2}$ 8 Hz, H(1)), 3.90 (dd, 1 H, $J_{3,4}$ 12, $J_{4,5}$ 2 Hz, H(4)), 3.70-3.40 (5 H, H(2), H(3), H(5), H(6), H(6')), 1.30 (s, 9 H, 3 X CH_3). Anal. calc. for $C_{16}H_{24}O_6$+0.75H_2O; C, 58.96; H, 7.90%; Found: C, 58.93; H, 8.05%.

4'-Cyanophenyl β-D-glucopyranoside (16)

The acetylated compound (**15**) was prepared according to Koenigs and Knorr from acetobromoglucose (2.250 g, 5.47 mmol) and 4-cyanophenol (1.150 g, 9.65 mmol), and was recrystallized from ethanol to give white needles (0.562 g, 1.25 mmol, 23%). This material (0.395 g, 0.880 mmol) was deacetylated with sodium methoxide/methanol, and the product glucoside (**16**) was recrystallized from ethanol to produce light pink prismatic crystals (0.206 g, 0.732 mmol, 83%). M.p.188-189°C (lit.[52] m.p.193-194°C); Rf 0.27; ^{1}H nmr (D_2O): δ 7.75 (d, 2 H, J 8 Hz, H(3'), H(5')), 7.20 (d, 2 H, J 8 Hz, H(2'), H(6')), 5.25 (d, 1 H, $J_{1,2}$ 8 Hz, H(1)), 3.95 (dd, 1 H, $J_{3,4}$ 11, $J_{4,5}$ 2 Hz, H(4)), 3.75 (dd, 1 H, $J_{2,3}$ 6, $J_{3,4}$ 11 Hz, H(3)), 3.70-3.45 (4 H, H(2), H(5), H(6), H(6')). Anal. calc. for $C_{13}H_{15}O_6N$; C, 55.50; H, 5.39; N, 4.98%; Found: C, 55.51; H, 5.44; N, 4.82%.

3'-Nitrophenyl β-D-glucopyranoside (18)

The acetylated compound (**17**) was prepared according to Koenigs and Knorr from acetobromoglucose (2.569 g, 6.25 mmol) and 3-nitrophenol (1.348 g, 9.69 mmol), and was recrystallized from ethanol to give white needles (0.402 g, 0.856 mmol, 14%). This material (0.300 g, 0.639 mmol) was deacetylated with sodium methoxide/methanol, and the product glucoside (**18**) was recrystallized from ethanol to produce fine white needles (0.169 g, 0.561 mmol, 88%). M.p.166-168°C (lit.[52] m.p. 166-168°C); Rf 0.34; ^{1}H nmr (D_2O): δ 8.00 (m, 2 H, H(2'), H(4')), 7.50 (m, 2 H, H(5'), H(6')), 5.20 (d, 1 H, $J_{1,2}$ 8 Hz, H(1)), 3.95 (dd, 1 H, $J_{3,4}$ 11, $J_{4,5}$ 2 Hz, H(4)), 3.75-3.45 (5 H, H(2), H(3), H(5),

H(6), H(6')). Anal. calc. for $C_{12}H_{15}O_8N$; C, 47.84; H, 5.03; N, 4.65%; Found: C, 47.60; H, 5.07; N, 4.45%.

β-Naphthyl β-D-glucopyranoside (20)

The acetylated compound (**19**) was prepared according to Koenigs and Knorr from acetobromoglucose (1.662 g, 4.04 mmol) and β-naphthol (1.404 g, 9.73 mmol), and was recrystallized from ethanol to give white needles (0.325 g, 0.687 mmol, 17%). This material (0.252 g, 0.530 mmol) was deacetylated with sodium methoxide/methanol, and the product glucoside (**20**) was recrystallized from ethanol to produce fine white needles (0.071 g, 0.230 mmol, 43%). M.p.184-186°C; Rf 0.34; ^{1}H nmr (CD_3OD): δ 7.80 (m, 3 H, aromatic), 7.50-7.25 (m, 4 H, aromatic), 5.10 (d, 1 H, $J_{1,2}$ 7 Hz, H(1)), 3.95 (dd, 1 H, $J_{3,4}$ 11, $J_{4,5}$ 2 Hz, H(4)), 3.75 (dd, 1 H, $J_{2,3}$ 5, $J_{3,4}$ 11 Hz, H(3)), 3.55-3.35 (4 H, H(2), H(5), H(6), H(6')). Anal. calc. for $C_{16}H_{18}O_6$; C, 62.73; H, 5.93%; Found: C, 62.53; H, 5.89%.

3',5'-Dichlorophenyl β-D-glucopyranoside (22)

The acetylated compound (**21**) was prepared according to Koenigs and Knorr from acetobromoglucose (2.498 g, 6.08 mmol) and 3,5-dichlorophenol (1.630 g, 11.1 mmol), and was recrystallized from ethanol to give fine white needles (0.362 g, 0.734 mmol, 12%). This material (0.249 g, 0.505 mmol) was deacetylated with sodium methoxide/methanol. Product (**22**) precipitated after 1 hour, and was recrystallized from ethanol to produce white needles (0.100 g, 0.308 mmol, 61%). M.p.215-217°C; Rf 0.28; ^{1}H nmr (CD_3OD): δ 7.90 (d, 1 H, J 2 Hz, H(4')), 7.15 (d, 2 H, J 2 Hz, H(2'), H(6')), 5.10 (d, 1 H, $J_{1,2}$ 8 Hz, H(1)), 3.90 (dd, 1 H, $J_{3,4}$ 11, $J_{4,5}$ 3 Hz, H(4)), 3.70 (dd, 1 H, $J_{2,3}$ 6, $J_{3,4}$ 11 Hz, H(3)), 3.50-3.30 (4 H, H(2), H(5), H(6), H(6')). Anal. calc. for $C_{12}H_{14}O_6Cl_2$+CH_3OH; C, 43.70; H, 3.95%; Found: C, 43.11; H, 3.81%.

2',4',6'-Trichlorophenyl β-D-glucopyranoside (24)

The acetylated compound (**23**) was prepared according to Koenigs and Knorr from acetobromoglucose (2.499 g, 6.08 mmol) and 2,4,6-trichlorophenol (1.982 g, 10.0 mmol). The product precipitated after 1.5 hours, and was recrystallized from ethanol to give flat white needles (0.802 g, 1.52 mmol, 25%). This material (0.202 g, 0.383 mmol), was deacetylated with AGX-8 ion exchange resin (0.030g). Product (**24**) was recrystallized from 7:1 ethyl acetate/methanol to produce white flakes (0.105 g, 0.291 mmol, 76%). M.p.190-194°C (dec.); Rf 0.51; ^{1}H nmr (CD_3OD): δ 7.40 (s, 2 H, H(3'), H(5')), 5.20 (d, 1 H, $J_{1,2}$ 8 Hz, H(1)), 3.90 (dd, 1 H, $J_{3,4}$ 14, $J_{4,5}$ 2 Hz, H(4)), 3.65 (dd, 1 H, $J_{2,3}$ 6, $J_{3,4}$ 14 Hz, H(3)), 3.60-3.40 (4 H, H(2), H(5), H(6), H(6')). Anal. calc. for $C_{12}H_{13}O_6Cl_3$+1.5H_2O; C, 37.26; H, 3.91%; Found: C, 37.14; H, 3.51%.

2',5'-Dinitrophenyl β-D-glucopyranoside (26)

The acetylated compound (**25**) was prepared according to Koenigs and Knorr from acetobromoglucose (1.075 g, 2.62 mmol) and 2,5-dinitrophenol (0.992 g, 5.39 mmol), and was recrystallized from ethanol to give slightly yellow needles (0.537 g, 1.04 mmol, 40%). This material (0.325 g, 0.632 mmol) was deacetylated with HCl/methanol, and the product glucoside (**26**) was recrystallized from methanol/dichloromethane, and hexane to produce yellowish plates (0.115 g, 0.332 mmol, 53%). M.p.166-168°C; Rf 0.34; ^{1}H nmr: δ 8.30 (d, 1 H, J 2 Hz, H(6')), 8.00 (m, 2 H, H(3'), H(4')), 5.25 (d, 1 H, $J_{1,2}$ 8 Hz, H(1)), 3.95 (dd, 1 H, $J_{3,4}$ 14, $J_{4,5}$ 2 Hz, H(4)), 3.70 (dd, 1 H, $J_{2,3}$ 5, $J_{3,4}$ 14 Hz, H(3)), 3.60-3.30 (4 H, H(2), H(5), H(6), H(6')). Anal. calc. for $C_{12}H_{14}O_{10}N_2$; C, 41.62; H, 4.08; N, 8.09%; Found: C, 41.15; H,4.19; N, 7.77%.

3',4'-Dinitrophenyl β-D-glucopyranoside (28)

The acetylated compound (**27**) was prepared according to Koenigs and Knorr from acetobromoglucose (0.876 g, 2.13 mmol) and 3,4-dinitrophenol (0.503 g, 2.73 mmol),

and was recrystallized from ethanol to give white needles (0.213 g, 0.413 mmol, 19%). This material (0.150 g, 0.292 mmol) was deacetylated with HCl/methanol, and the product glucoside (**28**) was recrystallized from methanol/dichloromethane/hexane to produce yellowish plates (0.076 g, 0.219 mmol, 75%). M.p.152-153°C ; Rf 0.34; ^{1}H nmr (CD_3OD): δ 8.15 (d, 1 H, $J_{5',6'}$ 11 Hz, H(5')), 7.65 (d, 1 H, $J_{2',6'}$ 2 Hz, H(2')), 7.50 (dd, 1 H, $J_{5',6'}$ 11, $J_{2',6'}$ 2 Hz, H(6')), 5.20 (d, 1 H, $J_{1,2}$ 8 Hz, H(1)), 3.95 (dd, 1 H, $J_{3,4}$ 14, $J_{4,5}$ 2 Hz, H(4)), 3.70 (dd, 1 H, $J_{2,3}$ 5, $J_{3,4}$ 14 Hz, H(3)), 3.60-3.30 (4 H, H(4), H(5), H(6), H(6')). Anal. calc. for $C_{12}H_{14}O_{10}N_2$+1.5H_2O; C, 38.61; H, 4.59; N, 7.51%; Found: C, 38.61; H, 4.51; N, 7.30%.

4'-Chloro-2'-Nitrophenyl β-D-glucopyranoside (30)

The acetylated compound (**29**) was prepared according to Koenigs and Knorr from acetobromoglucose (1.202 g, 2.92 mmol) and 4-chloro-2-nitrophenol (0.921 g, 5.30 mmol). Product crystallized after two hours and was recrystallized from ethyl acetate/petroleum ether to give white needles (0.554 g, 1.10 mmol, 38%). This material (0.120 g, 0.239 mmol) was deacetylated with sodium methoxide, and the product glucoside (**30**) was recrystallized from methanol/dichloromethane/hexane to produce yellowish crystals (0.037 g, 0.110 mmol, 46%). M.p.159-160°C ; Rf 0.28; ^{1}H nmr (CD_3OD): δ 7.85 (d, 1 H, $J_{3',5'}$ 2 Hz, H(3')), 7.60 (dd, 1 H, $J_{3',5'}$ 2, $J_{5',6'}$ 11 Hz, H(5')), 7.45 (d, 1 H, $J_{5',6'}$ 11 Hz, H(6')), 5.10 (d, 1 H, $J_{1,2}$ 8 Hz, H(1)), 3.95 (dd, 1 H, $J_{3,4}$ 14, $J_{4,5}$ 2 Hz, H(4)), 3.70 (dd, 1 H, $J_{2,3}$ 6, $J_{3,4}$ 14 Hz, H(3)), 3.60-3.35 (3 H, H(5), H(6), H(6')). Anal. calc. for $C_{12}H_{14}O_8NCl$+0.5H_2O; C, 41.81; H, 4.39; N, 4.06%; Found: C, 41.50; H, 4.33; N, 3.77%.

1.5. Deuterated Aryl β-D-Glucopyranosides

4'-Bromophenyl {1-^{2}H}-β-D-glucopyranoside (32)

The acetylated compound (**31**) was prepared according to Koenigs and Knorr from D-acetobromoglucose (0.292 g, 0.710 mmol) and 4-bromophenol (0.202 g, 1.13 mmol), and was recrystallized from ethanol to give white needles (0.080 g, 0.159 mmol, 22%). This material (0.065 g, 0.129 mmol) was deacetylated with sodium methoxide/methanol, and the product glucoside (**32**) was recrystallized from ethanol to produce fine white needles (0.015 g, 0.045 mmol, 35%). M.p.175-177°C; Rf 0.31; ^{1}H nmr (D_2O): δ 7.55 (d, 2 H, J 9 Hz, H(3'), H(5')), 7.05 (d, 2 H, J 9 Hz, H(2'), H(6')), 3.95 (dd, 1 H, $J_{3,4}$ 14, $J_{4,5}$ 2 Hz, H(4)), 3.70 (dd, 1 H, $J_{2,3}$ 5, $J_{3,4}$ 14 Hz, H(3)), 3.60-3.40 (4 H, H(2), H(5), H(6), H(6')). Anal. calc. for $C_{12}H_{15}DO_6Br$; C, 42.87; H, 4.64%; Found: C, 42.84; H, 4.54%.

4'-Nitrophenyl {1-^{2}H}-β-D-glucopyranoside (34)

The acetylated compound (**33**) was prepared according to Koenigs and Knorr from D-acetobromoglucose (1.022 g, 2.49 mmol) and 4-nitrophenol (0.710 g, 5.10 mmol), and was recrystallized from ethanol to give white needles (0.404 g, 0.859 mmol, 35%) This material (0.355 g, 0.754 mmol) was deacetylated with sodium methoxide/methanol. The product (**34**) crystallized after 2 hours, and was recrystallized from ether to produce fine white needles (0.156 g, 0.516 mmol, 68%). M.p. 164-166°C ; Rf 0.25; ^{1}H nmr (D_2O): δ 8.20 (d, 2 H, J 9 Hz, H(3'), H(5')), 7.10 (d, 2 H, J 9 Hz, H(2'), H(6')), 3.95 (dd, 1 H, $J_{3,4}$ 12, $J_{4,5}$ 2 Hz, H(4)), 3.70 (dd, 1 H, $J_{2,3}$ 4, $J_{3,4}$ 12 Hz, H(3)), 3.65-3.40 (4 H, H(2), H(5), H(6), H(6')). Anal. calc. for $C_{12}H_{14}DNO_8$: C, 47.68; H, 5.03; N, 4.63; Found: C, 47.44; H, 5.20; N, 4.47%.

3'-Nitrophenyl {1-^{2}H}-β-D-glucopyranoside (36)

The acetylated compound (**35**) was prepared according to Koenigs and Knorr from D-acetobromoglucose (0.300 g, 0.728 mmol) and 3-nitrophenol (0.500 g, 3.60 mmol), and was recrystallized from ethanol to give white needles (0.100 g, 0.212 mmol, 29%). This material (0.073 g, 0.16 mmol) was deacetylated with sodium methoxide/methanol, and the product glucoside (**36**) was recrystallized from ethanol to produce fine white needles (0.024 g, 0.079 mmol, 50%). M.p.166-167°C; Rf 0.32; ^{1}H nmr (D_2O): δ 8.00 (m, 2 H, H(2'), H(4')), 7.50 (m, 2 H, H(5'), H(6')), 3.95 (dd, 1 H, $J_{3,4}$ 11, $J_{4,5}$ 2 Hz, H(4)), 3.75-3.45 (5 H, H(2), H(3), H(5), H(6), H(6')). Anal. calc. for $C_{12}H_{14}DO_8N$; C, 47.68; H, 5.35; N, 4.63%; Found: C, 47.48; H, 5.06; N, 4.50%.

β-Naphthyl {1-^{2}H}-β-D-glucopyranoside (38)

The acetylated compound (**37**) was prepared according to Koenigs and Knorr from D-acetobromoglucose (0.961 g, 2.34 mmol) and β-naphthol (0.722 g, 5.00 mmol), and was recrystallized from ethanol to give white needles (0.376 g, 0.791 mmol, 34%). This material (0.120 g, 0.252 mmol) was deacetylated with sodium methoxide/methanol, and the product glucoside (**38**) was recrystallized from ethanol to produce fine white needles (0.065 g, 0.210 mmol, 83%). M.p.186-187°C; Rf 0.34; ^{1}H nmr (CD_3OD): δ 7.80 (m, 3 H, aromatic), 7.50-7.25 (4 H, aromatic), 3.95 (dd, 1 H, $J_{3,4}$ 11, $J_{4,5}$ 2 Hz, H(4)), 3.75 (dd, 1 H, $J_{2,3}$ 5, $J_{3,4}$ 11 Hz, H(3)), 3.55-3.35 (4 H, H(2), H(5), H(6), H(6')). Anal. calc. for $C_{16}H_{17}DO_6$+H_2O; C, 59.86; H, 6.21%; Found: C, 59.96; H, 6.15%.

2',4'-Dinitrophenyl {1-^{2}H}-β-D-glucopyranoside (40)

The acetylated compound (**39**) was obtained from Leise Berven. This material (0.523 g, 1.02 mmol), was deacetylated with HCl/methanol, and the product glucoside (**40**) was recrystallized from methanol/dichloromethane/acetone to produce fine white needles (0.165 g, 0.475 mmol, 47%). M.p.98-100°C; Rf 0.25; ^{1}H nmr (CD_3OD): δ

8.80 (d, 1 H, $J_{3',5'}$ 2 Hz, H(3')), 8.45 (dd, 1 H, $J_{5',6'}$ 11, $J_{3',5'}$ 2 Hz, H(5')), 7.65 (d, 1 H, $J_{5',6'}$ 11 Hz, H(5')), 3.95 (dd, 1 H, $J_{3,4}$ 14, $J_{4,5}$ 2 Hz, H(4)), 3.75 (dd, 1 H, $J_{2,3}$ 5, $J_{3,4}$ 14 Hz, H(3)), 3.60-3.30 (4 H, H(2), H(5), H(6), H(6')). Anal. calc. for $C_{12}H_{13D}O_{10}N_2+0.5H_2O+C_3H_6O$; C, 43.48; H, 5.12; N, 6.76%; Found: C, 43.62; H, 4.88; N, 7.00%.

1.6. Aryl 2-Deoxy-2-Fluoro-β-D-Glucopyranosides

4'-Nitrophenyl 2-deoxy-2-fluoro-β-D-glucopyranoside (42)

The acetylated compound (**41**) was prepared according to Koenigs and Knorr from 2F-acetobromoglucose (1.022 g, 2.75 mmol) and 4-nitrophenol (0.710 g, 5.10 mmol), and was recrystallized from ethanol to give white needles (0.404 g, 0.941 mmol, 34%). This material (0.355 g, 0.827 mmol) was deacetylated with sodium methoxide/methanol. The product (**42**) crystallized after 2 hours, and was recrystallized from ether to produce fine white needles (0.156 g, 0.514 mmol, 62%). M.p. 142-144°C; Rf 0.64; ^{1}H nmr (CD_3OD): δ 8.20 (d, 2 H, J 9 Hz, H(3'), H(5')), 7.10 (d, 2 H, J 9 Hz, H(2'), H(6')), 5.35 (dd, 1 H, $J_{1,2}$ 8, $J_{1,F}$ 3 Hz, H(1)), 4.50-4.25 (m, 1 H, $J_{1,2}$ 8, $J_{2,3}$ 10, $J_{2,F}$ 48 Hz, H(2)), 4.00 (dd, 1 H, $J_{3,4}$ 9, $J_{4,5}$ 2 Hz, H(4)), 3.65-3.45 (m, 4 H, H(3), H(5), H(6), H(6')). ^{19}F nmr (C_3D_6O): δ -123.22 (s). Anal. calc. for $C_{12}H_{14}O_7NF$; C, 47.52; H, 4.68; N, 4.62%; Found: C, 47.66; H, 4.68; N, 4.61%.

3',4'-Dinitrophenyl 2-deoxy-2-fluoro-β-D-glucopyranoside (44)

The acetylated compound (**43**) was prepared according to Koenigs and Knorr from 2F-acetobromoglucose (0.370 g, 0.997 mmol) and 3,4-dinitrophenol (0.420 g, 2.28 mmol). A complex mixture resulted which was purified twice by flash chromatography

(solvent system I; 1:1 ethyl acetate/hexane: solvent system II; 2:1 $CHCl_3$/ethyl acetate), and the product was crystallized from ethanol/water to give white solid (0.048 g, 0.101 mmol, 10%). This material (0.038 g, 0.080 mmol) was deacetylated with HCl/methanol, and the product glucoside (**44**) was recrystallized from methanol/dichloromethane/acetone to produce yellowish needles (0.024 g, 0.069 mmol, 87%). M.p. 138-139°C (dec.); Rf 0.73; ^1H nmr (CD_3OD): δ 8.15 (d, 1 H, $J_{5',6'}$ 11 Hz, H(5')), 7.65 (d, 1 H, $J_{2',6'}$ 2 Hz, H(2')), 7.50 (dd, 1 H, $J_{5',6'}$ 11, $J_{2',6'}$ 2 Hz, H(6')), 5.48 (dd, 1 H, $J_{1,2}$ 8, $J_{1,F}$ 3 Hz, H(1)), 4.50-4.25 (dt, 1 H, $J_{1,2}$ 8, $J_{2,3}$ 8, $J_{2,F}$ 51 Hz, H(2)), 3.85 (dd, 1 H, $J_{3,4}$ 8, $J_{4,5}$ 2 Hz, H(4)), 3.60-3.30 (m, 4 H, H(3), H(5), H(6), H(6')). ^{19}F nmr (C_3D_6O): δ -120.86 (s). Anal. calc. for $C_{12}H_{13}O_9N_2F+0.5H_2O$; C, 40.34; H, 3.96; N, 7.84%; Found: C, 40.29; H, 4.19; N, 7.69%.

2',4',6'-Trichlorophenyl 2-deoxy-2-fluoro-β-D-glucopyranoside (46)

The acetylated compound (**45**) was prepared according to Koenigs and Knorr from 2F-acetobromoglucose (0.200 g, 0.539 mmol) and 2,4,6-trichlorophenol (0.204 g, 1.03 mmol), precipitated after 2 hours, and was recrystallized from ethanol to give white needles (0.138 g, 0.283 mmol, 59%). This material (0.100 g, 0.205 mmol) was deacetylated with sodium methoxide/methanol, and the product glucoside (**46**) was recrystallized from acetone/dichloromethane/hexane to produce off-white solid (0.045 g, 0.124 mmol, 60%). M.p. 165-167°C (dec.); Rf 0.70; ^1H nmr (CD_3OD): δ 7.40 (s, 2 H, H(3'), H(5')), 5.30 (dd, 1 H, $J_{1,2}$ 8, $J_{1,F}$ 3 Hz, H(1)), 4.45-4.20 (dt, 1 H, $J_{1,2}$ 8, $J_{2,3}$ 8, $J_{2,F}$ 49 Hz, H(2)), 3.85-3.30 (5 H, H(3), H(4), H(5), H(6), H(6')). ^{19}F nmr (C_3D_6O): δ -122.34 (s). Anal. calc. for $C_{12}H_{12}O_5Cl_3F+0.5H_2O$; C, 38.88; H, 3.63; Found: C, 38.88; H, 3.49.

4'-Chloro-2'-Nitrophenyl 2-deoxy-2-fluoro-β-D-glucopyranoside (48)

The acetylated compound (**47**) was prepared according to Koenigs and Knorr from 2F-acetobromoglucose (0.225 g, 0.607 mmol) and 4-chloro-2-nitrophenol (0.330, 1.90 mmol). Product crystallized after two hours and was recrystallized from ethyl acetate/petroleum ether to give white needles (0.075 g, 0.162 mmol, 27%). This material (0.065 g, 0.140 mmol) was deacetylated with sodium methoxide, and the product glucoside (**48**) was recrystallized from ethyl acetate/hexane to produce yellowish crystals (0.038 g, 0.113 mmol, 81%). M.p.122-124°C ; Rf 0.30; ^{1}H nmr: δ 7.85 (d, 1 H, $J_{3',5'}$ 2 Hz, H(3')), 7.60 (dd, 1 H, $J_{3',5'}$ 2, $J_{5',6'}$ 11 Hz, H(5')), 7.45 (d, 1 H, $J_{5',6'}$ 11 Hz, H(6')), 5.40 (dd, 1 H, $J_{1,2}$ 8, $J_{1,F}$ 3 Hz, H(1)), 4.40-4.15 (dt, 1 H, $J_{1,2}$ 8, $J_{2,3}$ 8, $J_{2,F}$ 49 Hz, H(2)), 3.95 (dd, 1 H, $J_{3,4}$ 14, $J_{4,5}$ 2 Hz, H(4)), 3.60-3.30 (4 H, H(3), H(5), H(6), H(6')). ^{19}F nmr (C_3D_6O): δ -123.01 (s). Anal. calc. for $C_{12}H_{13}O_7NFCl+0.5H_2O$; C, 41.56; H, 4.08; N, 4.04%; Found: C, 41.25; H, 4.41; N, 3.70%.

2',5'-Dinitrophenyl 2-deoxy-2-fluoro-β-D-glucopyranoside (50)

The acetylated compound (**49**) was prepared according to Koenigs and Knorr from 2F-acetobromoglucose (0.300 g, 0.809 mmol) and 2,5-dinitrophenol (0.463, 2.52 mmol). A complex mixture resulted which was purified twice by flash chromatography (solvent system I; 1:1 ethyl acetate/hexane: solvent system II; 1:2.5 ethyl acetate/hexane), and the product was crystallized from ethanol/water to give yellowish solid (0.046 g, 0.101 mmol, 10%). This material (0.040 g, 0.084 mmol) was deacetylated with HCl/methanol, and the product glucoside (**50**) was recrystallized from acetone/dichloromethane to produce yellowish crystals (0.018 g, 0.052 mmol, 62%). M.p.122-124°C ; Rf 0.30; ^{1}H nmr: δ 8.30 (d, 1 H, J 2 Hz, H(6')), 8.00 (m, 2 H, H(3'), H(4')), 5.57 (dd, 1 H, $J_{1,2}$ 8, $J_{1,F}$ 3 Hz, H(1)), 4.40-4.20 (dt, 1 H, $J_{1,2}$ 8, $J_{2,3}$ 8, $J_{2,F}$ 49 Hz, H(2)), 3.95 (dd, 1 H, $J_{3,4}$ 14, $J_{4,5}$ 2 Hz, H(4)), 3.80-3.40 (4 H, H(3), H(5), H(6), H(6')). ^{19}F nmr (C_3D_6O): δ

-122.34 (s). Anal. calc. for $C_{12}H_{13}O_7NFCl+0.5H_2O+CH_2Cl_2$; C, 35.31; H, 3.65; N, 6.34%; Found: C, 35.35; H, 3.98; N, 6.31%.

2',4'-Dinitrophenyl 2-deoxy-2-fluoro-{1-^{2}H}-β-D-glucopyranoside (50)

The acetylated compound (**49**) was obtained from Leise Berven as an anomeric mixture (approximately 5% α), and was purified by preparative tlc, as follows. The material (0.045 g) was dissolved in ethyl acetate and spotted onto 6 glass tlc plates which were developed for approximately 1 hour (solvent; 1.5:1 $CHCl_3$/ethyl acetate). The bands of α- and β-glucosides were visualized under U.V. light, scraped separately off the plates, the gel collected and washed thoroughly with ethyl acetate. The solvent was removed in vacuo and the product crystallized from ethyl acetate/petroleum ether. The anomerically pure compound (β) (0.038 g, 0.080 mmol) was deacetylated with HCl/methanol, and the product (**50**) was recrystallized from acetone/dichloromethane/hexane to produce yellowish needles (0.016 g, 0.046 mmol, 58%). M.p. 123-126°C; Rf 0.60; ^{1}H nmr (CD_3OD): δ 8.75 (d, 1 H, $J_{3',5'}$ 2 Hz,H(3')), 8.50 (dd, 1 H, $J_{3',5'}$ 2, $J_{5',6'}$ 10 Hz, H(5')), 7.65 (d, 1 H, $J_{5',6'}$ 10 Hz, H(6')), 4.45-4.20 (dd, 1 H, $J_{2,3}$ 10, $J_{2,F}$ 51 Hz, H(2)), 3.93 (dd, 1 H, $J_{3,4}$ 10, $J_{4,5}$ 4 Hz, H(4)), 3.82-3.60 (m, 3 H, H(3), H(5), H(6)), 3.50 (m, 1 H, H(6')). ^{19}F nmr (C_3D_6O): δ -121.87 (s). Anal. calc. for $C_{12}H_{12}DO_9N_2F+2.5H_2O$; C, 40.83; H, 4.46; N, 7.27%; Found: C, 40.75; H, 4.40; N, 6.70%.

2. Enzymology

2.1. General Procedures

pABG-5 β-Glucosidase was generously provided by the Department of Microbiology, University of British Columbia. All absorbance measurements were made on a PU-8800 UV-Visible Spectrophotometer equipped with a circulating water bath.

Matched quartz cells were employed for all measurements except rates of hydrolysis of 4'-nitrophenyl-β-D-glucopyranoside, for which plastic cells were used. All cells used in this work had a 1 cm path length.

2.2. Extinction Coefficients

All extinction coefficients (ε) were determined at 37° C in 50 mM phosphate buffer at pH 6.8, using matched quartz cells. Phenols and glucosides were dried in vacuo over P_2O_5, weighed, and dissolved in a known volume of buffer. The stock solutions were diluted with buffer to give maximum absorbance values of 0.1 to 0.2. A wavelength scan was performed to determine λ_{max}, the wavelength of maximal absorbance, of the phenol and of the glucoside, and the assay wavelength was chosen as a point of maximal absorbance difference between phenol and glucoside. Accurate absorbance values of both phenol and glucoside were recorded at that wavelength, and extinction coefficients were determined from Beer's law:

$$\varepsilon = \frac{A}{bc} \qquad (23)$$

where A is absorbance, b is cell path length (1 cm in this work), and c is the concentration of the solution (M).

The extinction coefficient difference (Δε) between phenol and glucoside is used to convert the observed rate of change of absorbance (ΔA/min) during enzymatic hydrolysis to rate of phenol release (ΔmM/min):

$$v = \Delta A/\text{min} \div \Delta\varepsilon \qquad (24)$$

Extinction coefficients of the glucosides were verified in the following manner. A solution of glucoside of known absorbance at a specific wavelength was incubated with β-glucosidase until hydrolysis was complete. The concentration of phenol released was determined from the final absorbance, and since this is assumed to be equal to the initial

glucoside concentration, $\varepsilon_{glucoside}$ could be calculated. In cases where the two values of ε determined were different, the hydrolysis results were considered to be more accurate.

Extinction coefficients of the 2-deoxy-2-fluoroglucosides were assumed to be the same as those of the unsubstituted glucosides.

2.3. Determinations of K_m and k_{cat} for Hydrolysis of Aryl β-D-Glucopyranosides by pABG-5 β-Glucosidase

All kinetic measurements were performed at 37°C in 50 mM phosphate buffer (pH 6.8) containing 0.1% bovine serum albumin (BSA). Enzyme concentration and reaction times were chosen such that less than 10% of the total substrate was consumed, thus ensuring linear kinetics. (Enzyme concentrations used are given in the legends of the appropriate figures in Appendix III).

The rate of enzymic hydrolysis at each substrate concentration was determined as follows. Substrate stock, buffer and BSA were combined in a quartz spectrophotometer cell to give the appropriate substrate concentration. The cell was then equilibrated at 37°C, and pABG-5 β-glucosidase was injected into the cell. The rates of hydrolysis were followed spectrophotometrically at the appropriate wavelength of maximal absorbance difference between glucoside and the released phenol. Approximate values of K_m and k_{cat} were determined by measuring initial rates at three substrate concentrations covering a wide range. Accurate values were then found by measuring rates at seven to ten substrate concentrations ranging from approximately 0.15 times the value of K_m to 7 times K_m. The data are presented in this work as double reciprocal plots according to the method of Lineweaver and Burk[67], but this method was not used for calculating kinetic parameters due to the inaccuracy introduced by the non-linear error span. The values of K_m and k_{cat}

were calculated from a weighted non-linear regression analysis, using the Curvefitter program written for an Apple IIe computer by I. P. Street.

2.4. Determinations of K_i and k_i for Aryl 2-Deoxy-2-Fluoro-β-D-Glucopyranosides

Three different methods were employed in determining the kinetic parameters of inactivation of pABG-5 β-glucosidase by aryl 2-deoxy-2-fluoro-β-D-glucopyranosides, depending on the rate of inactivation.

2.4.1. Method of Phenolate Burst (Rapid Inactivation)

K_i and k_i were determined by following the rate of release of phenolate ion during inactivation of the enzyme, at a series of inactivator concentrations. Assay conditions were identical to those used with the normal aryl glucosides, but since each molecule of enzyme releases only one molecule of phenolate ion (and is then inactivated), a high enzyme concentration (~4 μM) must be used in order to obtain a reasonable absorbance change over the course of inactivation.

The inactivator stock solution was appropriately diluted with buffer and BSA in a quartz cell to afford the desired inactivator concentrations. The cells were then placed in the spectrophotometer cell block and equilibrated at 37°C. Because the rate of inactivation was quite high, enzyme was injected into the inactivation mixture and mixed quickly using a plastic stirring device without removing the cell from the cell block. This procedure minimized the time between addition of enzyme and start of absorbance detection, and thus the phenolate burst during inactivation could be observed at fairly high concentrations of inactivator. Absorbance values were recorded every seven seconds until the enzyme was fully inactivated.

The rate constant at each inactivator concentration, k_{obs}, can be calculated by plotting the fraction of active enzyme remaining *vs.* time, and fitting the data to an exponential decay function:

$$\frac{[E]_t}{[E]_o} = \exp\{-k_{obs}t\}, \qquad (25)$$

where $[E]_o$ is the initial concentration of enzyme.

Since the amount of phenol released during the course of the reaction is exactly equal to the amount of enzyme that has been inactivated, the fraction of active enzyme remaining can be determined from the absorbance change due to phenol released during the inactivation:

$$\frac{[E]_t}{[E]_o} = \frac{A_\infty - A_t}{A_\infty}, \qquad (26)$$

where A_t is the absorbance of the inactivation mixture at time t, and A_∞ is the absorbance at $t = \infty$, when the enzyme is fully inactivated. Thus, k_{obs} at each inactivator concentration was found by plotting $\frac{A_\infty - A_t}{A_\infty}$ vs. time and fitting the data to Equation 25 using an exponential fitting program on an Apple IIe computer. The overall K_i and k_i were determined by fitting the rate constants to Equation 27, a variation of the Michaelis-Menten equation, using the Curvefitter weighted regression program described previously.

$$k_{obs} = \frac{k_i [I]}{K_i + [I]} \qquad (27)$$

The observed rate constants are plotted according to Lineweaver-Burk for convenient visual inspection, and are presented in Appendix III.

2.4.2. Method of Phenolate Burst (Slow Inactivation).

Kinetic parameters for very slow substrates were determined in the same manner as with the rapid inactivators described above, by following the increase in absorbance due to release of phenolate ion at several different concentrations of inactivator. However, since the inactivation occurs quite slowly, absorbance values were recorded at 5 minute intervals for 16 to 18 hours. A control cell containing only inactivator solution showed no spontaneous hydrolysis over the course of the experiment. A second control containing enzyme and 0.1% BSA demonstrated no loss of enzyme activity over 18 hours at 37°C. (Activity was measured several times during the experiment by removal of an aliquot from the control cell and measuring the initial rate of hydrolysis of PNPG at saturating concentration.) Initial rates of inactivation were determined by plotting absorbance vs. time and measuring the initial slopes. Values of K_i and k_i were calculated using the Curvefitter weighted regression program, as described previously. The data are presented in Lineweaver-Burk fashion in Appendix III.

2.4.3. Method of Time-Dependent Inactivation

Solutions containing inactivator at several concentrations and 0.1% BSA were incubated at 37°C. pABG-5 β-Glucosidase was added to this inactivation mixture, and activity was tested at 1-2 minute intervals until the enzyme was fully inactivated. The residual activity at each time interval was found by diluting aliquots (10 μL) of the inactivation mixture into a relatively large volume (2 mL) of 4'-nitrophenyl-β-D-glucopyranoside at saturating concentration (~1 mM), and measuring the rate of release of 4-nitrophenolate ion, which is directly proportional to the amount of active enzyme remaining. This residual activity was plotted against time, and k_{obs} at each inactivator concentration was calculated using the exponential fitting program described in Section

2.4.1. The values of K_i and k_i were obtained from the Curvefitter weighted regression program.

2.5. α-Secondary Kinetic Isotope Effect Values for Aryl β-D-Glucopyranosides

The α-secondary kinetic isotope effects were determined by comparison of initial rates of hydrolysis of protio and deuterio substrates at high concentration, approximately ten times the value of K_m. This ensures that the enzyme is fully saturated with substrate, and thus slight differences in substrate concentration will cause no measurable difference in rate. To insure consistent enzyme concentration, a volume of appropriately diluted enzyme sufficient for the entire experiment was prepared (containing 0.1% BSA), and aliquots of this solution were pipetted into quartz cells, and then equilibrated at 37°C. Small volumes (50-100μL) of substrate solution were injected into the cell, and initial velocity determined. Rates of protio and deuterio substrates were measured alternately until a total of nine or ten rates for each compound had been determined. The values of k_H and k_D were calculated as the average of the initial rates.

Because observed rate differences between protio and deuterio glucosides could be due to trace contaminants of some unknown inhibitor, the kinetic isotope effect values were confirmed at higher substrate concentration, up to twenty times K_m if possible. If the deuterium substitution is indeed the sole source of the observed rate effect, the value of k_H/k_D should be the same at both concentrations.

The wavelength used for the kinetic isotope effect determination for 3'-nitrophenyl-β-D- glucopyranoside was chosen as 375 nm (slightly different from the K_m and k_{cat} assay wavelength of 380 nm) in order to obtain a somewhat larger extinction coefficient difference between glucoside and released phenol. All other isotope effect experiments were performed at the same wavelength as the K_m and k_{cat} determinations.

APPENDIX I
BASIC CONCEPTS OF ENZYME CATALYSIS

An understanding of the processes which contribute to enzyme catalysis is essential to the interpretation of kinetic data. The following sections will address several topics:

1. the treatment of kinetic data,
2. the kinetics of enzyme inactivation,
3. the definition of kinetic parameters in terms of free energy changes, and
4. the importance of enzyme-transition state complementarity to enzyme catalysis.

1. Fundamental Equations of Enzyme Kinetics[61]

The basic equation of enzyme kinetics is the Michaelis-Menten equation:

$$v = \frac{[E]_o[S]k_{cat}}{K_m + [S]} \qquad (28)$$

v is the velocity of the reaction (measured as rate of breakdown of substrate or appearance of product), $[E]_o$ is the total enzyme concentration, [S] is the substrate concentration, k_{cat} is the catalytic constant, and K_m is termed the Michaelis constant.

Note that v will exhibit "saturation kinetics" with respect to [S]; that is, when [S] « K_m, v will increase linearly with [S], but at high substrate concentration, v approaches a limiting value, $V_{max} = k_{cat}[E]_o$.

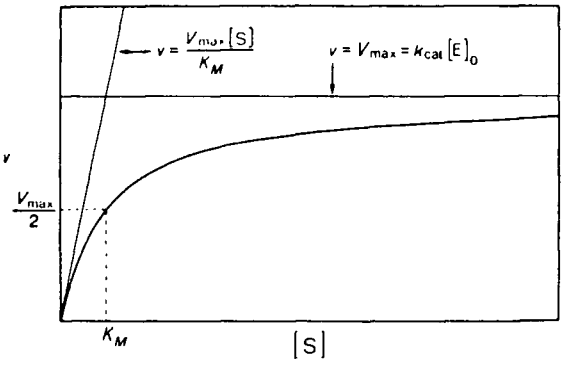

Figure 22. Velocity vs. substrate concentration for a typical enzymatic reaction.

K_m is that substrate concentration where $v = V_{max}/2$. The value of K_m may be treated as an apparent dissociation constant for all enzyme-bound species. That is,

$$\frac{[E][S]}{\Sigma[ES]} = K_m \qquad (29)$$

K_m is therefore used as an indicator of the stability of the bound enzyme-substrate complex. A substrate with a low K_m is said to bind tightly to the enzyme.

Note from the Michaelis-Menten equation that when $[S] \ll K_m$, the equation reduces to

$$v = \frac{k_{cat}}{K_m}[E]_o[S] \qquad (30)$$

Since [S] is low, most of the enzyme is unbound, and $[E]_o \approx [E]$, thus;

$$v = \frac{k_{cat}}{K_m}[E][S] \qquad (31)$$

k_{cat}/K_m is therefore an apparent second-order rate constant for the reaction of <u>free</u> enzyme with <u>free</u> substrate. k_{cat}/K_m is the indicator of the overall catalytic efficiency of the enzyme.

A very convenient form of graphical representation of enzymic rate data is that of Lineweaver and Burk[67] (Figure 23). This converts the Michaelis-Menten equation into a linear plot which can highlight data which deviate from the expected behavior. The relationship is found by inverting both sides of the Michaelis-Menten equation:

$$\frac{1}{v} = \frac{1}{V_{max}} + \frac{K_m}{V_{max}[S]} \qquad (32)$$

Graphing 1/v vs. 1/[S] results in a straight line with y-intercept equal to $1/V_{max}$, x-intercept equal to $-1/K_m$, and slope K_m/V_{max}.

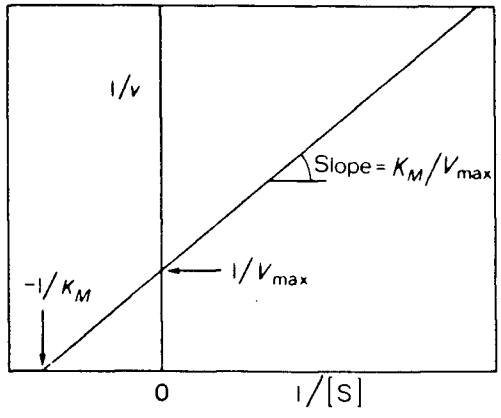

Figure 23. A typical Lineweaver-Burk plot.

2. Kinetics of Inactivation of pABG-5 β-glucosidase

The kinetic mechanism proposed for "retaining" glycosidases consists of binding, glycosylation, and deglycosylation steps, and can be expressed as in Scheme 16.

$$E + GX \underset{k_{-1}}{\overset{k_1}{\rightleftharpoons}} E \cdot GX \xrightarrow[HX]{k_2} E\text{-}G \xrightarrow[H_2O]{k_3} E + GOH$$

Scheme 16. Kinetic model for a "retaining" glycosidase.

When k_3 is extremely slow relative to k_2, all of the enzyme rapidly accumulates as the covalent glycosyl-enzyme complex, and the rate of glycosylation can be determined, even when X is a highly activated leaving group (as in the case of the 2-deoxy-2-fluoro-β-D-glucopyranosides). If [GX] is much greater than $[E]_o$, i.e. [GX] - $[E]_o \approx$ [GX], the concentration of GX is essentially constant over the course of the reaction, and the kinetics are pseudo-first-order with respect to enzyme concentration. The Michaelis-Menten equation for this inactivation can be written as:

$$v = \frac{k_i[E]_o[GX]}{K_i + [GX]} \qquad (33)$$

where k_i is the rate constant of inactivation and K_i is the apparent dissociation constant for all species of enzyme-bound inactivator (compare Equation 29). Since [GX] is assumed constant over the course of the reaction, Equation 33 can be rewritten as:

$$v = k_{obs}[E]_t \qquad (34)$$

where

$$k_{obs} = \frac{k_i[GX]}{K_i + [GX]} \qquad (35)$$

The value of k_{obs} at each inactivator concentration can be determined by fitting this velocity data to a standard exponential decay function. Also, since each molecule of HX released corresponds to one molecule of enzyme inactivated,

$$v = \frac{d[HX]}{dt} = -\frac{d[E]_t}{dt} \qquad (36)$$

and

$$-\frac{d[E]_t}{dt} = k_{obs}[E]_t \qquad (37)$$

$$-\frac{d[E]_t}{[E]_t} = k_{obs}\,dt \qquad (38)$$

Therefore,

$$\ln \frac{[E]_t}{[E]_o} = -k_{obs}\,t \qquad (39)$$

By substituting k_{obs} values into Equation 35, the inactivation parameters k_i and K_i can be determined.

3. Transition State Stabilization and Enzyme Catalysis

All catalysts function by stabilizing the transition state of a reaction, thus lowering the energy barrier for product formation, and accelerating the reaction rate. Enzymes are unique as catalysts in that they specifically bind their substrates within a well-defined active site. However, since the substrate structure is continually changing during the course of the reaction, the enzyme can only be fully complementary to one form of the substrate. It

will be shown here that enzymes achieve maximal efficiency by being complementary to the transition state for reaction of their substrate, rather than to the ground state.

Figure 24 shows how the kinetic parameters of a typical enzyme reaction, consisting of a binding step and a catalytic step, can be defined in terms of the free energy changes which occur along the reaction pathway.

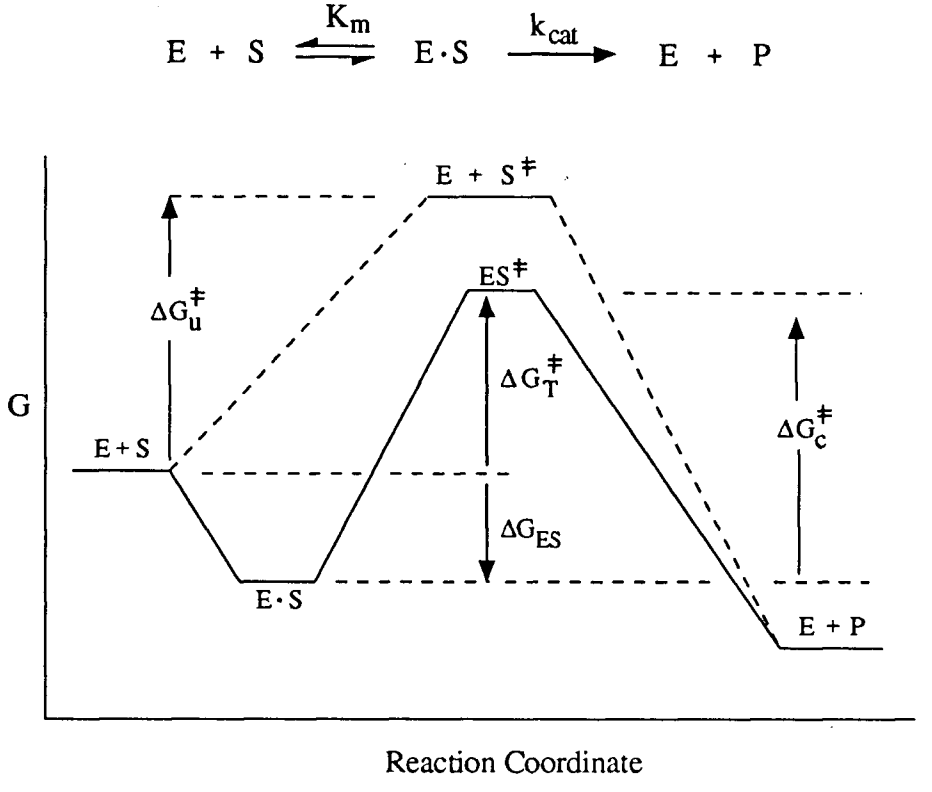

Figure 24. Free energy diagram for a typical enzymic reaction (solid line) and its corresponding uncatalyzed reaction (dashed line).

K_m equals $\exp\{-\Delta G_{ES}/RT\}$, k_{cat} is equal to $(\mathbf{k}T/h)\exp\{-\Delta G_c^{\ddagger}/RT\}$, and k_{cat}/K_m is equal to $(\mathbf{k}T/h)\exp\{-\Delta G_T^{\ddagger}/RT\}$. ($\mathbf{k}$ is the Boltzmann constant, and h is Planck's constant). The level of E·S may be higher or lower than E + S depending on the exact reaction conditions. (This represents the limiting case wherein the dissociation of the Michaelis complex to free

enzyme and substrate is much faster than turnover to product, so K_m is equal to K_S, the dissociation constant of the Michaelis complex.)

Now, suppose that an extra amount of binding energy, ΔG_R, is available which may be realized at the ground state but not at the transition state. For example, a hydrogen-bonding contact might be present at the ground state, but is lost at the transition state. Such a situation is depicted in Figure 25A. Figure 25B represents the case wherein ΔG_R is realized at the transition state, but not at the ground state (only the events leading to the transition state are shown in Figure 25).

When the ground state is stabilized, relative to that in the reaction depicted in Figure 24, ΔG_{ES} is increased by ΔG_R, and thus K_m is lowered (tighter binding). However, $\Delta G_c^{\ddagger}$ is also increased by this ground state stabilization, and k_{cat} is reduced. The value of k_{cat}/K_m, the rate constant for free enzyme and substrate proceeding to the transition state, is unaffected by the increased stability of the ground state. In Figure 25B, where $ES^{\ddagger}$ is preferentially stabilized, both k_{cat} and k_{cat}/K_m will be increased as a result of realizing ΔG_R at the transition state.

Comparison of the two outcomes in Figure 25 shows that when the enzyme is complementary to the transition state rather than to the ground state:

1. the activation energy ($\Delta G_c^{\ddagger}$) is lower, and therefore k_{cat} is higher,
2. k_{cat}/K_m, the measure of overall enzyme efficiency, is increased by a factor of

$$\exp(\Delta G_R/RT).$$

Thus stabilization of the transition state is of utmost importance to the catalytic power of enzymes.

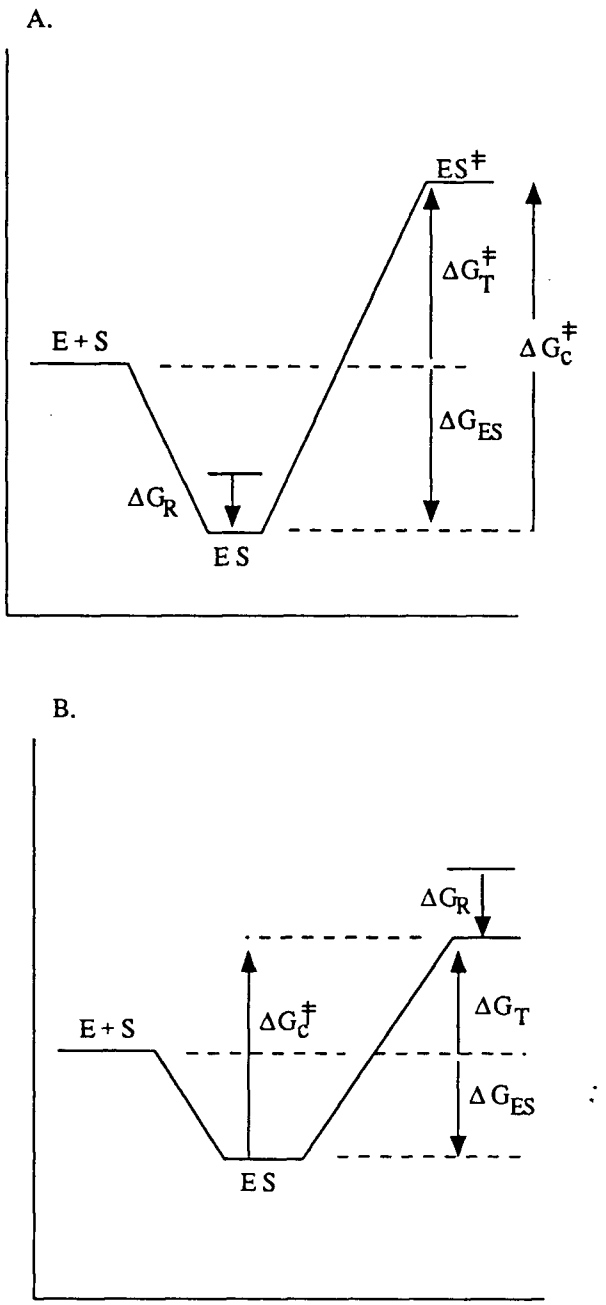

Figure 25. Free energy diagram of an enzymic reaction involving: A. Maximum enzyme-substrate complementarity at the ground state: B. Maximum enzyme-substrate complementarity at the transition state.

APPENDIX II

ORIGIN AND INTERPRETATION OF KINETIC ISOTOPE EFFECTS

1. Introduction

An isotope effect is defined as a difference in reaction rate or position of equilibrium brought about by an isotopic substitution in a reactant. The term "kinetic isotope effect" is used to indicate a rate as opposed to an equilibrium process. It is given by the ratio of rate constants for isotopically unsubstituted and substituted compounds, k_{light}/k_{heavy} (k_H/k_D for deuterium effects).

Isotope effects are very useful as probes of reaction mechanism because they do not perturb the electronic nature of the system, since according to the Born-Oppenheimer principle, the electronic structure of a molecule is essentially insensitive to differences in nuclear masses[81]. This is especially important in exploring enzyme mechanisms, where a more drastically altered substrate could cause a change in the reaction pathway.

This discussion will focus on deuterium isotope effects, but the principles are equally valid for heavier elements, e.g. $^{16}O/^{18}O$, $^{12}C/^{13}C$.

2. Theory

2.1. Primary Isotope Effects[82]

A primary isotope effect occurs in a reaction in which a bond to the isotopically substituted atom is broken or formed in the rate-determining step. Any bond, for example a C-H bond, may be thought of as a harmonic oscillator undergoing a series of characteristic vibrations which impart some energy to the molecule, its zero-point energy. The energy associated with these vibrations is related to the mass of the atoms which are vibrating: $E_0 = 1/2h\nu$, where h is Planck's constant, and the vibrational frequency, ν, is defined as:

$$\nu = \frac{1}{2\pi}\sqrt{K/\mu} \qquad (40)$$

K is the force constant of the bond and μ the reduced mass of the oscillating system. (K does not vary with isotopic substitution). Since deuterium has a higher mass than hydrogen, the vibrations of the C-D bond contribute less to the zero-point energy than the corresponding C-H bond. Therefore, substituting deuterium for hydrogen results in a lowering of the molecule's zero-point energy. When the bond to hydrogen (or deuterium) is cleaved, a vibrational degree of freedom is converted to a translational degree of freedom on passing through the transition state, and so no longer contributes an energy difference at the transition state. (The isotopically substituted and unsubstituted molecules are considered to pass through the same transition state). Thus the lower zero-point energy of the C-D bond results in a higher energy of activation for bond cleavage, and a slower rate of reaction (Figure 26).

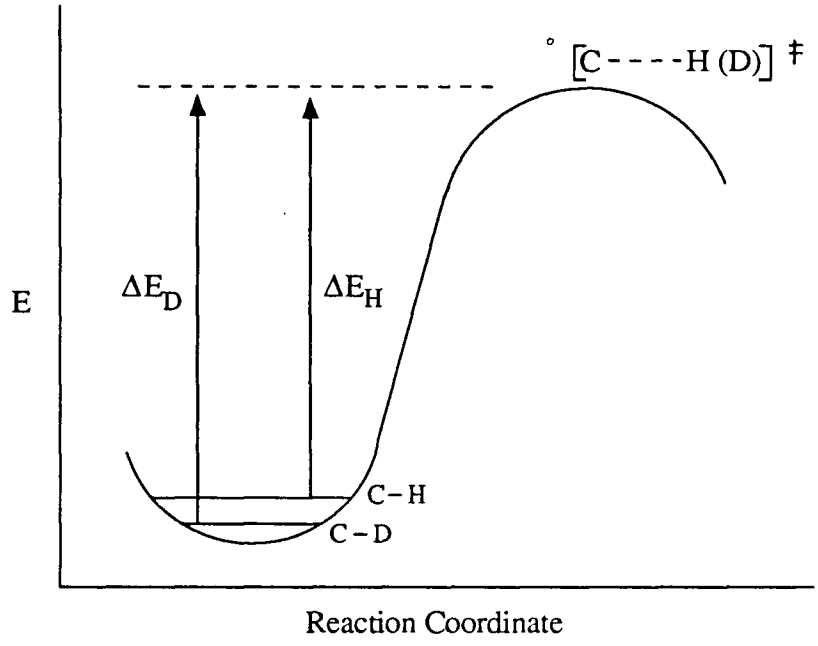

Figure 26. Origin of a primary isotope effect due to deuterium substitution. The substitution causes a difference in zero-point vibrational energy in the ground state, but not at the transition state; thus $k_H > k_D$.

Primary deuterium kinetic isotope effects have a theoretical maximum value of about 7. Typical k_H/k_D values are in the range 2 to 7. An isotope effect in this range is strong evidence for a mechanism which involves C-H(D) bond breaking in the rate-determining step. The magnitude of the isotope effect gives a qualitative indication of where the transition state lies in relation to products and reactants. A value approaching the theoretical maximum implies nearly complete bond cleavage at the transition state. A lower value indicates a transition state that more closely resembles the reactants, where little bond cleavage has occurred.

2.2. Secondary Kinetic Isotope Effects

A secondary kinetic isotope effect is a difference in reaction rate brought about by the isotopic substitution of atoms to which no bonds are broken or formed during the course of the reaction. These effects are the result of rehybridization of the reacting center in the rate-determining step. They are classified as α, β, or remote (γ, δ), depending on their position relative to the reaction center. α-substitutions are those where the isotope is directly attached to the atom undergoing covalency change; β-effects involve substitution on an atom adjacent to the reaction center.

2.2.1. α-Secondary Kinetic Isotope Effects[83]

α-Secondary deuterium isotope effects arise from changes in the bending frequencies of isotopic bonds in reaching the transition state. The difference in zero-point energy between isotopically-labelled reactants (discussed in Section 2.1) can be altered in one of two ways in reaching the transition state, depending on the changes in the relevant force constants of the isotopic vibrational mode.

A change from sp^3 to sp^2 hybridization at the transition state results in a "freeing up" of the C-H(D) bending mode (i.e. a lower bending frequency), decreasing the force constant, K, of the vibration. Since the difference in zero-point energies of the C-H and C-

D bonds is proportional to $(K/\mu)^{1/2}$, the energy levels will be closer together at the transition state. This will result in a lower activation energy, and thus a faster rate, for the hydrogen-substituted molecule than for the deuterium-substituted species (Figure 27, Case A). This is a "normal" isotope effect, with $k_H/k_D > 1.0$. The converse of this will apply when the rate-determining step involves rehybridization from sp^2 to sp^3 (Figure 27, Case B). The force constant increases at the transition state, driving the C-H and C-D levels farther apart. A reaction of this type will exhibit an isotope effect < 1.0.

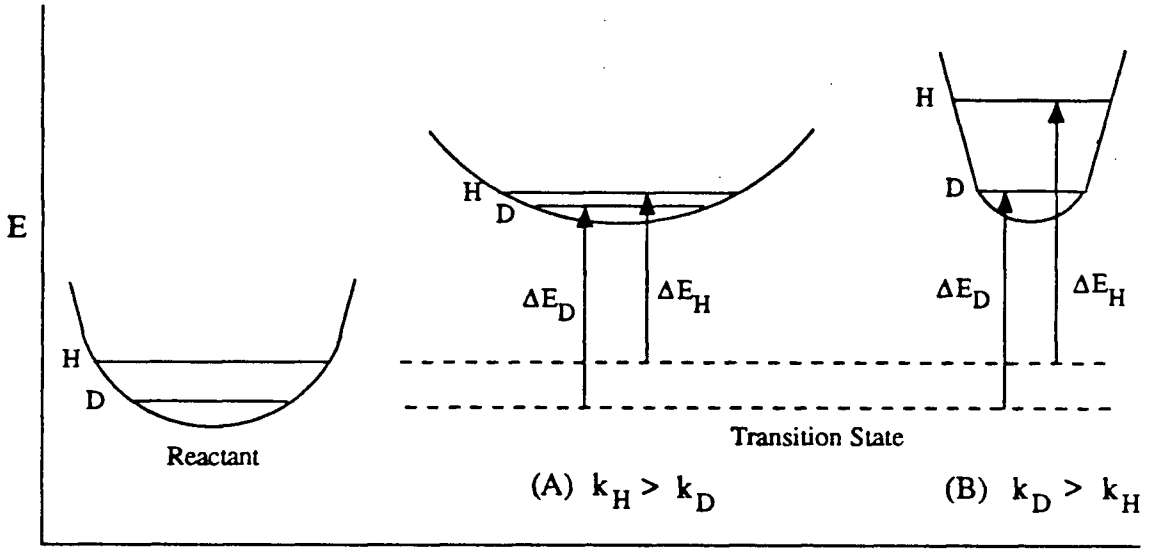

Figure 27. Energy profiles illustrating the change in zero-point energy difference between H- and D-substituted species on going to the transition state. (A). "Normal" isotope effect; the force constant of the bond decreases upon approaching the transition state. (B). "Inverse" isotope effect; the force constant of the bond increases upon proceeding to the transition state.

A normal α-secondary deuterium kinetic isotope effect can have a maximum value of about 1.40, but generally a value of 1.10 to 1.25 is considered indicative of a large

degree of sp^3 to sp^2 rehybridization at the transition state. A k_H/k_D value of 1.00 implies an S_N2 mechanism. However, S_N2 reactions can have secondary isotope effects $\neq$ 1.00. Temperature dependence and theoretical calculations of such isotope effects have indicated that relative degrees of bond breaking and bond formation, as well as temperature, affect the magnitude of the observed isotope effect.

2.2.2. β-Secondary Kinetic Isotope Effects [84]

β-Deuterium kinetic isotope effects are observed in S_N1 reactions and are believed to arise from weakening of the C-H(D) bond by hyperconjugation with the adjacent electron-deficient carbon atom (Figure 28). Since deuterium is slightly electron-donating with respect to hydrogen, a C-D bond is stronger and the electrons are less available for hyperconjugation to stabilize the positive charge. Therefore, the deuterium-substituted molecule will be less stable at the transition state and have a higher energy of activation, thus exhibiting a normal isotope effect. Strong evidence for this is the fact that β-k_H/k_D values correlate very well with the electron demand at the carbonium-ion center. When the molecule contains electron-releasing substituents, they decrease the need for hyperconjugative stabilization of the carbonium ion, and thereby decrease the isotope effect. Typical β-kinetic isotope effects range from approximately 5 to 15% per deuteron.

β-Secondary kinetic isotope effects are also extremely dependent upon molecular geometry, since proper spatial arrangement is required for orbital overlap. If the C-H(D) bond is orthogonal to the electron-deficient p-orbital, there can be no hyperconjugation. In fact, there may in this case be an inverse effect due to induction, since the deuterium is slightly more electron-donating. These inverse effects are usually quite small, no more than 5%.

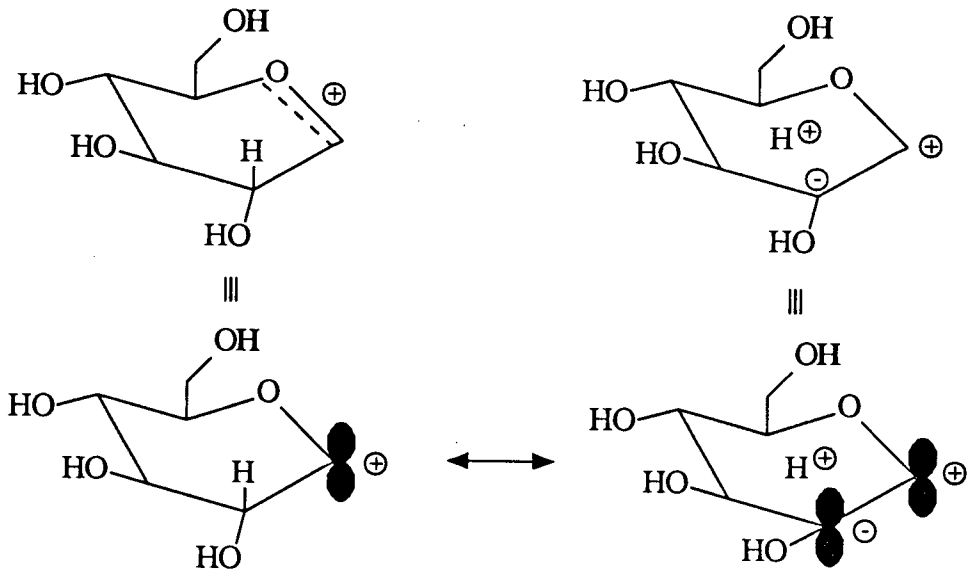

Figure 28. Hyperconjugation in an oxocarbonium ion.[67]

APPENDIX III

GRAPHICAL REPRESENTATION OF KINETIC DATA

1. Lineweaver-Burk Plots for Hydrolysis of Aryl β-D-Glucopyranosides by pABG-5 β-Glucosidase.

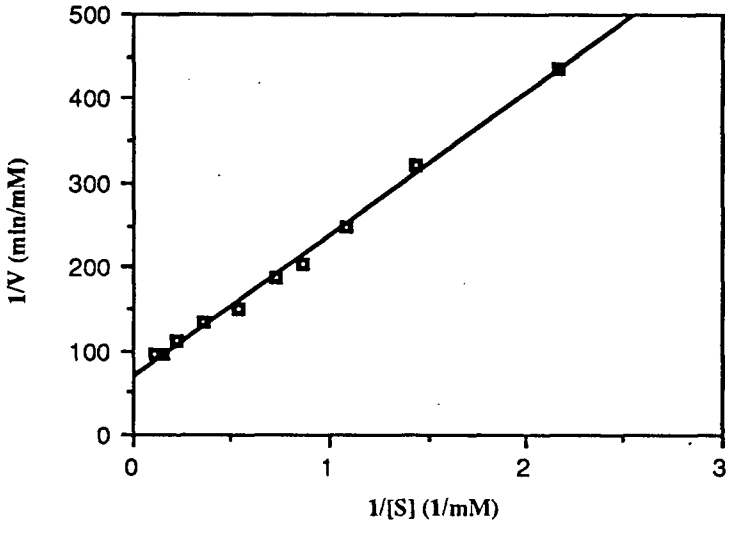

Figure 29. Hydrolysis of phenyl β-D-glucopyranoside.
Enzyme concentration = 2.65 x 10^{-3} mg/mL.

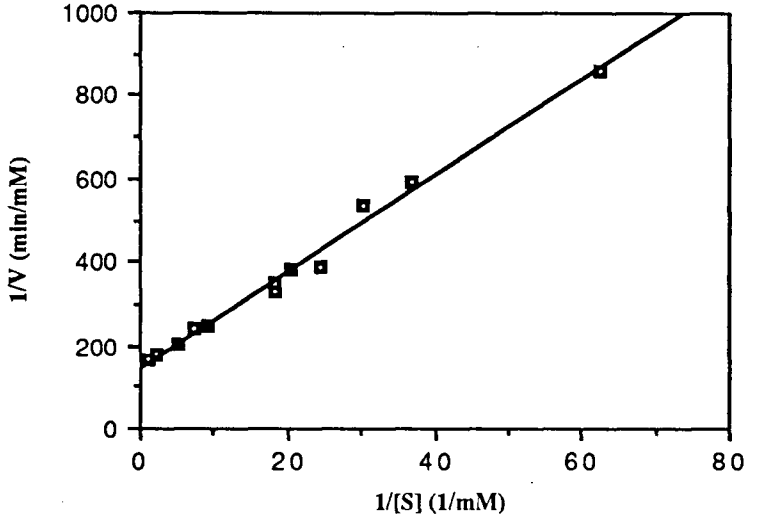

Figure 30. Hydrolysis of 4'-t-butylphenyl β-D-glucopyranoside.
Enzyme concentration = 1.45 x 10^{-3} mg/mL.

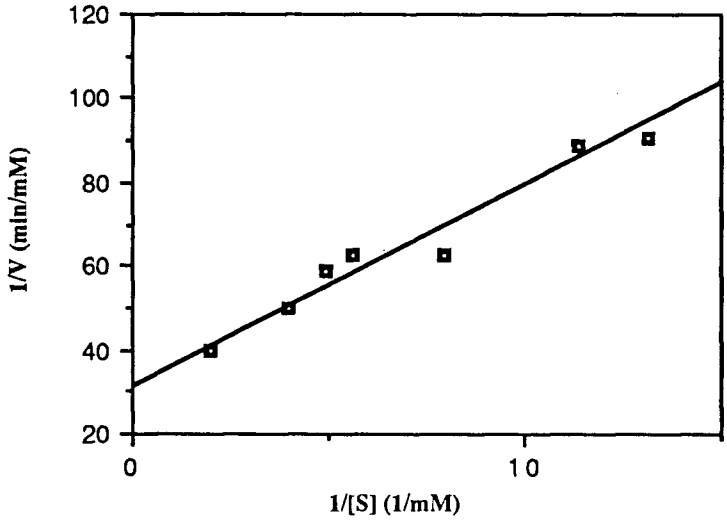

Figure 31. Hydrolysis of β-naphthyl β-D-glucopyranoside.
Enzyme concentration = 1.33 x 10^{-3} mg/mL.

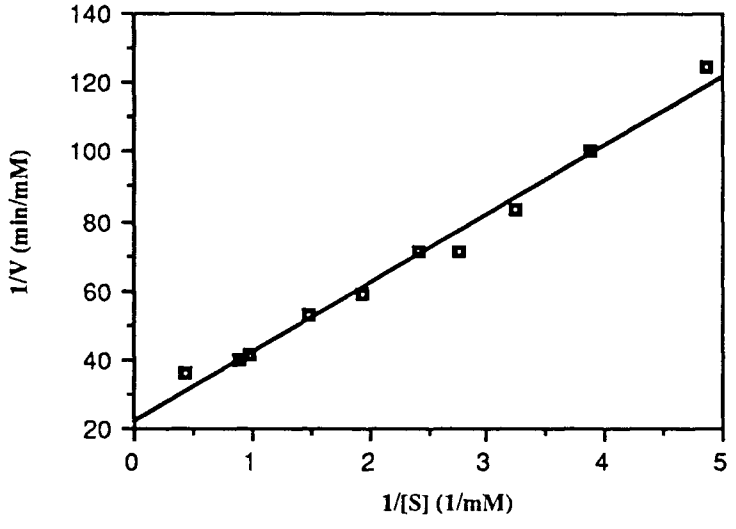

Figure 32. Hydrolysis of 4'-chlorophenyl β-D-glucopyranoside.
Enzyme concentration = 1.80 x 10^{-3} mg/mL.

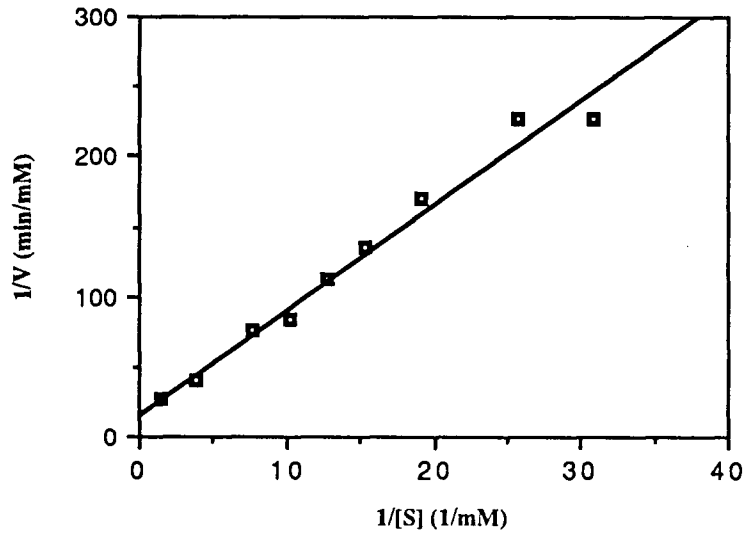

Figure 33. Hydrolysis of 4'-bromophenyl β-D-glucopyranoside.
Enzyme concentration = 1.42 x 10^{-3} mg/mL.

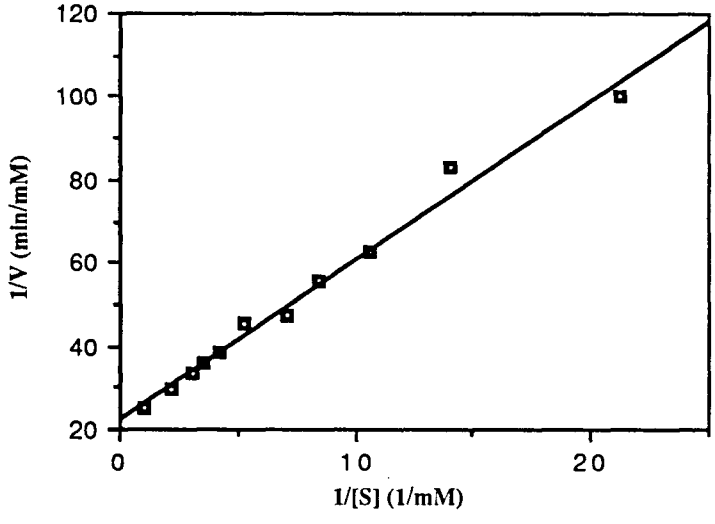

Figure 34. Hydrolysis of 4'-cyanophenyl β-D-glucopyranoside.
Enzyme concentration = 1.04 x 10^{-4} mg/mL.

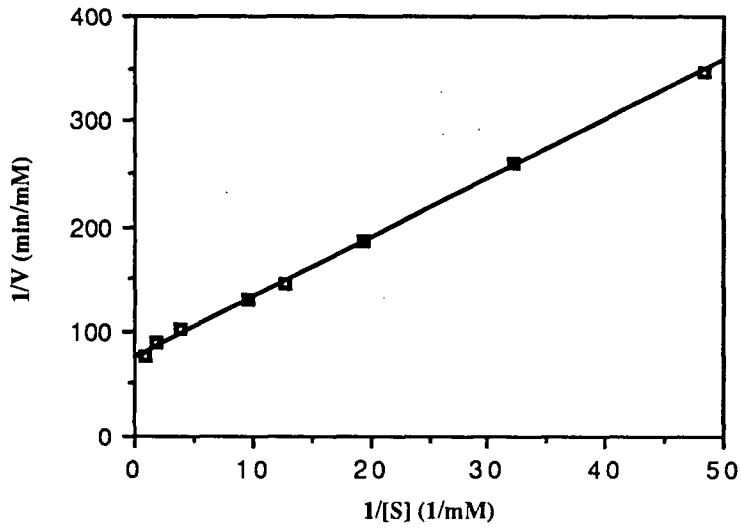

Figure 35. Hydrolysis of 4'-nitrophenyl β-D-glucopyranoside.
Enzyme concentration = 6.60 x 10^{-5} mg/mL.

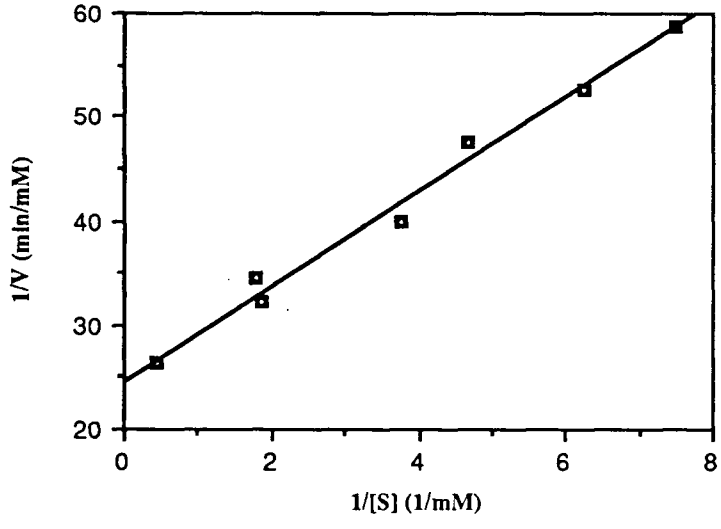

Figure 36. Hydrolysis of 3'-nitrophenyl β-D-glucopyranoside.
Enzyme concentration = 8.18 x 10^{-4} mg/mL.

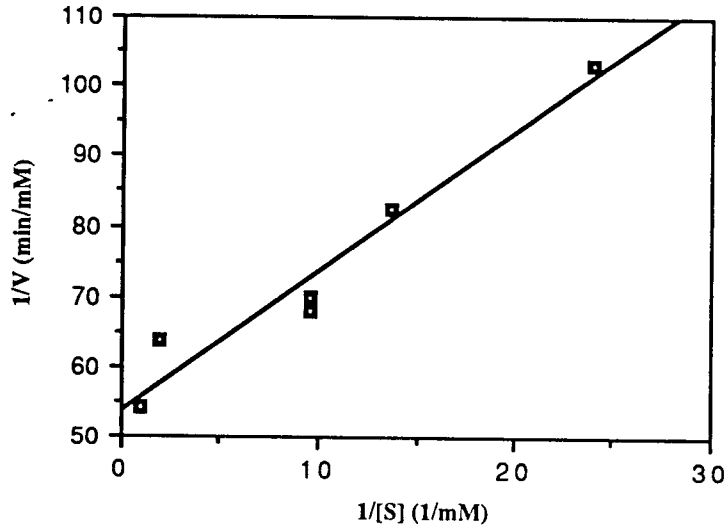

Figure 37. Hydrolysis of 2'-nitrophenyl β-D-glucopyranoside.
Enzyme concentration = 1.36 x 10^{-4} mg/mL.

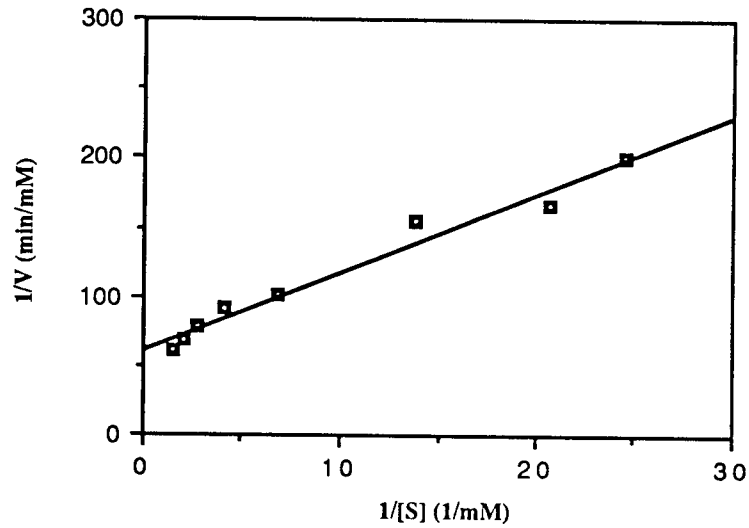

Figure 38. Hydrolysis of 3',5'-dichlorophenyl β-D-glucopyranoside.
Enzyme concentration = 1.58 x 10^{-4} mg/mL.

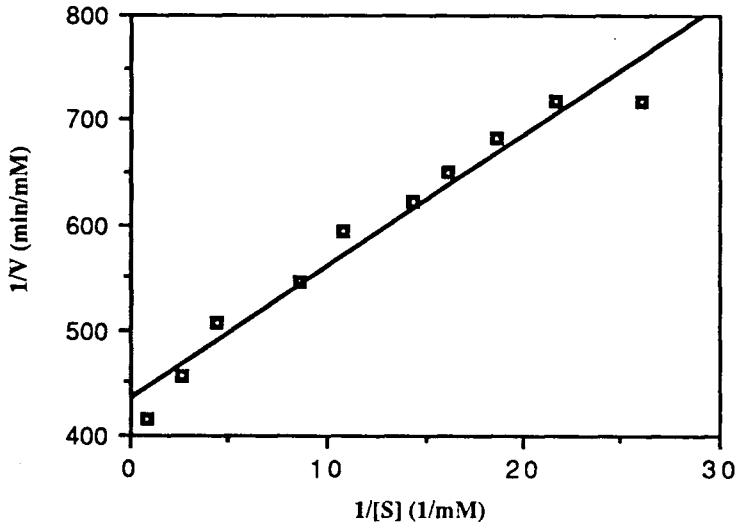

Figure 39. Hydrolysis of 3',4'-dinitrophenyl β-D-glucopyranoside.
Enzyme concentration = 1.33 x 10^{-5} mg/mL.

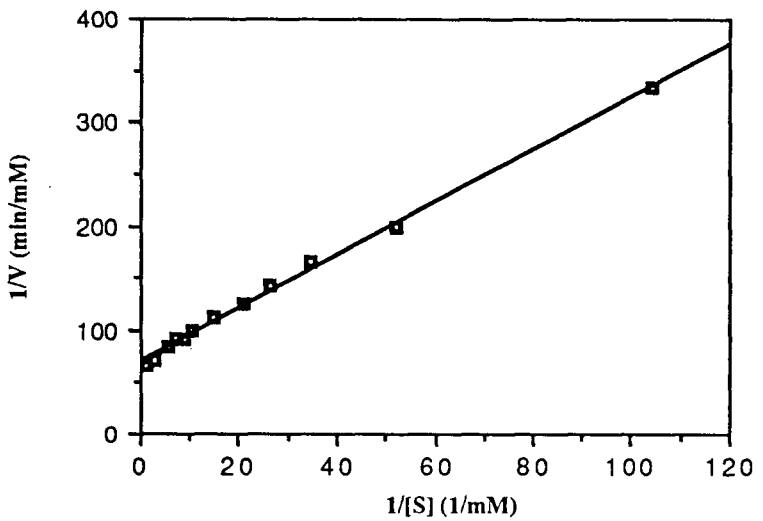

Figure 40. Hydrolysis of 2',5'-dinitrophenyl β-D-glucopyranoside.
Enzyme concentration = 2.48 x 10^{-5} mg/mL.

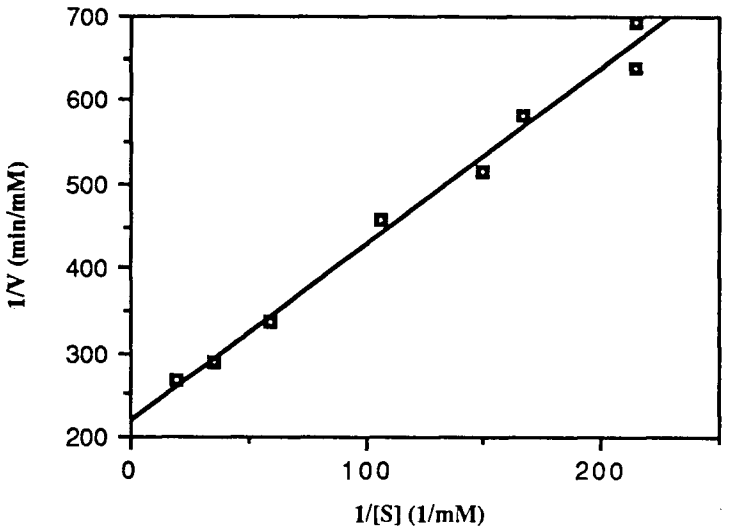

Figure 41. Hydrolysis of 2',4',6'-trichlorophenyl β-D-glucopyranoside.
Enzyme concentration = 1.58 x 10^{-5} mg/mL.

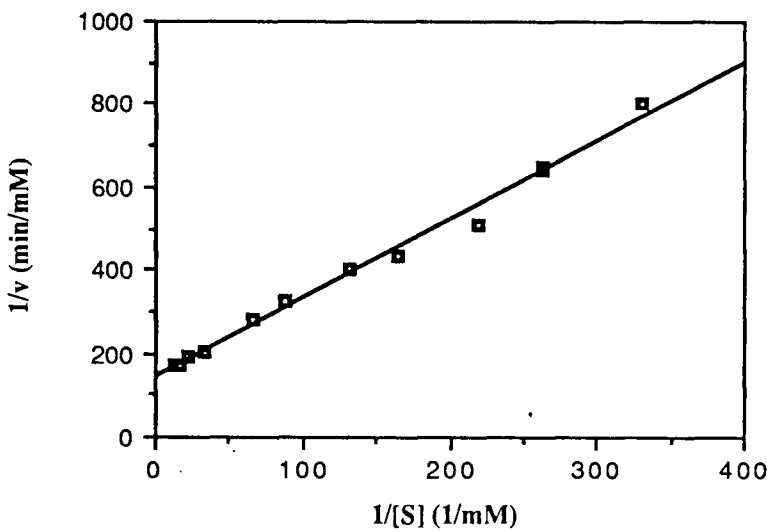

Figure 42. Hydrolysis of 4'-chloro-2'-nitrophenyl β-D-glucopyranoside.
Enzyme concentration = 3.99 x 10^{-5} mg/mL.

2. Inactivation of pABG-5 β-Glucosidase by 2-Deoxy-2-fluoro-β-D-glucopyranosides

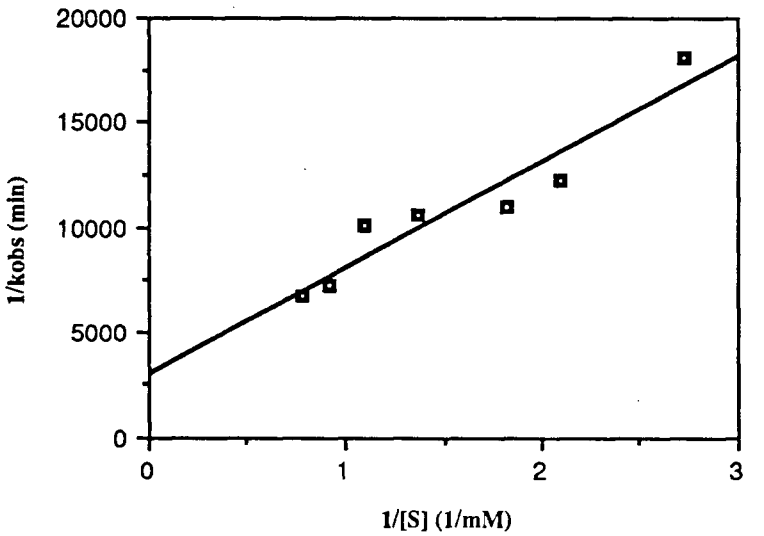

Figure 43. Inactivation of β-glucosidase by 4'-nitrophenyl 2-deoxy-2-fluoro-β-D-glucopyranoside.
Enzyme concentration = 4.56 x 10^{-1} mg/mL.

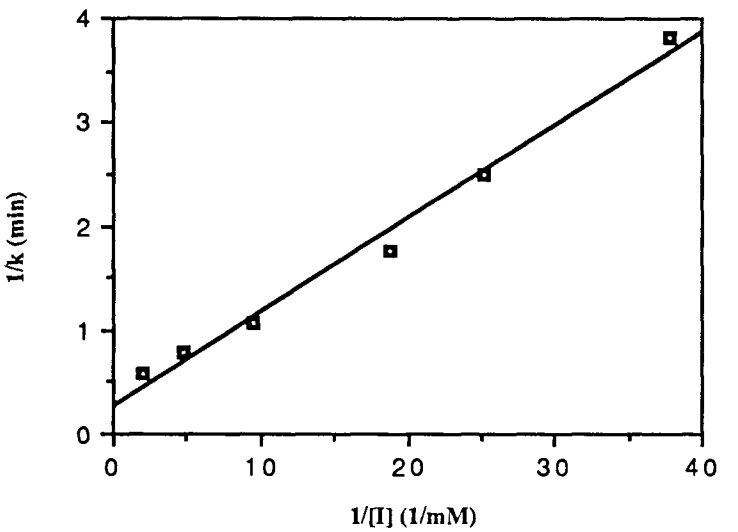

Figure 44. Inactivation of β-glucosidase by 2',4',6'-trichlorophenyl 2-deoxy-2-fluoro-β-D-glucopyranoside.
Enzyme concentration = 2.26 x 10^{-1} mg/mL.

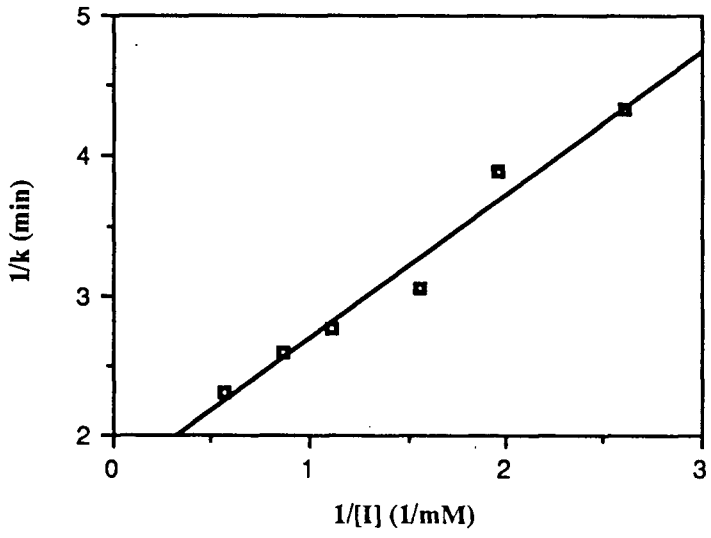

Figure 45. Inactivation of β-glucosidase by 3',4'-dinitrophenyl 2-deoxy-2-fluoro-β-D-glucopyranoside.
Enzyme concentration = 2.09 x 10^{-1} mg/mL.

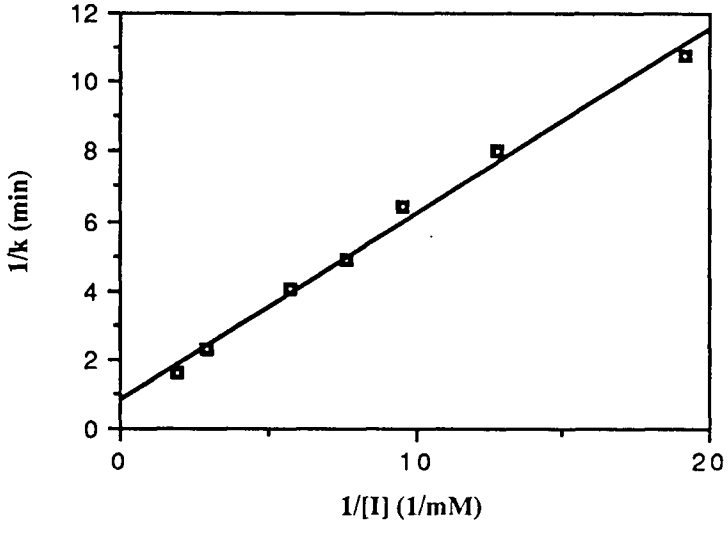

Figure 46. Inactivation of β-glucosidase by 4'-chloro-2'-nitrophenyl 2-deoxy-2-fluoro-β-D-glucopyranoside.
Enzyme concentration = 1.94 x 10^{-1} mg/mL.

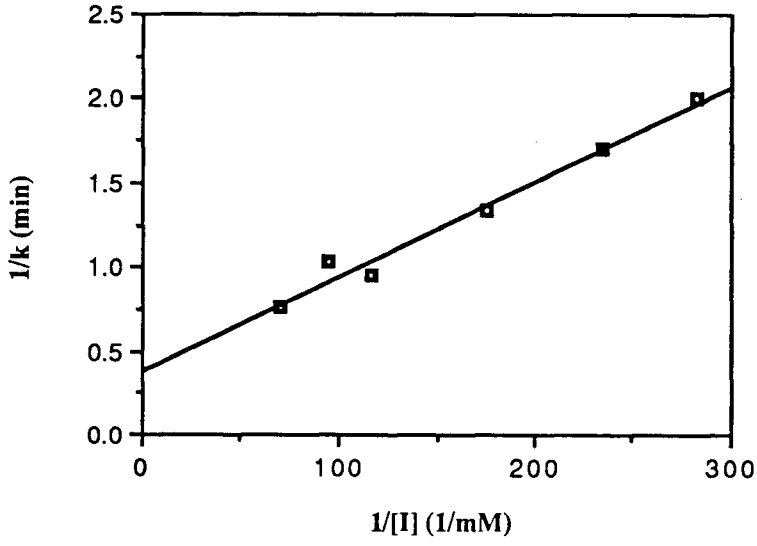

Figure 47. Inactivation of β-glucosidase by 2',5'-dinitrophenyl 2-deoxy-2-fluoro-β-D-glucopyranoside.
Enzyme concentration = 2.09 x 10^{-1} mg/mL.

REFERENCES

[1]Koshland, D. E. (1953) *Biol. Rev. 28*, 416.

[2]Anderson, W. F., Gruter, M. C., Remington, S. J., Weaver, L. H., & Matthews, B. W. (1981) *J. Molec. Biol. 147*, 523.

[3]Imoto, T., Johnson, L. N., North, A. C. T., Phillips, D. C., & Rupley, J. A. (1972), in *The Enzymes Vol. 7*, 3rd ed. (Boyer, P. D., Ed.) p. 665, Academic Press, New York.

[4]Bause, E., & Legler, G. (1974) *Hoppe-Seyler's Z. Physiol. Chem. 355*, 438.

[5]Legler, G., & Harder, A. (1978) *Biochim. Biophys. Acta 524*, 102.

[6]Herrchen, M., & Legler, G. (1984) *Eur. J. Biochem. 138*, 527.

[7]Withers, S. G., Warren, R. A. J., Street, I. P., Rupitz, R., Kempton, J. B., & Abersold, R. (1990) *J. Amer. Chem. Soc. 112*, 5887 .

[8]Stokes, T. M., & Wilson, I. B. (1972) *Biochemistry 11*, 1061.

[9]Blake, C. C. F., Mair, G. A., North, A. C. T., Phillips, D. C., & Sarma, V. R. (1967) *Proc. R. Society London Ser. B 167*, 365.

[10]Chiang, Y., & Kresge, A. J. (1985) *J. Amer. Chem. Soc. 107*, 6363.

[11]Weber, J. P., & Fink, A. L. (1980) *J. Biol. Chem. 255*, 9030.

[12]Withers, S. G., Street, I. P., & Dolphin, D. H. (1987) *J. Amer. Chem. Soc. 109*, 7530.

[13]Withers, S. G., & Street, I. P. (1988) *J. Amer. Chem. Soc. 110*, 8551.

[14]Sinnott, M. L., & Withers, S. G. (1974) *Biochem. J. 143*, 751.

[15]Legler, G., Sinnott, M. L., & Withers, S. G. (1980) *J. Chem. Soc. Perk. Trans. II*, 1376.

[16]Van Doorslaer, E., Opstal, O., Kersters-Hilderson, H., & DeBryune, C. K. (1984) *Bioorg. Chem. 12*, 158.

[17]Sinnott, M. L. (1987) in *Enzyme Mechanisms* (Page, M. I., & Williams, A., Eds.) p. 259, Universities Press, Belfast.

[18]Legler, G., & Julich, E. (1984) *Carbohydrate Res. 128*, 61.

[19]Dale, M. P., Kopfler, W. P., Chait, I., & Byers, L. D. (1986) *Biochemistry 25*, 2522.

[20]Chinchetru, M. A., Cabezas, J. A., & Calvo, P. (1989) *Int. J. Biochem. 21*, 469.

[21]Findlay, J., Levvy, G. A., & Marsh, C. A. (1958) *Biochem. J. 69*, 467.

[22]Pugh, D., Leaback, D. H., & Walker, P. G. (1957) *Biochem. J. 65*, 464.

[23]Niwa, T., Inouye, S., Tsuruoka, T., Koaze, Y., & Niida, T. (1970) *Agric. Biol. Chem. 34*, 966.

[24]Jones, C. C., Sinnott, M. L., & Souchard, I. J. L. (1977) *J. Chem. Soc. Perk. Trans. II*, 1191.

[25]Lehmann, J., & Schlesselmann, P. (1983) *Carbohydrate Res. 113*, 93.

[26]Loeffler, R. S. T., Sinnott, M. L., Sykes, B. D., & Withers, S. G. (1979) *Biochem J. 177*, 145.

[27]Legler, G., & Lotz, W. (1973) *Hoppe-Seyler's Z. Physiol. Chem. 354*, 243.

[28]Pauling, L. (1946) *Chem. Eng. News 24*, 1375.

[29]Roeser, K. R., & Legler, G. (1981) *Biochim. Biophys. Acta 657*, 321.

[30]Brockhaus, M., Dettinger, H. M., Kurz, G., Lehmann, J., & Wallenfels, K. (1979) *Carbohydrate Res. 69*, 264.

[31]Ballardie, F. W., Capon, B., Cuthbert, M. W., & Dearie, W. M. (1977) *Bioorg. Chem. 6*, 483.

[32]Han, Y. W., & Srinivasan, V. R. (1968) *J. Bacteriol. 100*, 1355.

[33]Day, A. G., & Withers, S. G. (1986) *Can. J. Biochem. Cell Biol. 64*, 914.

[34]Wakarchuk, W. W., Kilburn, D. G., Miller, R. C., & Warren, A. J. (1986) *Molec. Gen. Genetics 205*, 146.

[35]Love, D. R., Fisher, R., & Berquist, P. L. (1988) *Molec. Gen. Genetics 213*, 84.

[36]Johnson, C. D. (1973) *The Hammett Equation*, Cambridge University Press, New York.

[37]Barlin, G. B., & Perrin, D. D. (1966) *Quart. Rev. Chem. Soc. 20*, 75.

[38]Jaffe, H. H. (1953) *Chem. Rev. 53*, 191.

[39]Taft, R. W. (1960) *J. Phys. Chem. 64*, 1805.

[40]Van Bekkum, H., Verkade, P. E., & Wepster, B. M. (1959) *Rec. Trav. Chim. 78*, 815.

[41]Norman, R. O. C., Radda, G. K., Brimacombe, D. A., Ralph, P. D., & Smith, E. M. (1961) *J. Chem. Soc.*, 3247.

[42]Exner, O. (1972) in *Advances in Linear Free Energy Relationships* (Chapman, N. B., & Shorter, J., Eds.) p. 1, Plenum Press, London.

[43]Ritchie, C. D., & Sager, W.F. (1964) *Prog. Phys. Org. Chem. 2*, 323.

[44]Jaffe, H. H. (1953) *Science 118*, 246.

[45]Westheimer, F. H., & Metcalf, R. P. (1941) *J. Amer. Chem. Soc. 63*, 1339.

[46]Idoux, J. P., & Hancock, C. K. (1968) *J. Org. Chem. 33*, 3498.

[47]Clark, J., & Perrin, D. D. (1964) *Quart. Rev. Chem. Soc. 18*, 295.

[48]Hopkinson, A. C. (1969) *J. Chem. Soc. B*, 203.

[49]White, W. N., & Fife, W. K. (1961) *J. Amer. Chem. Soc. 83*, 3826.

[50]Schreck, J. O. (1971) *J. Chem. Ed. 48*, 103.

[51]Kirsch, J. F. (1972) in *Advances in Linear Free Energy Relationships* (Chapman, N. B., & Shorter, J., Eds.) p 369, Plenum Press, London.

[52]Nath, R. L., & Rydon, H. N. (1954) *Biochem. J. 57*, 1.

[53]Caplow, M., & Jencks, W. P. (1962) *Biochemistry 1*, 883.

[54]Riddle, B., & Jencks, W. P. (1971) *J. Biol. Chem. 246*, 3250.

[55]Sinnott, M. L., & Souchard, I. J. L. (1973) *Biochem. J. 133*, 89.

[56]Lowe, G., Sheppard, G., Sinnott, M. L., & Williams, A. (1967) *Biochem. J. 104*, 893.

[57]Dahlquist, F. W., Rand-Meir, T., & Raftery, M. A. (1969) *Biochemistry 8*, 4214.

[58]Craze, G.-A., Kirby, A. J., & Osborne, R. (1978) *J. Chem. Soc. Perk. Trans. II*, 357.

[59]Rosenberg, S. & Kirsch, J. F. (1981) *Biochemistry 20*, 3196.

[60]Withers, S. G., Street, I. P., & Percival, M. D. (1988) in *Fluorinated Carbohydrates: Chemical and Biochemical Aspects* (Taylor, N. F., Ed.) p. 59, American Chemical Society, Washington, D. C.

[61]Fersht, A. (1985) *Enayme Structure and Mechanism*, p.331, W. H. Freeman & Co., New York.

[62]Street, I. P., Armstrong, C. R., & Withers, S. G. (1986) *Biochemistry 25*, 6021.

[63]Street, I. P., Rupitz, K., & Withers, S. G. (1989) *Biochemistry 28*, 1581.

[64]Conchie, J., & Levvy, G. A. (1963) *Methods in Carbohydrate Chemistry II*, 335.

[65]Ballardie, F., Capon, B., Sutherland, J. D. G., Cocker, D., & Sinnott, M. L. (1973) *J. Chem. Soc. Perk. Trans. I*, 2418.

[66]Reed, L. A., Prabhakar, A. R., & Goodman, L. (1981) *J. Chem. Soc. Chem. Comm*, 760.

[67]Street, I. P. (1985) MSc Thesis, University of British Columbia.

[68]Lineweaver, H., & Burk, D. (1934) *J. Amer. Chem. Soc. 56*, 658.

[69]Reference 61, p. 107.

[70]Kortum, G., Vogel, W., & Andrussow, K. (1961) *Pure Appl. Chem. 1*, 450.

[71]Robinson, R. A., Davis, M. M., Paabo, M., & Bower, V. E. (1960) *J. Res. Nat. Bur. Stand. Sect. A 64*, 347.

[72]Ba-Saif, S. A., & Williams, A. (1988) *J. Org. Chem. 53*, 2204.

[73]Schowen, R. L. (1978) in *Transition States of Biochemical Processes* (Gandour, R. D. & Schowen, R. L., Eds.) pp 77-114, Plenum Press, New York.

[74]Berven, L. A., & Withers, S. G. (1986) *Carbohydr. Res. 156*, 282.

[75]Street, I. P. (1988) PhD Thesis, University of British Columbia.

[76]Rupitz, K., personal communication.

[77]Still, W. C., Kahn, M., & Mitra, M. (1977) *J. Org. Chem. 43*, 2923.

[78]Wolfrom, M. L., & Thompson, A. (1963) *Methods in Carbohydrate Chemistry II*, 213.

[79]Haynes, L. J., & Newth, F. J. (1955) *Adv. Carbohydrate Chemistry 10*, 213.

[80]Shelling, J. G., Dolphin, D. H., Wirz, P., Cobbledick, R. E., & Einstein, F. W. B. (1984) *Carbohydr. Res. 132*, 241.

[81]Klinman, J. P. (1978) in *Transition States of Biochemical Processes* (Gandour, R. D., & Schowen, R. L., Eds.) pp 165-200, Plenum Press, New York.

[82]Carey, F. A., & Sundberg, R. J. (1977) *Advanced Organic Chemistry Part A.*, p. 149, Plenum Press, New York.

[83]Hogg, J. L. (1978) in *Transition States of Biochemical Processes* (Gandour, R. D., & Schowen, R. L., Eds.) pp 201-224, Plenum Press, New York.

[84]Melander, L., & Saunders, W. H. (1980) *Reaction Rates of Isotopic Molecules*, Wiley Press, New York.